

NGNP and Hydrogen Production Preconceptual Design Report

SPECIAL STUDY 20.4: POWER CONVERSION SYSTEM

Revision 0

APPROVALS

Function	Printed Name and Signature	Date
Author	Gerard du Plessis M-Tech-Industrial (Pty) Ltd 	26 January 2007
Reviewer	Jan van Ravenswaay M-Tech Industrial (Pty) Ltd 	26 January 2007
Approval	Michael Correia Pebble Bed Modular Reactor (Proprietary) Ltd 	26 January 2007

Westinghouse Electric Company LLC
Nuclear Power Plants
Post Office Box 355
Pittsburgh, PA 15230-0355

©2007 Westinghouse Electric Company LLC
All Rights Reserved

LIST OF CONTRIBUTORS

Name and Organization	Date
Renée Greyvenstein Pebble Bed Modular Reactor (Proprietary) Ltd	November 2006
Scott Penfield, Fred Silady, Dan Mears, Dan Allen Technology Insights	December 2006

BACKGROUND INTELLECTUAL PROPERTY

Section	Title	Description
NONE		

REVISION HISTORY**RECORD OF CHANGES**

Revision No.	Revision Made by	Description	Date
0	G. du Plessis M-Tech Industrial (Pty) Ltd	Initial issue	31 January, 2007

DOCUMENT TRACEABILITY

Created to support the following Document(s)	Document Number	Revision
NGNP and Hydrogen Production Preconceptual Design Report	NGNP-01-RPT-001	0

LIST OF TABLES

Table 20.4.1: Cycle Input Parameters.....	22
Table 20.4.2: Operating Pressure for Cycle B at the Design Point.....	43
Table 20.4.3: Cycle B Heat Exchanger Duty and Turbo Machine Load for Cycle B	44
Table 20.4.4: Operating Pressure for Cycle H at the Design Point	47
Table 20.4.5: Cycle H Heat Exchanger Duty and Turbo Machine Load.....	48
Table 20.4.6: Operating Pressures for Cycle J at the Design Point	50
Table 20.4.7: Cycle J Heat Exchanger Duty and Turbo Machine Load	51
Table 20.4.8: Operating Pressures and Primary/Secondary Circuit Temperatures for Cycle L. 52	
Table 20.4.9: Cycle L Heat Exchanger Duties and Turbo Machine Loads	53
Table 20.4.10: Summary of Turbo Unit Model Inputs and Outputs.....	61
Table 20.4.11: Input Parameters to Cycle Analysis Tool	67

LIST OF FIGURES

Figure 20.4.1: Representative Brayton Cycle.....	9
Figure 20.4.2: Representative GTCC.....	10
Figure 20.4.3: Representative Rankine Cycle.....	10
Figure 20.4.4: Overview of Methodology	13
Figure 20.4.5: Option Tree for Choosing the Optimum PCS	15
Figure 20.4.6: Direct Brayton Cycles Under Investigation	17
Figure 20.4.7: Brayton T-S Diagrams for Various Rejected GTCC Configurations.....	18
Figure 20.4.8: Brayton T-S Diagrams for Various Recommended GTCC Configurations.....	19
Figure 20.4.9: Direct GTCCs Under Investigation.....	20
Figure 20.4.10: T-S Diagram Indicating Lost Work for (i) GTCC and (ii) Steam Cycle	21
Figure 20.4.11: Direct Rankine Cycle under Investigation	21
Figure 20.4.12: Direct Brayton Cycle Net Efficiency vs. Overall Pressure Ratio.....	24
Figure 20.4.13: Direct Brayton Cycle RIT vs. Overall Pressure Ratio.....	25
Figure 20.4.14: Direct Brayton Cycle Mass Flow Rate vs. Overall Pressure Ratio	25
Figure 20.4.15: Direct Brayton Cycle Relative Turbo Unit Size vs. Overall Pressure Ratio	26
Figure 20.4.16: Direct Brayton Cycle Relative Turbo Unit Size vs. Power Turbine Speed	27
Figure 20.4.17: Direct Brayton Cycle Relative Heat Exchanger Size vs. Overall Pressure Ratio.....	27
Figure 20.4.18: T-S Diagram of Cycle J.....	29
Figure 20.4.19: Direct GTCC Net Efficiency vs. Total Brayton Cycle Pressure Ratio	30
Figure 20.4.20: Direct GTCC RIT vs. Overall Brayton Pressure Ratio	30
Figure 20.4.21: Direct GTCC Mass Flow Rate vs. Overall Brayton Pressure Ratio.....	31
Figure 20.4.22: Direct GTCC Relative Turbo Unit Size vs. Overall Brayton Pressure Ratio.....	32

Figure 20.4.23: Direct GTCC Relative Heat Exchanger Size vs. Overall Brayton Pressure Ratio.....	33
Figure 20.4.24: Thermal Power Output vs. Pressure Ratio for Brayton Cycles and GTCCs.....	33
Figure 20.4.25: Indirect Cycle Configurations	36
Figure 20.4.26: Direct vs. Indirect Cycle Net Efficiency vs. Total Brayton Cycle Pressure Ratio.....	37
Figure 20.4.27: Series vs. Parallel Hydrogen Production Plant Configuration for Cycle B.....	38
Figure 20.4.28: Cycle B PCS Cycle Efficiency for a Series and Parallel PCHX Coupling vs. Hydrogen Production Plant Size.....	38
Figure 20.4.29: Cycle B and Cycle L PCS Net Cycle Efficiency for a Series PCHX Coupling vs. Hydrogen Production Plant Size	40
Figure 20.4.30: Net Cycle Efficiency vs. Brayton Overall Pressure Ratio.....	41
Figure 20.4.31: Net Cycle Efficiency vs. Turbine Inlet Temperature (Brayton Pressure Ratio Fixed at 3.1)	42
Figure 20.4.32: Numbering for Cycle B	43
Figure 20.4.33: T-S Diagram for the Design Point Operating Conditions of Cycle B.....	44
Figure 20.4.34: Numbering for Cycle H.....	46
Figure 20.4.35: T-S Diagram for the Design Point Operating Conditions of Cycle H.....	46
Figure 20.4.36: Heat Transfer vs. Temperature in Steam Generator.....	47
Figure 20.4.37: Numbering for Cycle J	49
Figure 20.4.38: T-S Diagram for the Design Point Operating Conditions of Cycle J.....	49
Figure 20.4.39: Heat Transfer vs. Temperature in Steam Generator.....	50
Figure 20.4.40: Numbering for Cycle L	51
Figure 20.4.41: T-S Diagram for the Rankine Section of Cycle L	52
Figure 20.4.42: Recuperator Efficiency vs. Heat Transfer Area for Recuperator	64
Figure 20.4.43: Heat Exchanger Efficiency vs. Heat Transfer Area for Coolers	65

ACRONYMS

Abbreviation or Acronym	Definition
DGS	Dry Gas Seal
DPP	Demonstration Power Plant
EMB	Electro Magnetic Bearing
GTCC	Gas-Turbine Combined Cycles
GT-MHR	Gas Turbine – Modular Helium Reactor
HPC	High Pressure Compressor
HPT	High Pressure Turbine
HTGR	High Temperature Gas Reactor
IHX	Intermediate Heat Exchanger
LPC	Low Pressure Compressor
LPT	Low Pressure Turbine
NGNP	Next Generation Nuclear Plant
PBMR	Pebble Bed Modular Reactor
PCHX	Process Coupling Heat Exchanger
PCS	Power Conversion System
PT	Power Turbine
RIT	Reactor Inlet Temperature
RPV	Reactor Pressure Vessel

TABLE OF CONTENTS

LIST OF TABLES 4

LIST OF FIGURES 4

ACRONYMS 6

20.4 POWER CONVERSION SYSTEMS 9

SUMMARY AND CONCLUSIONS 9

INTRODUCTION..... 12

BACKGROUND 12

OBJECTIVE 12

ANALYSIS METHODOLOGY 12

 Component Models 14

20.4.1 POWER CONVERSION SYSTEMS 15

20.4.1.1 BRAYTON CYCLES..... 16

20.4.1.2 GAS TURBINE COMBINED CYCLES 18

20.4.1.3 RANKINE CYCLES 21

20.4.2 RESULTS..... 22

20.4.2.1 ANALYSIS INPUTS 22

20.4.2.2 COMPARATIVE RESULTS 23

 20.4.2.2.1 Brayton Cycles 23

 20.4.2.2.2 Brayton Cycle Selection..... 28

 20.4.2.2.3 Gas Turbine Combined Cycles 28

 20.4.2.2.4 Gas Turbine Combined Cycle Selection 34

 20.4.2.2.5 Rankine Cycle 35

20.4.2.3 GENERAL RESULTS 35

 20.4.2.3.1 Direct vs. Indirect..... 35

 20.4.2.3.2 Series vs. Parallel 37

 20.4.2.3.3 Horizontal vs. Vertical Shaft and Bearing Arrangements..... 40

 20.4.2.3.4 Other..... 41

20.4.2.4 DESIGN POINT PARAMETERS 42

 20.4.2.4.1 Brayton Cycle (Cycle B)..... 43

 20.4.2.4.2 Gas Turbine Combined Cycles (Cycle H, J)..... 45

 20.4.2.4.3 Rankine Cycles (Cycle L) 51

20.4.3 SUMMARY AND RECOMMENDATIONS 54

REFERENCES..... 55

BIBLIOGRAPHY 56

DEFINITIONS 57

REQUIREMENTS..... 58

LIST OF ASSUMPTIONS..... 59

TECHNOLOGY DEVELOPMENT 60

APPENDICES 61

APPENDIX A: COMPONENT MODELS..... 61

APPENDIX B: INPUT PARAMETERS 67

APPENDIX C: SPECIAL STUDY 20.4 SLIDES 70

20.4 POWER CONVERSION SYSTEMS

SUMMARY AND CONCLUSIONS

The choice of a thermodynamic cycle configuration is a vital step in the preconceptual design phase of the Next Generation Nuclear Plant (NGNP). The cycle configuration directly influences the cycle efficiency and power output as well as operational flexibility, construction time and risks associated with the plant.

The objective of this special study is to compare various cycle configurations in order to identify representative Brayton, Combined and Rankine cycles for the NGNP. The most promising Brayton cycles, Gas-Turbine Combined cycles (GTCCs) and Rankine cycles were analyzed and compared with regard to thermodynamic performance and practical considerations when employed in conjunction with a given Pebble Bed Modular Reactor (PBMR). A representative cycle was chosen for each group of cycle configurations.

For the Brayton cycle configurations, this study has shown that a single-shaft cycle with inter-cooling would be the best option in terms of net cycle efficiency and turbo-unit size. The representative Brayton cycle, shown by Figure 20.4.1 has an optimum net cycle efficiency of 42.3%, which is achieved at an overall pressure ratio of approximately 3.2 (See Section 20.4.2.4.1).

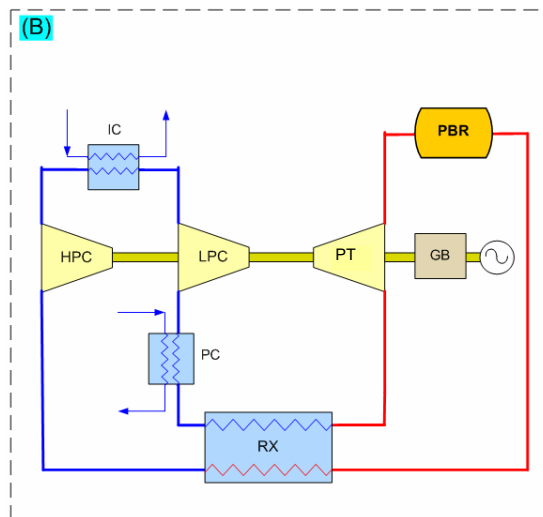


Figure 20.4.1: Representative Brayton Cycle

For the GTCCs, a single-shaft recuperative Brayton cycle without inter-cooling was found to be the most suitable cycle configuration. Although the cycle does not have the highest

net cycle efficiency (45.1%, see Section 20.4.2.4.2) of the GTCCs under investigation, the turbomachine employed by the cycle builds on the PBMR Demonstration Power Plant (DPP) design. The cycle shown by Figure 20.4.2 was therefore chosen as the representative GTCC on the basis of readiness of technology.

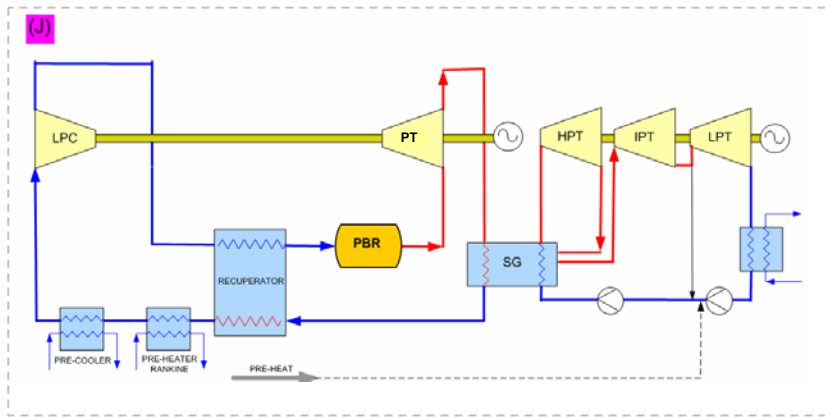


Figure 20.4.2: Representative GTCC

A single conventional Rankine cycle coupled to a PBMR through a steam generator was chosen as the representative Rankine cycle – refer to Figure 20.4.3. The representative Rankine configuration uses proven Rankine cycle technology and has a net cycle efficiency of 41.2% (See Section 20.4.2.2.5).

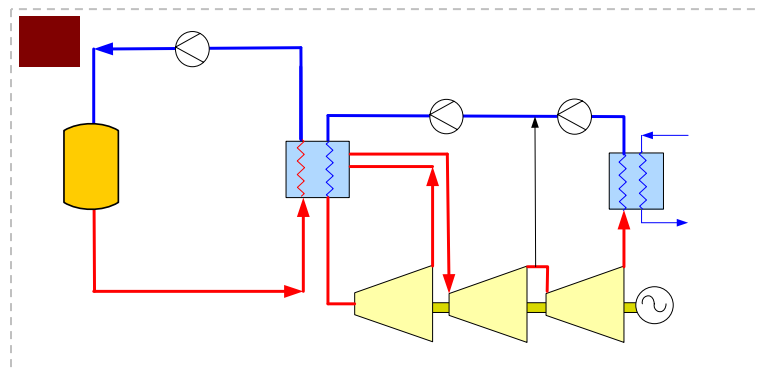


Figure 20.4.3: Representative Rankine Cycle

The influence of a direct versus indirect power conversion system (PCS) was also investigated for each group of cycle configurations. As expected, it was indicated that the net cycle efficiency of the cycles in each group decreases for an indirect configuration. Special Study 20.3 [2] comments on the practical considerations associated with direct versus indirect coupled PCSs.

The influence of the coupling configuration of the hydrogen plant with the PCS, as well as the size of the hydrogen production plant, was also considered. The sensitivity of cycle efficiency to the hydrogen plant size was compared for Brayton and Rankine cycles. It was found that the net cycle efficiency of the representative Rankine cycle is not as sensitive to the coupling configuration and hydrogen production plant size as the representative Brayton cycle. Special Study 20.3 [2] comments on the practical considerations associated with series versus parallel coupled PCSs.

Finally, the design point parameters for the representative cycle configurations are presented together with a diagram showing the major components of each cycle.

Considering the results presented by this study it is recommended that the three selected representative cycles are evaluated further in NGNP Special Study 20.3 [2] in order to identify the optimum cycle configuration for the NGNP application.

INTRODUCTION

Background

The choice of a thermodynamic cycle configuration is a vital step in the preconceptual design phase of the NGNP. The cycle configuration directly influences the cycle efficiency, power output, operational flexibility, maintenance, construction time and risks associated with the plant. It is therefore essential to investigate various cycle configurations and assess each cycle's feasibility with regard to these parameters before deciding on a cycle configuration for the NGNP.

Identifying the optimum Power Conversion System (PCS) is a complex and integrated problem; it is difficult to assess the feasibility of each cycle during the preconceptual phase. An integrated approach is therefore needed to highlight the underlying parameters that will influence the feasibility of a particular cycle. An integrated decision-supporting tool that systematically compares various cycle configurations based on the same input parameters was therefore employed to evaluate the performance of different cycle configurations as a function of various design parameters. The cycle analysis tool employed for the comparison of the different cycle configurations (CYCLE-C) was previously developed by Pebble Bed Modular Reactor (Pty) Ltd. [1].

Objective

The objective of this special study is to analyze and compare various Brayton cycles, Gas-Turbine Combined cycles (GTCCs) and a conventional Rankine cycle in terms of thermodynamic performance and practical considerations when employed in conjunction with a Pebble Bed Modular Reactor (PBMR). The objective is to identify a near-optimum design for each cycle configuration from which a representative Brayton cycle, GTCC and Rankine cycle can be identified. Another special study "High Temperature Process Heat, Transfer and Transport," [2] will select the optimum cycle for the NGNP from the short-list of representative cycles.

In selecting the three representative cycles, this study also considers the technology maturity and design point parameters, together with a list of the major components for each representative cycle configuration. In addition, a commentary on vertical and horizontal shaft and bearing arrangements for Brayton cycles is included.

Analysis Methodology

Thermodynamic performance and practical considerations are the main parameters used to compare the various cycle configurations. The following methodology is used to compare the various cycle configurations – refer to Figure 20.4.4.

- A thermodynamic cycle analysis is performed for each configuration based on a fixed reactor pressure loss coefficient, fixed heat exchanger effectiveness and fixed percentages for pressure loss through the piping and heat exchangers. The turbo machine leak flows are calculated as fixed percentages of the total cycle flow (however, percentages differ for multiple shaft configurations).
- Component models for the turbine, compressor, heat exchanger and blower are used together with the boundary values from the cycle analyses to perform a conceptual design of these components.
- The turbo machine designs are optimized by ensuring the minimum size for each machine (assuming fixed isentropic efficiencies).
- The temperatures, pressures and cycle efficiency of each configuration are calculated for various pressure ratios, turbine inlet temperatures and power turbine speeds.

Since it is anticipated that the size of the NNGP’s initial hydrogen plant demonstration will be relatively small [2] compared to the reactor size, the hydrogen production plant will not be directly considered in the analyses when comparing the various PCS cycle configurations. However, the influence of the hydrogen plant growth path from prototype to commercial plant on the PCS cycle efficiency is subsequently evaluated for two representative cycle configurations from the Brayton cycle and Rankine cycle groups.

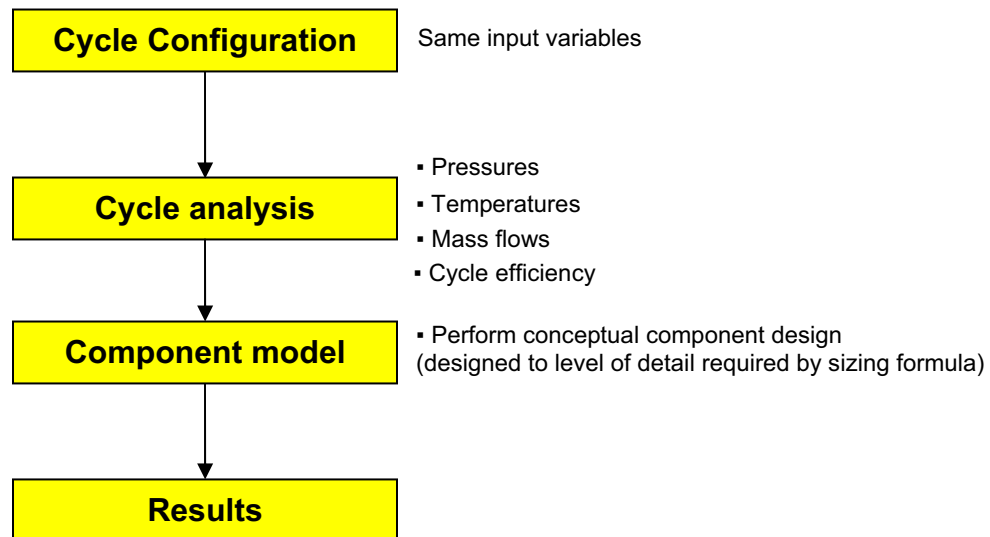


Figure 20.4.4: Overview of Methodology

In order to perform a conceptual design of the major components in each cycle configuration, component models are required. Component models were developed only for the turbo machines, the heat exchangers and the blowers. The same reactor configuration was utilized for all the cycles [1].

The reactor inlet temperature (RIT) for the GTCCs and also the turbo machine sizes for the Brayton cycles of the GTCC are optimized to ensure, respectively, the maximum GTCC efficiency and minimum Brayton turbo machine size. After the thermodynamic cycle analysis has been performed and optimized (to ensure maximum cycle efficiency), the turbo units are optimized (to ensure the smallest possible machine for a given set of inputs - see next section). This process is repeated over a wide range of operating conditions.

The above analysis process of calculating and optimizing using CYCLE-C was done within the ISO 9001:2000 quality assurance system of M-Tech along with the quality management systems (QMS) of M-Tech [5]. Further more, M-Tech conforms to ANSI-10.4 (1987) [6] and other internationally accepted standards with respect to C++ programming.

Component Models

Appendix A provides more detailed discussions concerning the turbo machine, heat exchanger and blower component models mentioned below. This study only presents the results for the turbo machine and heat exchanger sizes.

Turbo Machines

The size of the turbo unit is calculated as a function of compressor and turbine tip radius (r_t), number of stages (z) and proportionality constants. The component model is used to determine the compressor and turbine tip radius, number of stages, etc. at each specified operating point. The component model is a function of the temperature difference over the machine (dT), the mass flow through the machine (\dot{m}), the inlet density (ρ_{inlet}), the work coefficient (ψ), the flow coefficient (ϕ), the maximum blade stress (σ_{max}), the blade density (ρ_{blade}), the blade stress safety factor (SF), the rotational speed (N), the axial velocity (Ca) and the hub-tip-ratio (htr). The machine is optimized to ensure the smallest size, while staying within all the design limitations.

Heat Exchangers

The heat exchanger's size is assumed to be directly proportional to the heat transfer area. For the recuperator, pre-cooler and inter-cooler the component models are applied to determine the appropriate heat transfer area (A) for a fixed heat transfer coefficient (U), whereas for the IHX the component models determine the heat transfer area for a fixed approach temperature.

Blower

The blower size model is a function of the blower power output and, consequently, the component model only solves for the blower power.

20.4.1 POWER CONVERSION SYSTEMS

This section presents the different cycle configurations under investigation. Various Brayton cycles, GTCC cycles and a Rankine cycle for comparison are given, and it is explained why the specific variations of these configurations were chosen.

For a specific PCS, one needs to assess whether a direct or indirect cycle is best. This study only presents the effect on cycle efficiency for direct versus indirect cycles, while Special Study 20.3 2 addresses practical considerations. Should one choose an indirect cycle, the choice of which fluid to use arises. It is assumed that a PBMR will be used and that helium would, therefore, be used as the coolant for all the direct cycles. This study only investigates the use of helium for the indirect cycle PCS; however Special Study 20.3 2 considers different fluid options for the Secondary Heat Transport System. Figure 20.4.5 shows the option tree for the different categories of PCS configurations.

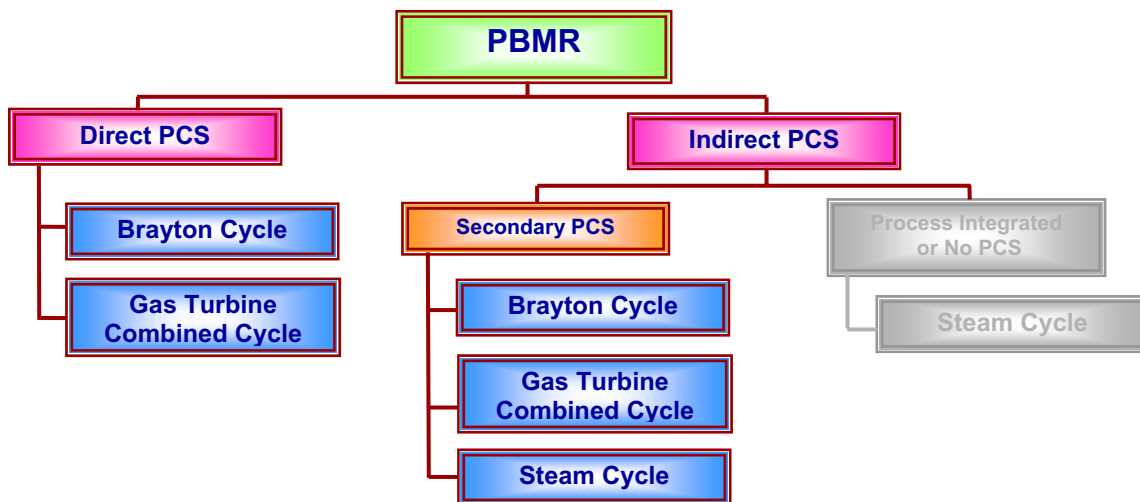


Figure 20.4.5: Option Tree for Choosing the Optimum PCS

20.4.1.1 Brayton Cycles

Brayton cycle configurations mainly differ from each other with regard to number of shafts, orientation of shafts, inter-cooling and whether or not a recuperator is employed for waste heat recovery. The number of shafts impact directly on the plant controllability, the number of compressors and turbines, the turbo machine design, risk and cost. The turbo machine design impacts on the turbo efficiency, which influences the net cycle efficiency. Inter-cooling and waste heat recovery also impact directly on the cycle efficiency. The effect of each of these parameters on the efficiency and practicalities needs to be evaluated for each of the various options. Cycles A to E shown in Figure 20.4.6 were identified as possible Brayton configurations:

- Cycle A: Single shaft, recuperative Brayton cycle.
- Cycle B: Single shaft, recuperative Brayton cycle with inter-cooling.
- Cycle C: Two shaft, recuperative Brayton cycle with inter-cooling.
- Cycle D: Three shaft, recuperative Brayton cycle with inter-cooling.
- Cycle E: Three shaft, recuperative Brayton cycle with two-step inter-cooling.

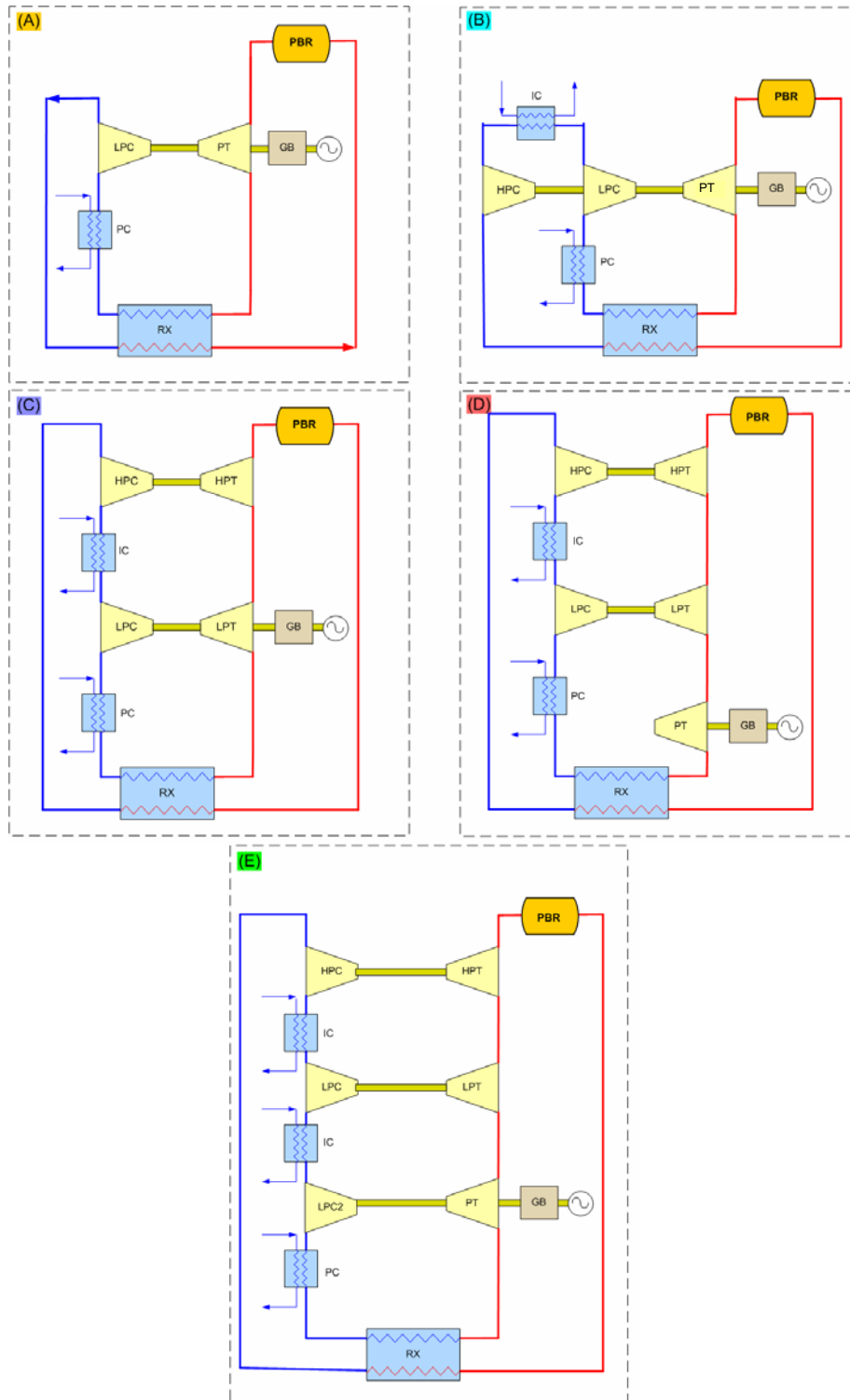


Figure 20.4.6: Direct Brayton Cycles Under Investigation
 (A) Single-shaft, (B) Single-shaft with inter-cooling, (C) Two-shaft with inter-cooling,
 (D) Three-shaft with inter-cooling, (E) Three-shaft with two-step inter-cooling.

20.4.1.2 Gas Turbine Combined Cycles

GTCCs reject heat at low temperatures in the condenser and are, therefore, generally more efficient than Brayton cycles. For the Brayton section of the GTCC, the number of shafts needs to be determined as well as whether inter-cooling and waste heat recovery are necessary. Added complexities are the questions of where the steam generator should be situated in the Brayton cycle layout and how to customize the steam plant to exactly match the Brayton cycle.

Figure 20.4.7 (i) represents the T-s diagram of a single-shaft inter-cooled Brayton cycle, in which the recuperator has been replaced with a steam generator. The reactor inlet temperature (RIT) for the PBMR is limited to a minimum of approximately 280°C if the existing Reactor Pressure Vessel (RPV) material is to be used without re-qualification. In the absence of the recuperator, the RIT drops to approximately 100°C. This is below the minimum RIT and therefore Cycle (i) is disqualified. Because of the limit on the RIT, a recuperator is introduced.

Figure 20.4.7 (ii) represents the T-s diagram of a single-shaft inter-cooled Brayton cycle, with both a recuperator and steam generator. The penalty incurred with placing the steam generator at the lower end is that the recuperator is very ineffective, and that the maximum temperature for the steam plant is limited to approximately 200°C. Cycle (ii) will therefore have both an inefficient Brayton cycle due to low recuperator effectiveness and also a low Rankine cycle efficiency due to the low steam temperature; therefore Cycle (ii) is not advised.

Figure 20.4.7 (iii) represents the T-s diagram of a single-shaft inter-cooled Brayton cycle in which the steam generator is coupled in parallel with the recuperator through a three-pass heat exchanger. Although the steam plant efficiency will be increased because of the higher temperatures, the Brayton section is still inefficient due to the ineffective recuperator. Cycle (iii) is, therefore, also not advisable.

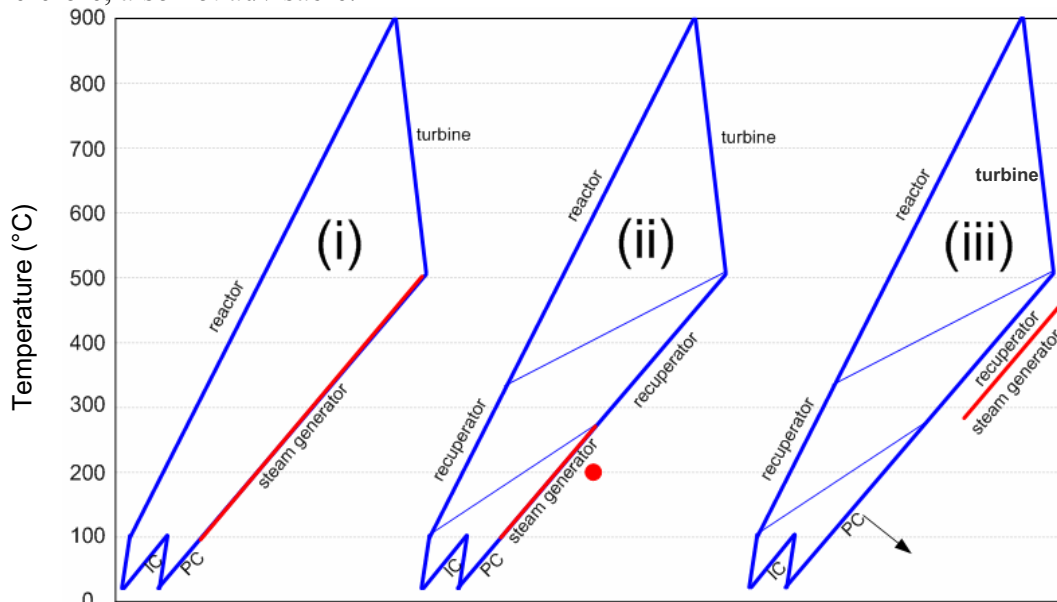


Figure 20.4.7: Brayton T-S Diagrams for Various Rejected GTCC Configurations

Figure 20.4.8 (iv-A) represents the T-s diagram of a single-shaft inter-cooled recuperative Brayton cycle, where the steam generator is utilized at the higher end with the recuperator at the lower end. The advantage is that the steam plant has a high steam temperature, while the recuperator is still working effectively. Note that the RIT is low which results in lower mass flows for the same reactor outlet temperature when compared to the Brayton cycle without the steam generator. Since reactor velocities are to be limited, the lower RIT implies that this configuration will enable the use of increased reactor power levels compared to a Brayton cycle. The lower RIT results in a lower duty, smaller recuperator. This cycle is proposed to be investigated – see Cycle G of Figure 20.4.9.

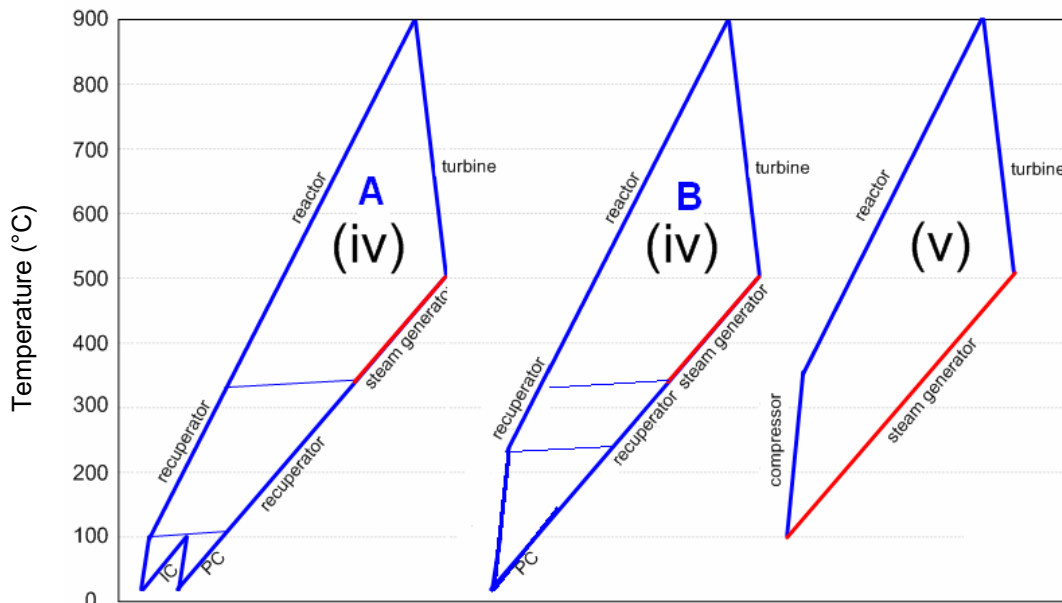


Figure 20.4.8: Brayton T-S Diagrams for Various Recommended GTCC Configurations

An alternative to Cycle G (Figure 20.4.8 (iv-A)) is shown in Figure 20.4.8 (iv-B) where the fluid is compressed after the pre-cooler and the inter-cooler and the high-pressure compressor (HPC) is removed – see Cycle J of Figure 20.4.9. It is noted that the recuperator size is smaller now and also that more heat is available in the pre-cooler to be effectively used to pre-heat the water in the Rankine cycle before entering the steam-generator. Another alternative shown in

Figure 20.4.8 (v) is to remove the pre-cooler and directly compress the fluid after the steam generator. In this case a recuperator will not be needed since the RIT is already in the region of 400°C - see Cycle H of Figure 20.4.9.

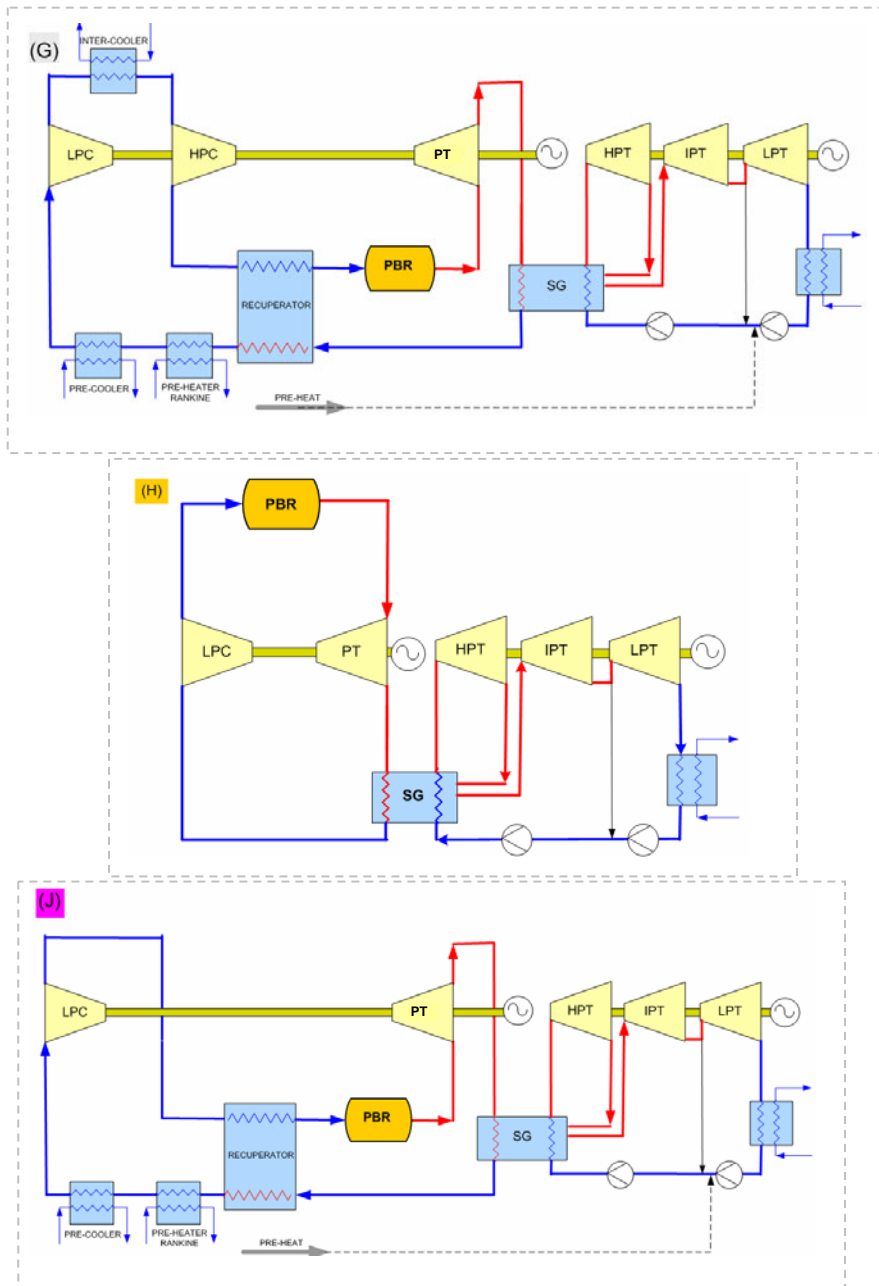


Figure 20.4.9: Direct GTCCs Under Investigation

(G) Single-shaft recuperative Brayton with inter-cooling (H) Single-shaft Brayton without inter-cooling (J) Single-shaft recuperative Brayton without inter-cooling.

20.4.1.3 Rankine Cycles

The maximum steam temperature for conventional steam plants varies. However 540°C presents a typical maximum steam temperature for coal-fired steam plants. Thus, steam plants effectively utilize heat only below 650°C. The shaded areas in Figure 20.4.10 indicate lost work in the system – heat which is available, but not utilized. Rankine cycles, therefore, do not fully utilize the heat from high temperature nuclear reactors; however, Rankine cycles could provide flexible solutions when incorporated with a hydrogen production plant. If a hydrogen production plant is coupled to a Rankine cycle, the high-temperatures provided by the PBMR can be utilized by the hydrogen production plant, while the excess heat available at lower temperatures is ideally suited for a bottoming Rankine cycle. A Rankine cycle will therefore be included as a possible cycle configuration in this investigation.

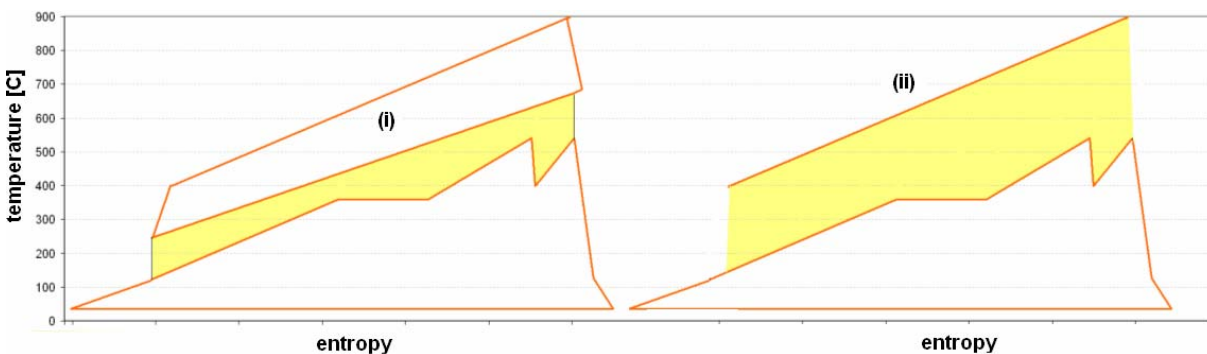


Figure 20.4.10: T-S Diagram Indicating Lost Work for (i) GTCC and (ii) Steam Cycle

Figure 20.4.11 presents the Rankine cycle under investigation where a PBMR is coupled directly to a steam generator of a conventional Rankine cycle.

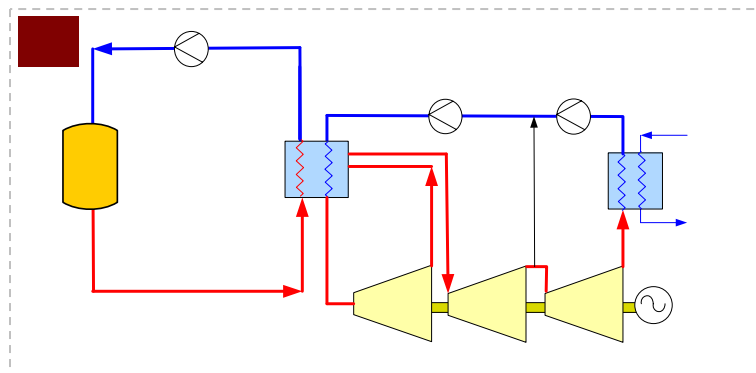


Figure 20.4.11: Direct Rankine Cycle under Investigation

20.4.2 RESULTS

This section presents the results obtained from the cycle analyses of the various cycle configurations [1]. From these results, a representative Brayton cycle, GTCC and Rankine cycle are chosen.

The performance of an indirect Brayton cycle, GTCC and a Rankine cycle is compared to the equivalent direct cycle configurations. The influence of a series versus parallel coupled hydrogen production plant on the PCS is also presented.

20.4.2.1 ANALYSIS INPUTS

In order to compare the various cycle configurations, all the input parameters to the analyses, except the turbo machine leak flows, are kept constant. Table 20.4.1 shows the major input parameters for the Brayton cycles, GTCCs and the Rankine cycles under investigation. Refer to Appendix B for a more detailed list of inputs to the cycle analysis tool.

Table 20.4.1: Cycle Input Parameters

Generic Inputs	
PBMR power	500 MW _{th}
Primary and Secondary fluid	Helium
Brayton Cycle Inputs	
Turbine inlet temperature	900°C
Min Helium coolant temperature	22.5°C
$\eta_{\text{compressor}}$	89%
η_{turbine}	91%
η_{blower}	80%
Compressor outlet axial velocity	135 m/s
$\eta_{\text{recuperator}}$	97%
IHX pressure drop	0.5% of inlet pressure
Piping pressure drop	0.2% of inlet pressure
Brayton cycle House load	6.5 MW _e (assumed)
Primary circuit maximum pressure	9 MPa
IHX approach temperatures (indirect cycles)	50°C
Secondary circuit pressure (indirect cycles)	8.8 MPa (assumed)
GTCC Inputs	
Cycle (G), (J) House load*	$0.8 \cdot HL_{\text{Brayton}} + 0.0085 \cdot \text{Power}_{\text{Rankine}}$
Cycle (H) House load*	$0.6 \cdot HL_{\text{Brayton}} + 0.0085 \cdot \text{Power}_{\text{Rankine}}$

Rankine Cycle Inputs	
Maximum steam pressure	18 MPa
Condenser temperature	35°C
Turbine exhaust quality	>0.88
η_{turbine}	89%
η_{pump}	72%
Steam Generator pressure drop	3% of inlet pressure
Re-heater pressure drop	3% of inlet pressure
Piping pressure drop	Ignored
Rankine House load	$0.0085 * \text{Power}_{\text{Rankine}}$
Pinch temperature	30°C

* The Brayton cycle house load for Cycles G and J differs from that of Cycle H, since the relative size of the Brayton cycle section of Cycle H is smaller than the size of the Brayton cycle section of Cycles G and J – see subsequent text.

The following constraints should be taken into account when interpreting the results from the cycle analysis:

- The RIT is limited to a maximum of 500°C in order to limit the temperature of the core barrel below 427°C (to stay within material limitations).
- The average velocity through the reactor outlet slots is limited and corresponds to a maximum allowable mass flow rate of approximately 200 kg/s at a pressure level of 9 MPa. This limitation stems from the current PBMR DPP design, which has been optimized for maximum velocity in the reactor slots. In order to build on the PBMR DPP design with limited R&D and design development, the current reactor design is assumed.
- The maximum overall pressure ratio of the Brayton cycle turbo machines is limited to approximately 3.5 to enable practical helium gas turbine designs.
- For the Rankine cycles, the maximum steam temperature is limited to 540°C to enable the use of off-the-shelf Rankine cycle equipment.

20.4.2.2 COMPARATIVE RESULTS

This section compares the results obtained from the cycle analyses for the Brayton cycles, GTCCs and the Rankine cycle under investigation.

20.4.2.2.1 Brayton Cycles

Figure 20.4.12 presents the calculated net cycle efficiency as a function of the total pressure ratio for each of the five direct Brayton cycles. Figure 20.4.12 shows that, in general, the net cycle efficiency of a Brayton cycle is increased when the number of compression stages

with inter-cooling is increased. However, the contribution of each additional stage to the net cycle efficiency becomes less (from Cycle A to Cycle D to Cycle E).

Cycles B, C and D represent single-, two- and three-shaft Brayton cycles with a single inter-cooler. The net cycle efficiency of the single-shaft design is higher than the two-shaft and three-shaft designs. The reason for these differences can be ascribed to the higher leakage flows and the additional turbo machine diffuser losses accredited to multi-shaft systems.

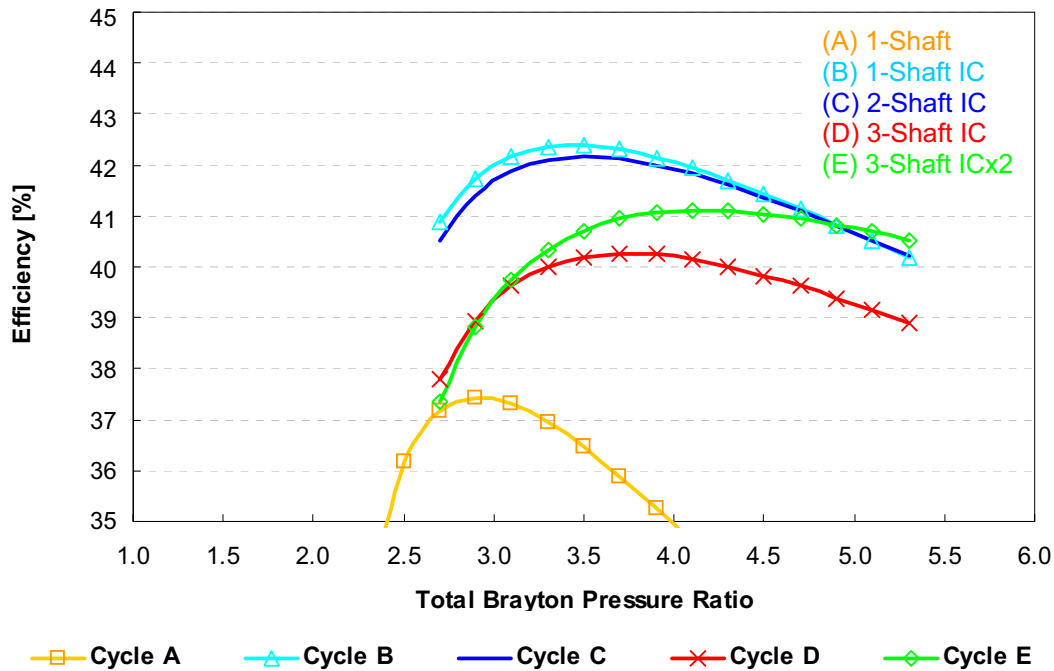


Figure 20.4.12: Direct Brayton Cycle Net Efficiency vs. Overall Pressure Ratio

Figure 20.4.13 and Figure 20.4.14 present the RIT and mass flow rate through the reactor as a function of the total pressure ratio for each of the cycles, respectively. The PBMR RIT is limited to 500°C (in order to limit the Core Barrel temperature below 427°C) and the mass flow rate through the reactor to approximately 200 kg/s at 9 MPa (in order to keep the reactor velocities below its limit).

It can be seen from Figure 20.4.13 that the pressure ratio of the Brayton cycles needs to be above 3.1 in order to limit the RIT to approximately 500°C.

From Figure 20.4.14 it can be seen that none of the direct Brayton cycles are able to operate at their maximum efficiencies without exceeding the maximum acceptable mass flow rate through the reactor at 500 MW_{th}. In order to operate within the reactor design envelope, the direct Brayton cycles would have to operate at pressure ratios of ~4.3, which exceed the predefined overall pressure ratio limitation of 3.5. Although viable for a 400 MW_{th} reactor, the 500 MW_{th} Brayton cycles are challenged due to the reactor velocity constraints that are

exceeded. The pressure ratio or recuperator efficiency must therefore be adapted to operate at 500 MW_{th}. This will result in a net cycle efficiency penalty.

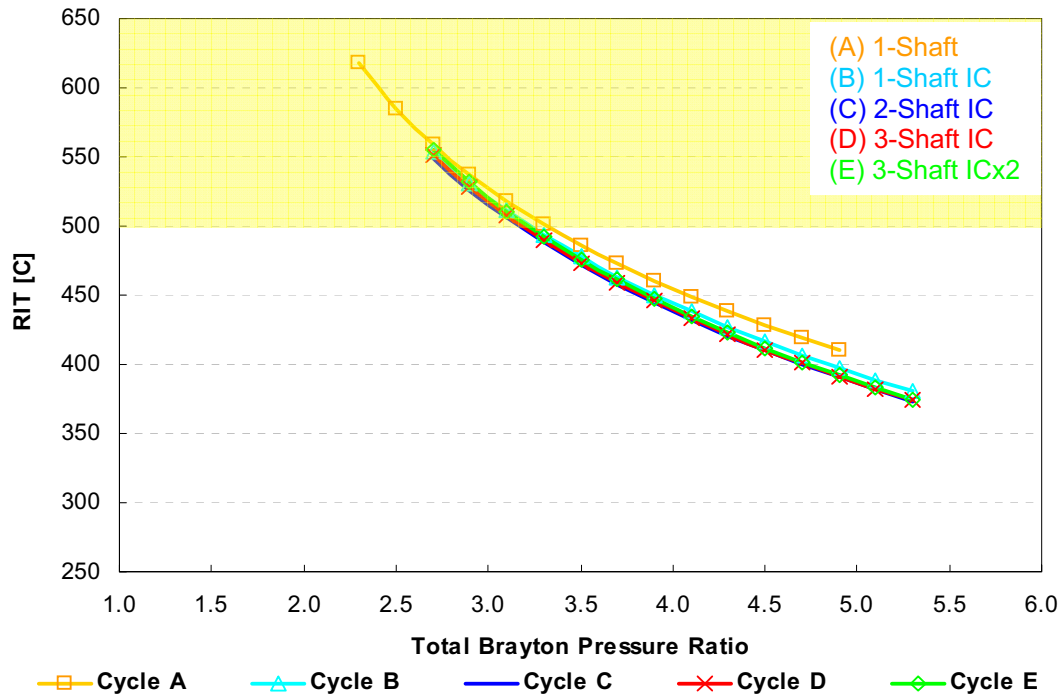


Figure 20.4.13: Direct Brayton Cycle RIT vs. Overall Pressure Ratio

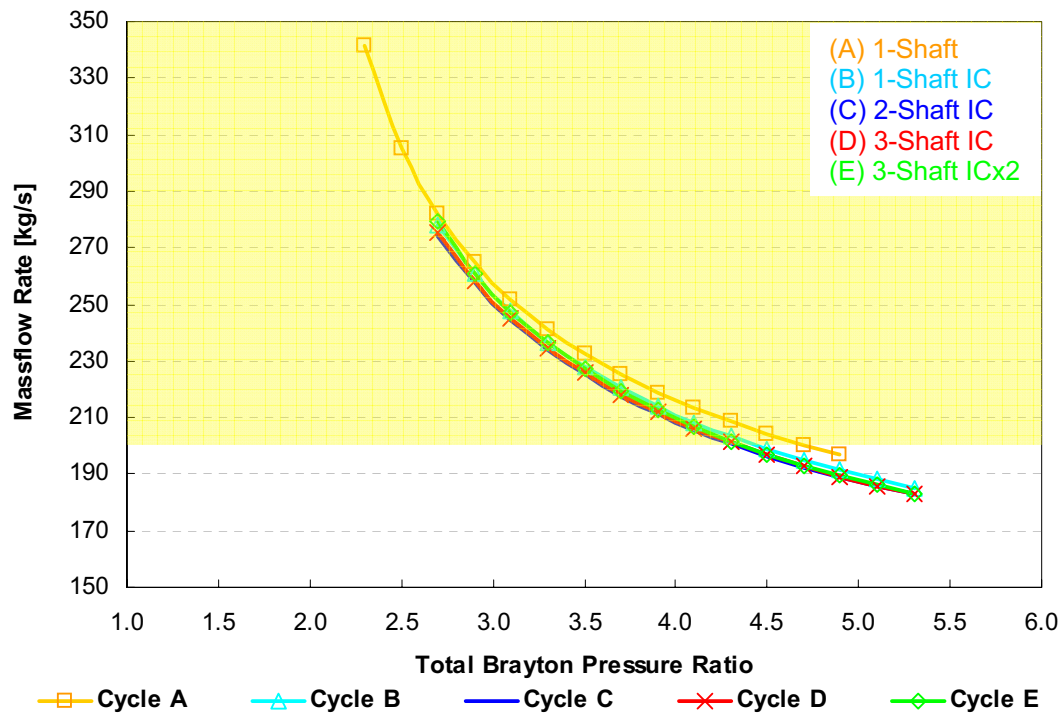


Figure 20.4.14: Direct Brayton Cycle Mass Flow Rate vs. Overall Pressure Ratio

Figure 20.4.15 presents the combined relative turbo machine size (all turbo machines in each cycle) as a function of the total pressure ratio. To obtain the relative turbo machine sizes, the turbo machine sizes are normalized relative to the smallest turbo machine size within the cycles. The multi-shaft designs (Cycles C, D and E) have lower gradients than the single-shaft designs (Cycles A and B). This is since the turbo machines, which are not constrained by the fixed power turbine speed, can be optimized with regards to power turbine size by increasing the machine rotational speeds, which results in smaller machines.

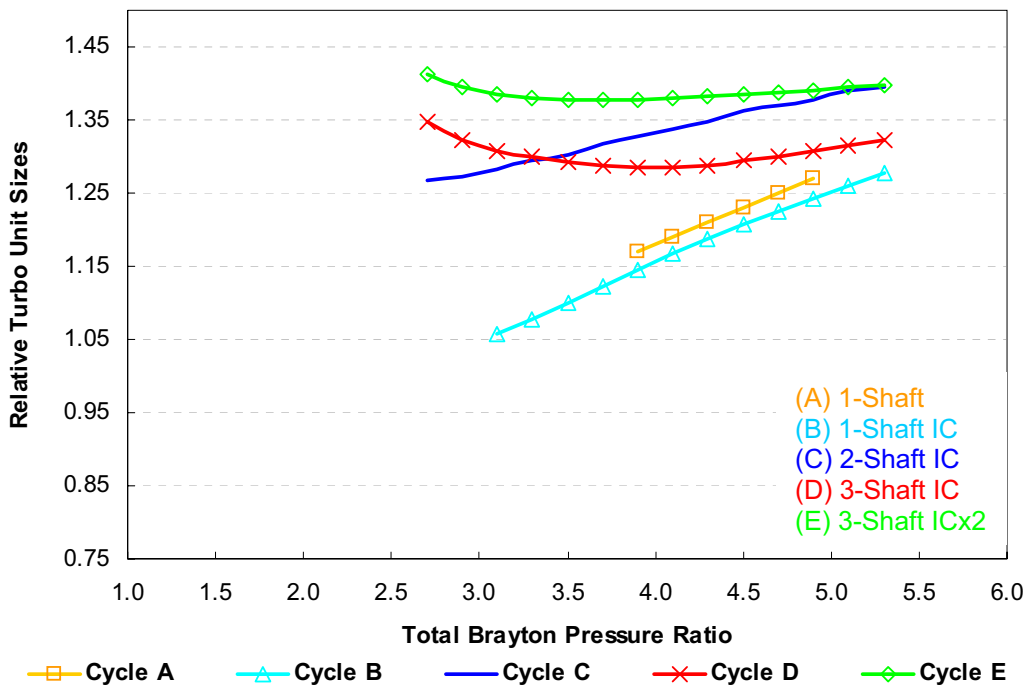


Figure 20.4.15: Direct Brayton Cycle Relative Turbo Unit Size vs. Overall Pressure Ratio

Figure 20.4.16 shows how the relative turbo machine size decreases as the power turbine rotational speed increases at a pressure ratio of 3.1. The turbine inlet temperature is fixed at 900°C. Figure 20.4.16 shows that the single-shaft designs only become smaller than the multi-shaft designs at power turbine speeds above ~78 rev/s (4680 rpm). Should the single-shaft design be chosen, it is advisable to employ a gearbox connecting it to the generator in order to allow operation at increased turbine speeds.

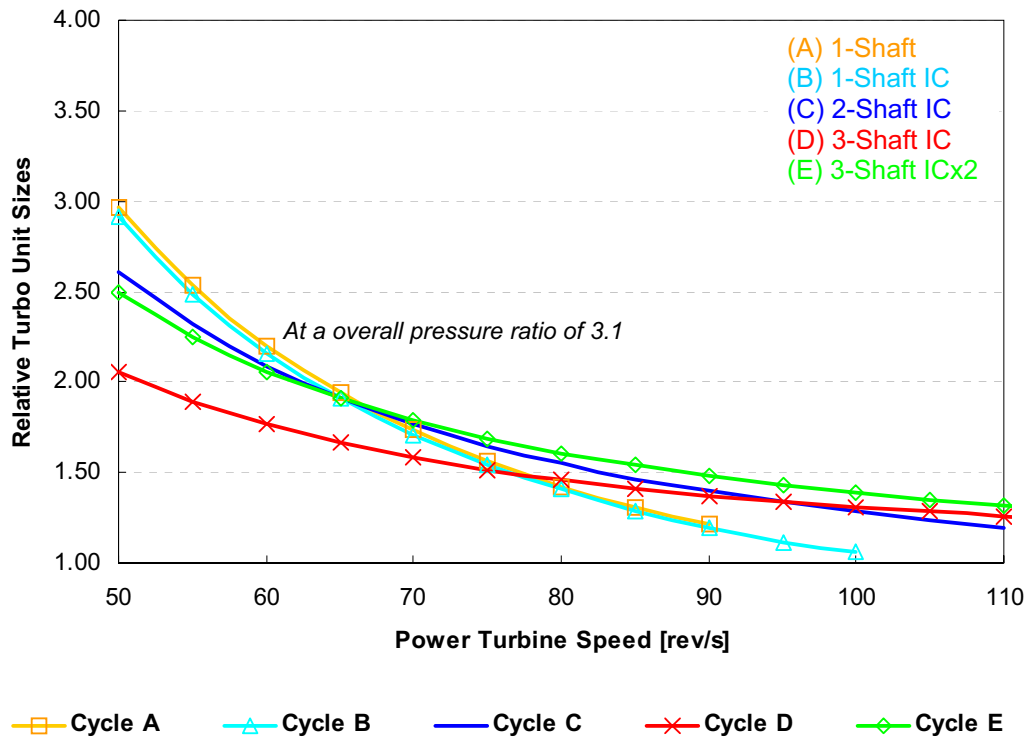


Figure 20.4.16: Direct Brayton Cycle Relative Turbo Unit Size vs. Power Turbine Speed

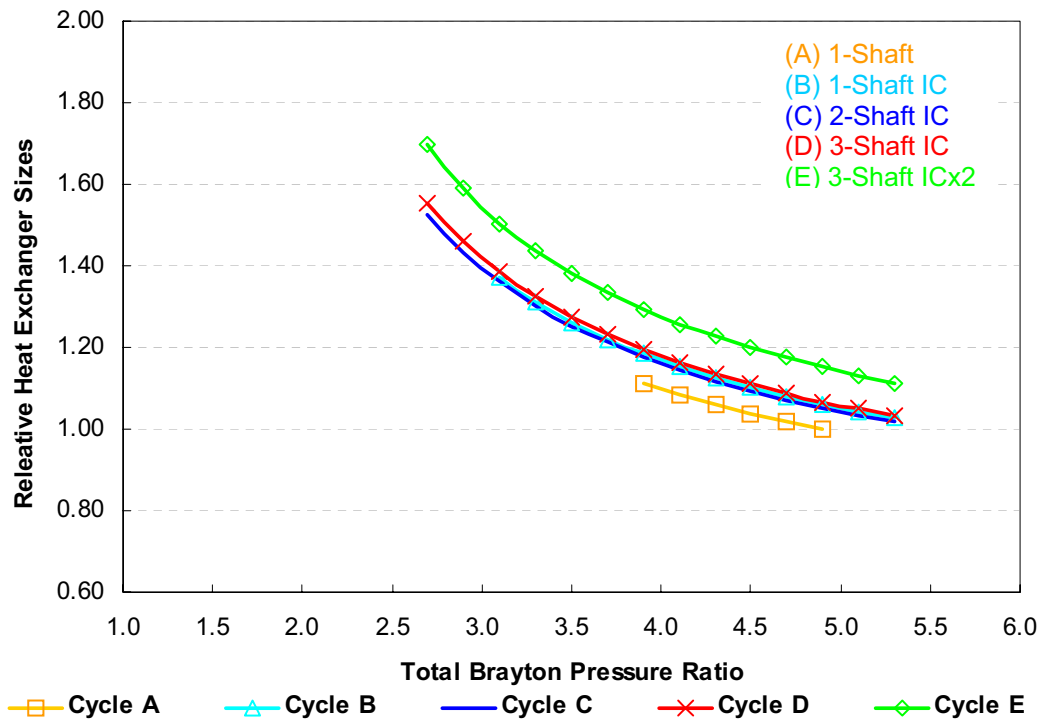


Figure 20.4.17: Direct Brayton Cycle Relative Heat Exchanger Size vs. Overall Pressure Ratio

Figure 20.4.17 shows the total heat exchanger area as a function of pressure ratio for each cycle. Since both the heat exchanger effectiveness and the heat transfer coefficient (U) are fixed, the heat transfer area of each heat exchanger is only a function of its mass flow rate. The mass flow rate decreases as the pressure ratio increases and therefore the size of the heat exchangers steadily decreases as well. The relative sizes of the heat exchangers are the same for the single-, two- and three-shaft inter-cooled Brayton cycles (B, C, D) because their mass flows are the same at each pressure ratio and the same number of heat exchangers are employed. The relative heat exchanger size of Cycle E is the largest of the direct cycles, due to the two-step inter-cooling. Cycle A has the smallest relative heat exchanger size of the direct cycles, since there is no inter-cooler present.

20.4.2.2.2 Brayton Cycle Selection

The Brayton cycles are compared against each other in terms of the following criteria:

- Performance (medium importance).
- Combined component size (low importance).
- Technical readiness (high importance).

Considering the above-mentioned results, it can be seen that the single-shaft design with inter-cooling (Cycle B) has the highest net cycle efficiency, as well as the lowest combined turbo unit size. Cycle B also has an advantage in terms of technical readiness over the other Brayton cycle configurations, since Cycle B represents the PBMR DPP design. Cycle B is selected as the representative Brayton cycle for further comparisons.

However, it should be noted that none of the Brayton cycles are able to operate at their maximum efficiencies within the reactor design envelope at 500MWt. The mass flow rate of all the Brayton cycles is larger than the maximum allowable mass flow of 200 kg/s at a reactor pressure level of 9 MPa.

20.4.2.2.3 Gas Turbine Combined Cycles

This section presents the results obtained for the GTCCs. Figure 20.4.18 shows the T-s diagram of Cycle J. The diagram illustrates the fit between the Rankine- and Brayton cycle sections of a GTCC. The T-s diagrams of the other GTCC configurations under investigation are presented in subsequent sections.

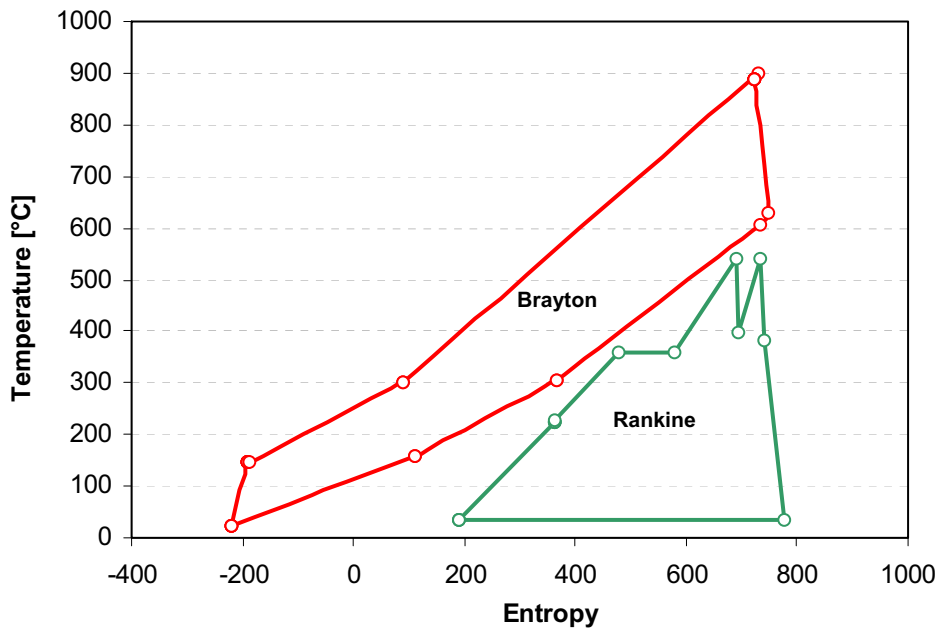


Figure 20.4.18: T-S Diagram of Cycle J

Figure 20.4.19 presents the net cycle efficiency as a function of the Brayton-section total pressure ratio. The high efficiencies of the GTCCs are attributed to the fact that the GTCCs reject heat at a lower cycle temperature in the condenser, whereas the Brayton cycles reject heat at higher average temperatures in the inter-cooler and pre-cooler.

It can be seen from Figure 20.4.19 that Cycle H has the highest net cycle efficiency. The difference in net cycle efficiency between Cycle G and Cycle J is reasonably small, since Cycles G and J have similar configurations and have been optimized through the use of pre-heating to utilize most of the waste heat.

The working point for Cycle H is at a pressure ratio of ~1.9, for Cycle G at ~2.4 and for Cycle J at ~2.2. These working points were chosen to correspond with the highest net cycle efficiency.

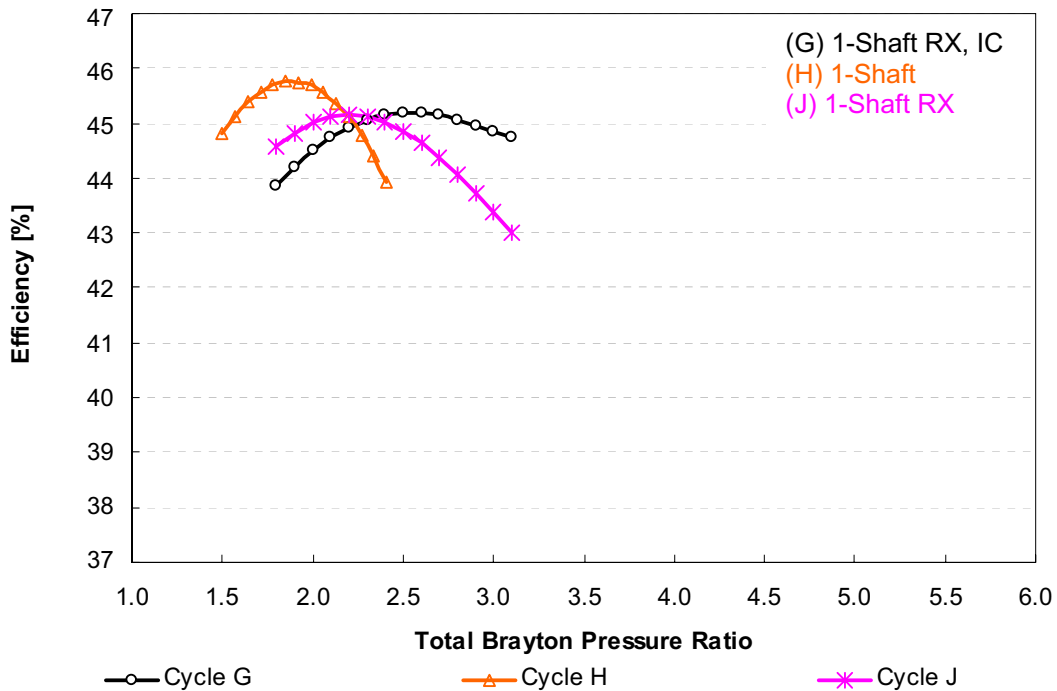


Figure 20.4.19: Direct GTCC Net Efficiency vs. Total Brayton Cycle Pressure Ratio

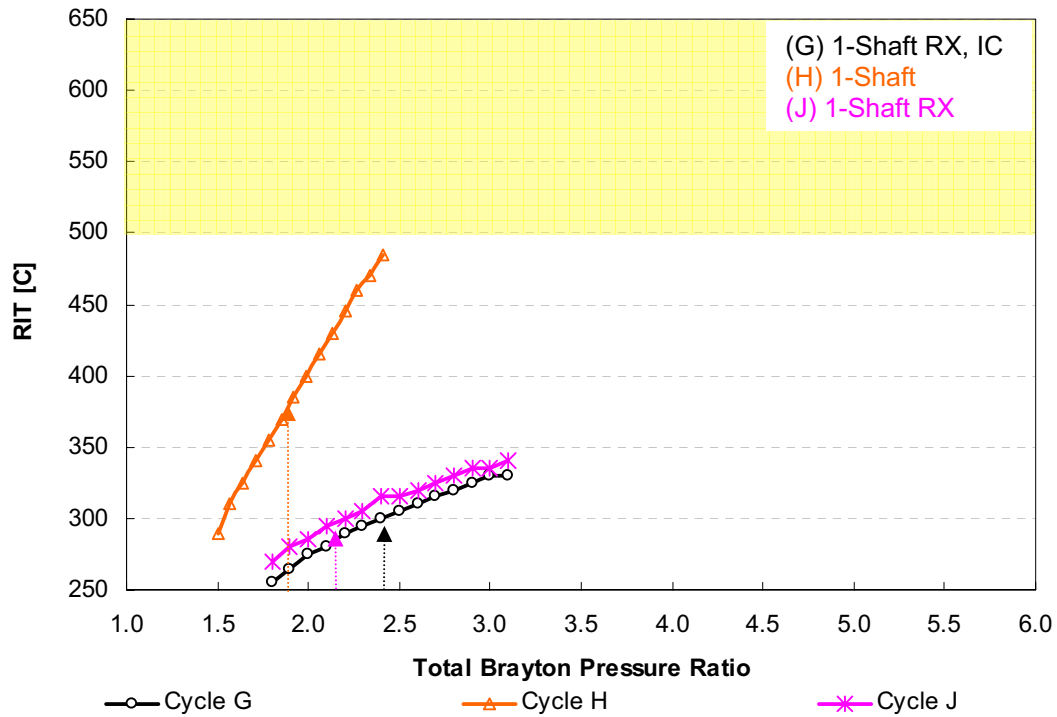


Figure 20.4.20: Direct GTCC RIT vs. Overall Brayton Pressure Ratio

Figure 20.4.20 and Figure 20.4.21 present the RIT and mass flow as a function of total Brayton-section pressure ratio. The addition of the Steam Generator for the GTCCs results in favorable lower RITs. From Figure 20.4.20, it can be seen that all the GTCCs are able to operate at their maximum cycle efficiencies within the RIT limitations of between 280°C and 500°C. It can be seen from Figure 20.4.21 that the mass flow rates of the GTCCs at their different working points are well within the reactor mass flow design envelope.

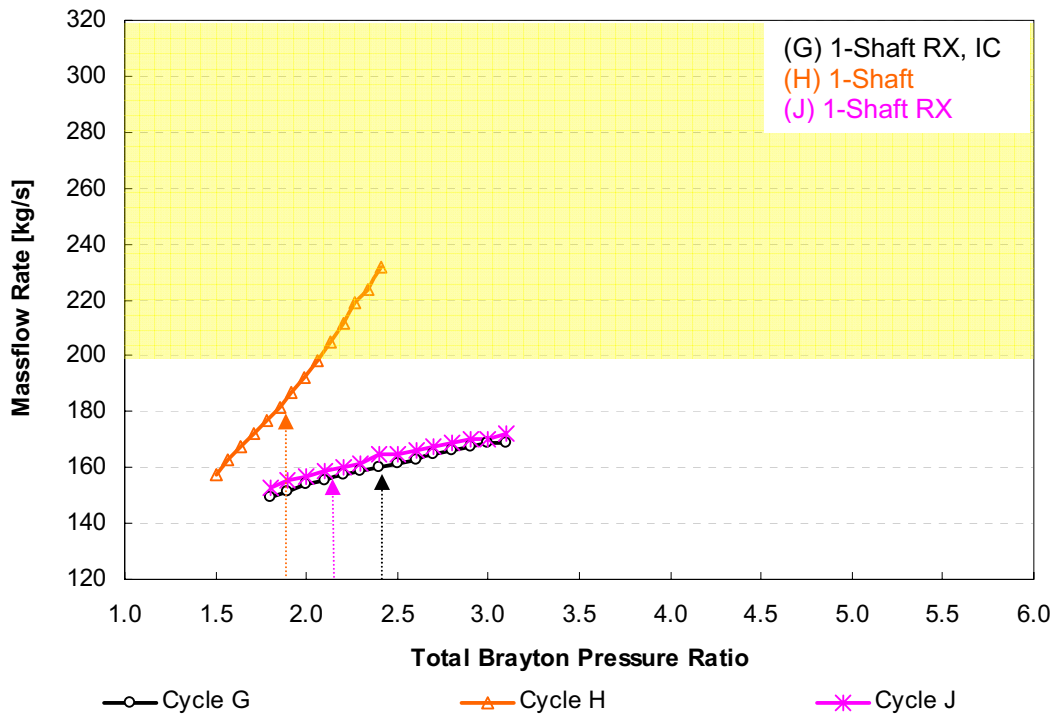


Figure 20.4.21: Direct GTCC Mass Flow Rate vs. Overall Brayton Pressure Ratio

Figure 20.4.22 presents the relative turbo unit size as a function of the total Brayton pressure ratio. To obtain the relative turbo machine sizes, the turbo machine sizes are normalized relative to the smallest turbo machine size within the cycles. The turbo machines of the GTCC are significantly smaller than the Brayton cycle machines due to the lower mass flows. Cycles H and J also have one less compressor than does Cycle G. The gradients of these cycles are similar, since all are single-shaft cycles.

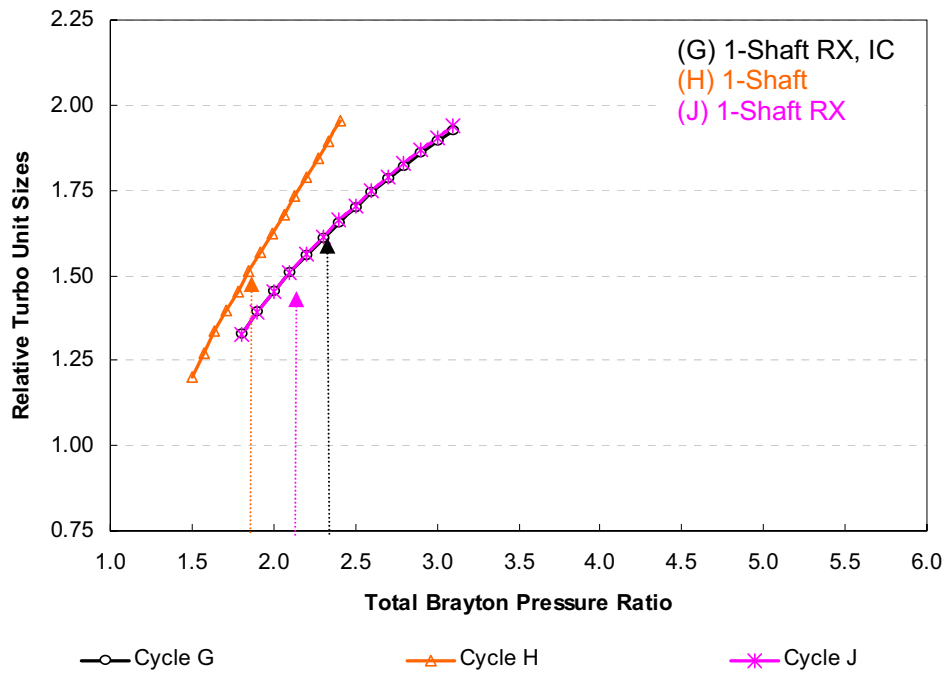


Figure 20.4.22: Direct GTCC Relative Turbo Unit Size vs. Overall Brayton Pressure Ratio

Figure 20.4.23 presents the relative heat exchanger size as a function of the total Brayton pressure ratio. Cycle H has no heat exchangers included in the Brayton cycle section. The relative size of the heat exchangers of Cycle G is larger than those of Cycle J. However, the heat exchangers of the GTCCs are relatively small compared to the Brayton cycle heat exchangers as a result of the reduced mass flows.

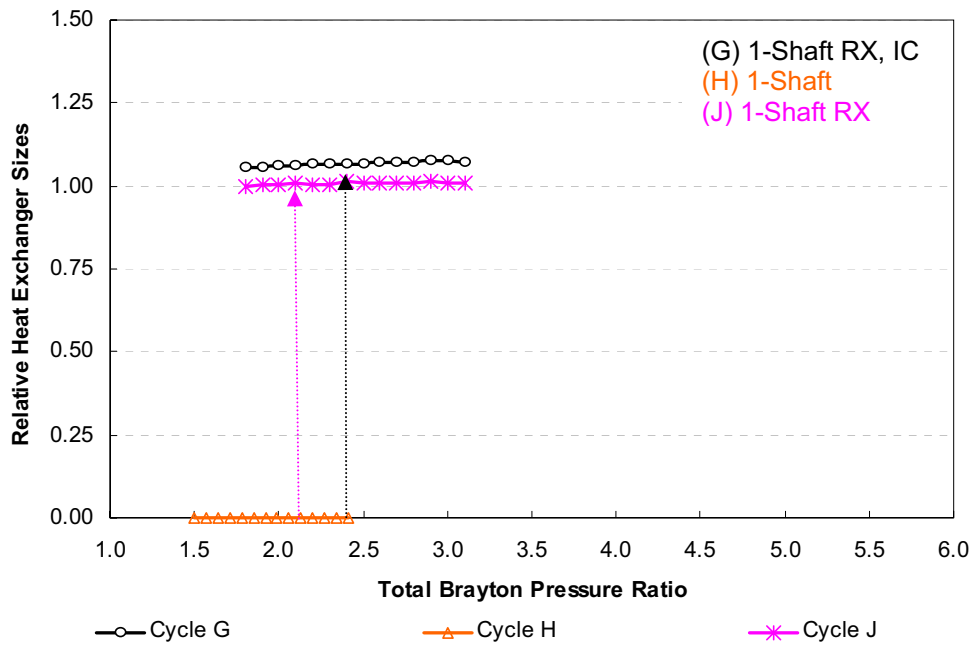


Figure 20.4.23: Direct GTCC Relative Heat Exchanger Size vs. Overall Brayton Pressure Ratio

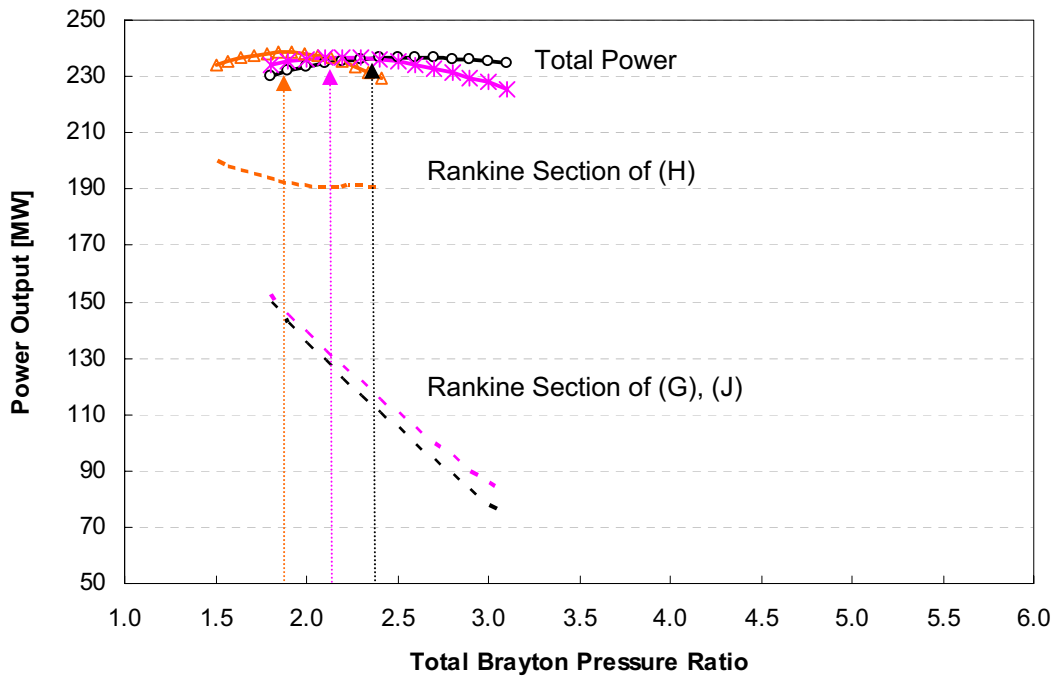


Figure 20.4.24: Thermal Power Output vs. Pressure Ratio for Brayton Cycles and GTCCs

Figure 20.4.24 presents the thermal work output as a function of total Brayton pressure ratio. The solid lines refer to the total thermal work output and the dotted lines refer to the thermal Rankine cycle work output. For Cycle G and Cycle J, it can be seen that only approximately 50% of the total thermal work output at the design point is produced by the steam plant. For Cycle H it can be seen that almost 80% of the total thermal work output is produced by the steam plant.

20.4.2.2.4 Gas Turbine Combined Cycle Selection

Cycle H has the highest net cycle efficiency (45.8%) of the GTCCs. However, the net cycle efficiencies of Cycle G and Cycle J are reasonably similar at 45.2% and 45.1%, respectively. Hence, only a marginal difference exists among the various GTCC efficiencies. Furthermore, note that all the GTCC configurations are able to operate at their maximum efficiency while staying within the reactor design envelope in terms of RIT and mass flow.

Since the performance of Cycle G and Cycle J is very similar, alternative criteria have to be considered to differentiate between the two. The GTCCs are compared against each other in terms of the following criteria:

- Performance (low importance).
- Combined component size (medium importance).
- Technology readiness (high importance).

In terms of performance, Cycle G has a slightly higher net cycle efficiency than Cycle J. Cycle G requires an additional compressor as well as an additional heat exchanger. These additional components marginally increase the complexity and combined component size (cost) of Cycle G compared to Cycle J and, hence, Cycle J is preferred over Cycle G.

Although Cycle H has a higher net cycle efficiency and fewer heat exchangers than Cycle J, Cycle J is preferred over Cycle H. In terms of technology maturity and readiness, Cycle J has the following advantages over Cycle H:

- Cycle J builds on the PBMR DPP Brayton cycle design with its turbo machines operating at similar conditions.
- Cycle H requires a new helium turbo machine design since the inlet temperature to the compressor is $\sim 200^{\circ}\text{C}$ (compared to $\sim 23^{\circ}$ for the PBMR DPP and Cycle J). Cycle H, therefore, requires additional cooling flow to cool down the turbo machine blades, which should result in a reduced net cycle efficiency (which is not accounted for by this study).

Cycle J is selected as the representative GTCC. It is perceived as lower risk, due to known Brayton turbo machinery that builds on the PBMR DPP design.

20.4.2.2.5 Rankine Cycle

The net cycle efficiency of the representative Rankine cycle (Cycle K) coupled directly to the PBMR was calculated as 41.2%. The RIT is 300°C with a mass flow rate of 160 kg/s in the primary loop. The steam generator has an inlet temperature of 900°C on the primary side, with a maximum steam temperature of 540°C on the secondary side, which utilizes reheat and regenerative heating.

Although the cycle efficiency appears high, one must bear in mind that conventional coal-fired steam plants operating at 540°C achieve net cycle efficiencies of between 33-37%. Up to 3% of the net cycle efficiency is lost due to furnace/boiler losses, which is equivalent to the reactor losses. Furthermore, the Rankine house load is scaled from existing coal-fire steam plants and is calculated as a percentage of power output which excludes all the systems required by coal plants.

Since only one Rankine cycle configuration is evaluated, Cycle K defaults as the representative Rankine cycle for further comparison.

20.4.2.3 General Results

20.4.2.3.1 Direct vs. Indirect

As mentioned previously, the influence of a direct vs. indirect cycle on the cycle efficiency is evaluated for two representative cycles from the Brayton cycle and Rankine cycle groups. One cycle from each of the different groups was randomly selected to determine the typical influence that an indirect cycle configuration would have on the cycle performance. For the Brayton cycles, GTCCs, and the Rankine cycles, Cycle B, Cycle H and Cycle K were chosen respectively. Figure 20.4.25 shows the indirect cycles under investigation. An approach temperature of 50°C was assumed for the intermediate heat exchanger (IHX) and helium was chosen as the primary and secondary heat transfer fluid.

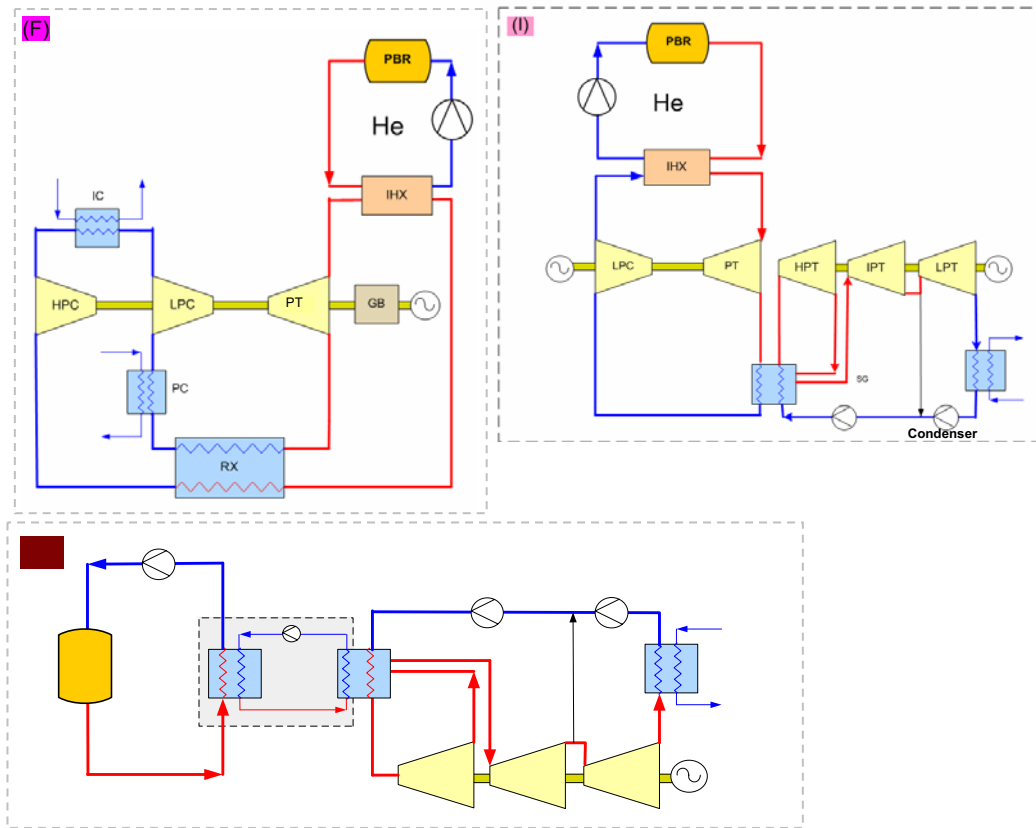


Figure 20.4.25: Indirect Cycle Configurations

- (F) Single-shaft indirect Brayton cycle with inter-cooling (Indirect version of Cycle B),
- (I) Single-shaft indirect GTCC without inter-cooling (Indirect version of Cycle H),
- (L) Indirect Rankine cycle (Indirect version of Cycle K).

Figure 20.4.26 compares the net cycle efficiencies of the direct cycles with the indirect cycles. It can be seen that the indirect Brayton cycle (Cycle F) has a net cycle efficiency of ~4% less than the equivalent direct Brayton cycle. The indirect GTCC (Cycle I) and the indirect Rankine cycle (Cycle L) are ~2% less efficient than the equivalent direct GTCC and Rankine cycle. The main reasons for the decrease in net cycle efficiency for the Brayton cycle and GTCC are the lower turbine inlet temperature caused by the drop in temperature over the IHX, together with the additional blower power required to circulate the primary fluid through the IHX. The blower requires additional power for circulation since the compressor efficiency is assumed to be 89% whereas the blower efficiency is assumed to be 80%. In the direct cycle, the compressor overcomes the pressure losses through the reactor and, for the indirect cycle, the blower overcomes the pressure losses through the reactor. The lower blower efficiency implies that a larger blower than compressor is required to overcome the reactor losses.

However, the decrease in net cycle efficiency suffered by the indirect Rankine cycle is only a result of the additional blower power required to circulate the helium through the IHX. The temperature drop across the IHX does not influence the efficiency of the Rankine cycle, since the maximum steam temperature remains the same. In the GTCC, part of the efficiency lost in the Brayton cycle, due to reduced turbine inlet temperature, is recovered in the Rankine section. In a configuration where the Rankine cycle is combined with a hydrogen production plant, an indirect coupling will be more beneficial from a safety point of view as the process coupling heat exchanger will then not be in the primary loop.

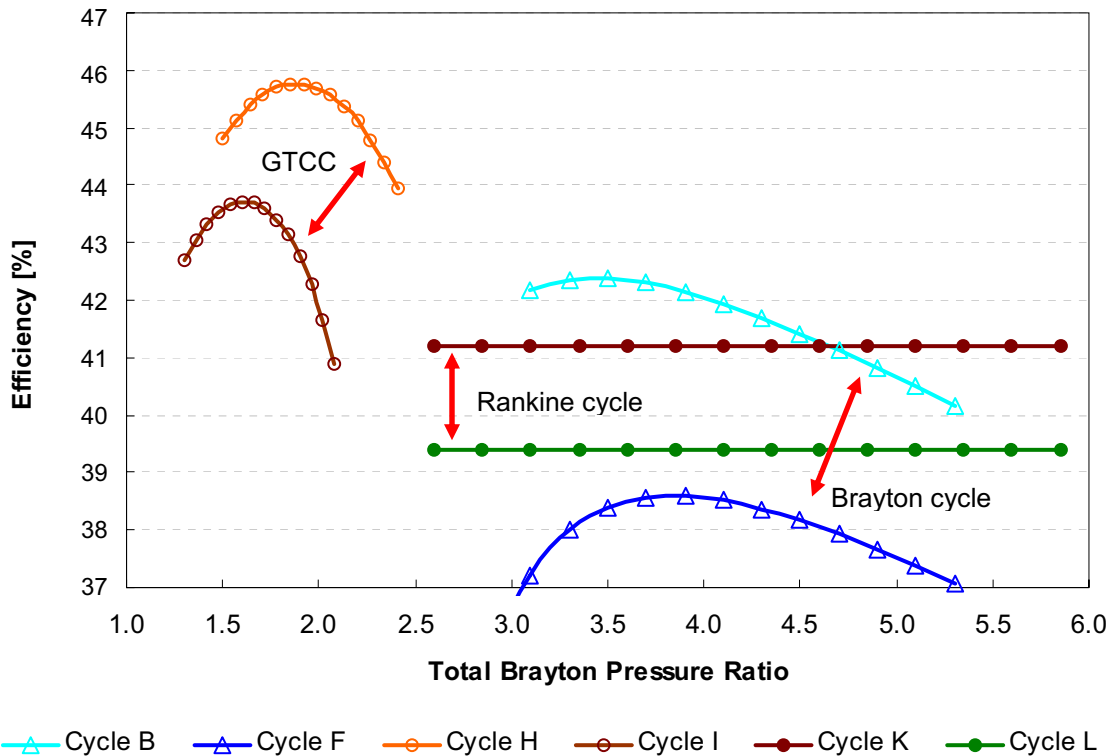


Figure 20.4.26: Direct vs. Indirect Cycle Net Efficiency vs. Total Brayton Cycle Pressure Ratio

20.4.2.3.2 Series vs. Parallel

In this section, the influence of the hydrogen production plant on the cycle efficiency of the PCS is investigated. Since the hydrogen production plant requires high-temperature heat, it can be coupled to the outlet of the reactor either in series or in parallel with the PCS. Figure 20.4.27 shows an example of a hydrogen production plant coupled in series and parallel to the reference Brayton cycle (Cycle B). Cycle B was chosen to illustrate the influence of a series vs. parallel process coupling on the performance of the PCS at uniform steady state operation at design conditions. Further detail on series and parallel coupling considerations and off design operations can be found in Special Study 20.3 [2].

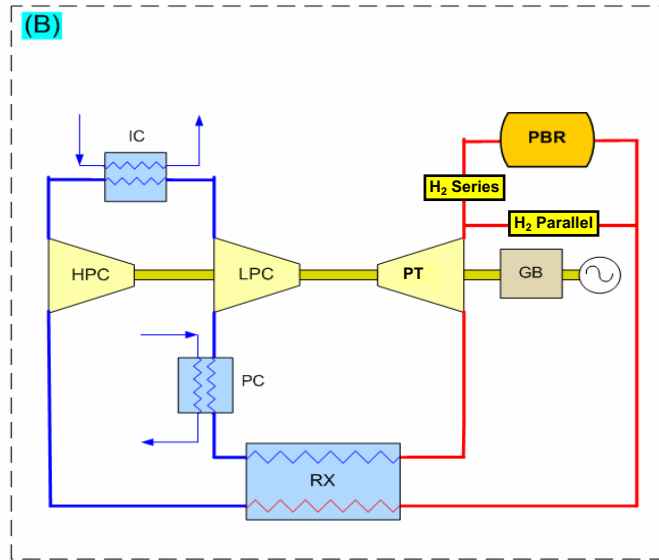


Figure 20.4.27: Series vs. Parallel Hydrogen Production Plant Configuration for Cycle B

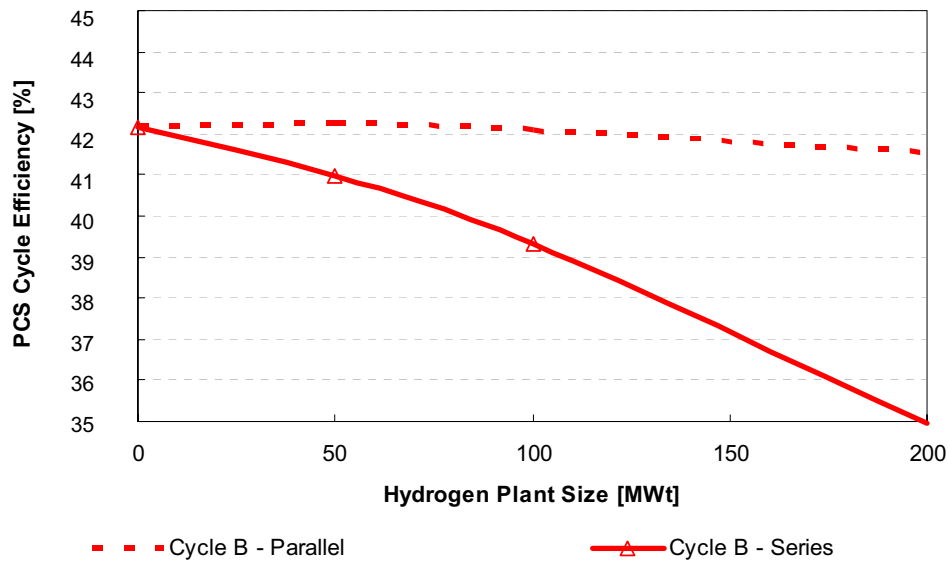


Figure 20.4.28: Cycle B PCS Cycle Efficiency for a Series and Parallel PCHX Coupling vs. Hydrogen Production Plant Size

Figure 20.4.28 shows the efficiency of the PCS of Cycle B as a function of the hydrogen production plant size for a series and parallel process coupling, respectively. Note that the Brayton cycle PCS is re-optimized for the different hydrogen production plant sizes along the curve. Note also that neither additional pressure losses through the IHX, the additional blower house load for a parallel configuration nor the hydrogen plant house load were incorporated in

calculating the cycle efficiency. It can be seen from Figure 20.4.28 that the efficiency of the Brayton cycle PCS decreases as the size of the hydrogen production plant increases for the series and the parallel configurations. However, the efficiency decrease suffered by the series configuration is more sensitive to an increase in the hydrogen production plant size than the parallel configuration. This is the result of lower turbine inlet temperatures. For the parallel configuration, the efficiency decrease is less sensitive to an increase in the hydrogen production plant size, since the turbine inlet temperature does not decrease. However, the parallel configuration requires an additional blower to circulate the heat transfer fluid through the PCHX. The efficiency decrease shown by Figure 20.4.28 for the parallel configuration is expected to be slightly more than indicated, since the additional blower power requirement, as well as the effect of mixing, is not taken into account here.

The parallel configuration also presents some design challenges. The parallel configuration requires an additional blower, at a high temperature, that has to be controlled and attention needs to be given to the mixing of fluid at the PCHX outlet with the cooler flow from the recuperator.

It is expected that the influence of a series coupled hydrogen production plant on the efficiency of a GTCC PCS will be similar for the Brayton cycle PCS. However, it is expected that the Rankine section of a GTCC will tend to level out the efficiency decrease of the Brayton section up to a certain hydrogen production plant size where after the Brayton section will influence the GTCC PCS efficiency significantly. The influence of the PCHX size is therefore not shown for the GTCC configurations.

Figure 20.4.29 shows the PCS cycle efficiency of a Brayton cycle (Cycle B) and a Rankine cycle (Cycle L) as a function of the hydrogen production plant size, respectively. The PCHX is coupled in series with Cycle B and Cycle L and both cycles are re-optimized for the different hydrogen production plant sizes (which implies that the Brayton cycle pressure ratio differs at each point on the curve and, hence, cannot be later compared with Figure 20.4.31). It can be seen from the figure that the PCS cycle efficiency of the Brayton cycle is more sensitive to an increase in the size of the hydrogen production plant than the Rankine PCS cycle efficiency. This is a result of the decrease in turbine inlet temperature for the Brayton cycle, which influences the PCS cycle efficiency negatively. The Rankine PCS does not experience a significant decrease in cycle efficiency since the steam generator outlet temperature is not affected. However, since the primary and secondary blower house load remains constant with an increase in hydrogen production plant size (decrease in Rankine cycle power output) the net cycle efficiency of the Rankine cycle is slightly penalized.

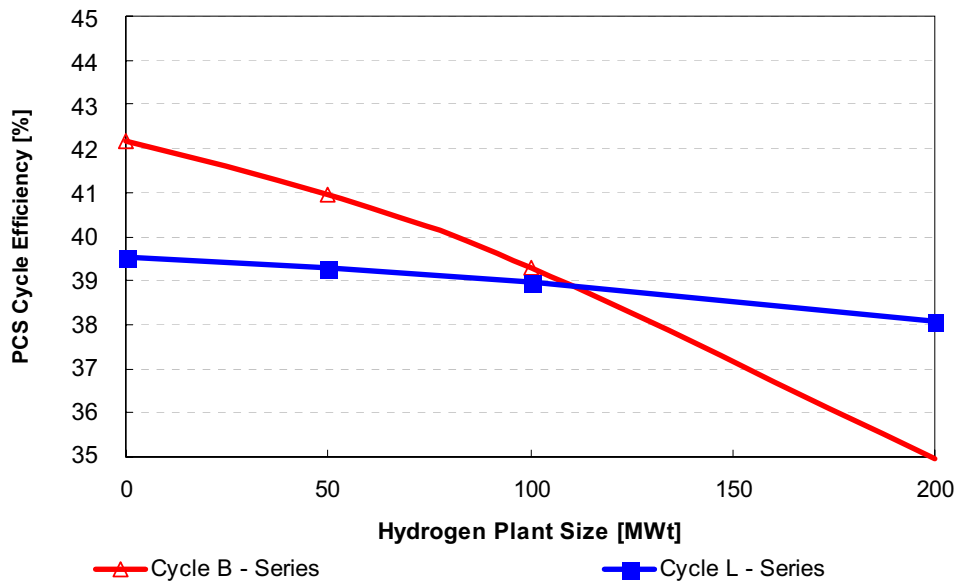


Figure 20.4.29: Cycle B and Cycle L PCS Net Cycle Efficiency for a Series PCHX Coupling vs. Hydrogen Production Plant Size

20.4.2.3.3 Horizontal vs. Vertical Shaft and Bearing Arrangements

Various shaft arrangements, the number of shafts and bearing types have been explored for HTGR designs. General Atomics’ GT-MHR design incorporates a single shaft, vertical design with electro magnetic bearings (EMBs). The PBMR earlier designs utilized a three shaft, vertical design with EMBs and then simplified the design to a single shaft, horizontal design [3].

In the PBMR Three-Shaft vertical arrangement, each shaft was operating at a different optimized speed (6000/7000/3000 rpm). EMBs were used on the high and low pressure units and a dry gas seal (DGS) with oil thrust bearing was used on the Power Turbine Generator unit with a radial EMB.

In the current PBMR Single-Shaft horizontal arrangement, the shaft is operating at 6000 rpm with a reduction gearbox to 3000 rpm for the generator. A gearbox with reduction to 3600 rpm could also be used. DGSs and oil bearings are used on the entire shaft. The reduced risk Single-Shaft arrangement was made possible due to developments in the areas of DGSs and high capacity gearbox technologies.

The Single-Shaft horizontal arrangement has the following advantages with respect to the prior Three-Shaft vertical arrangement:

- The horizontal turbo machine layout is an improved seismic design.
- Eliminates EMB penetrations (~1000) of the pressure boundary.

- Elimination of potentially unstable Power Turbine Generator operations during trip and subsequent restart.
- Less complex control system is required.
- Easier to balance shaft thrust forces.
- No large resistor bank required to maintain load on trip.
- Elimination of the start-up blower system.
- Conversion from 50 to 60 Hz simplified through gearbox gear ratios.
- Improved maintenance very similar to combustion gas turbine systems.
- No special rotor balancing facilities required; conventional commissioning.
- Reduced cost of turbo machinery equipment.
- Significantly lower R&D required, i.e., reduced development risk.

20.4.2.3.4 Other

This section presents some general results obtained for the different cycle configurations. Figure 20.4.30 compares the net cycle efficiency of the direct cycle configurations as function of the Brayton cycle overall pressure ratio. As mentioned previously the GTCCs have the highest net cycle efficiency compared to the Brayton and Rankine cycles. It should be noted that the Rankine cycle (Cycle K) efficiency is not a function of the Brayton cycle overall pressure ratio, since Cycle K does not have a Brayton cycle section.

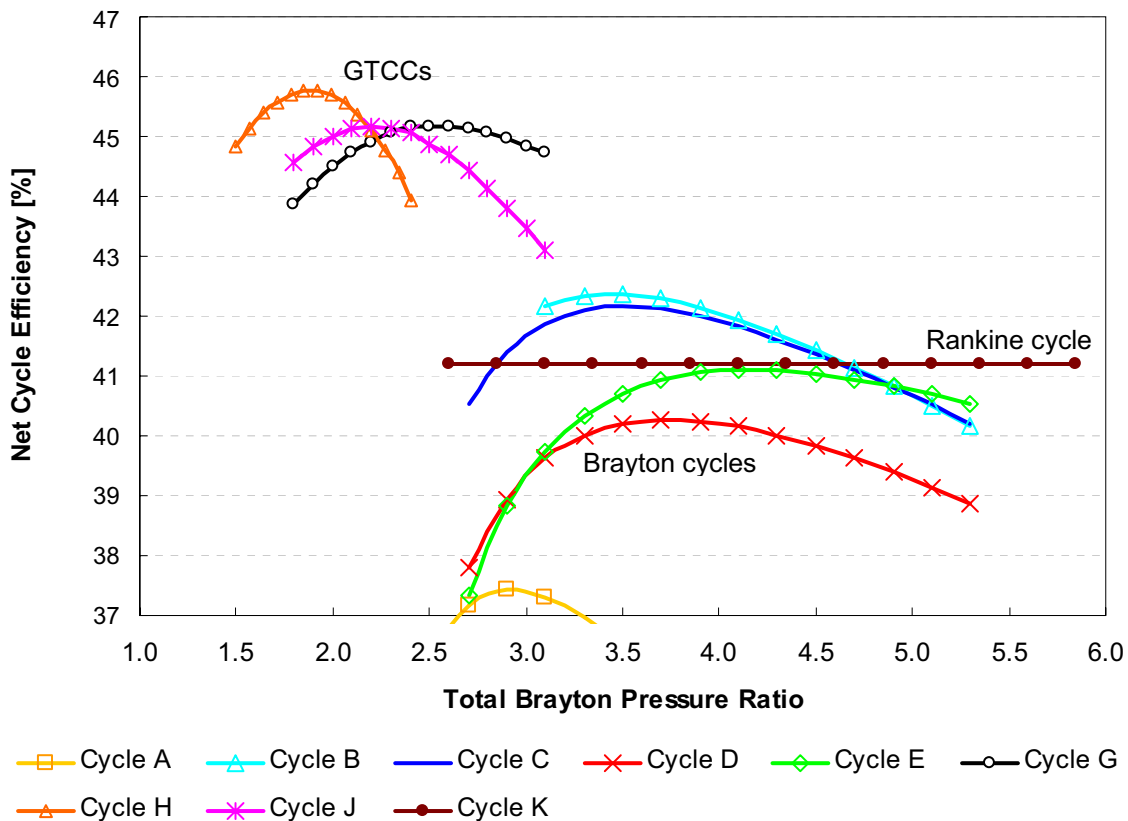


Figure 20.4.30: Net Cycle Efficiency vs. Brayton Overall Pressure Ratio

Figure 20.4.31 shows the influence of the net cycle efficiency as a function of the turbine inlet temperature. It is seen that the net cycle efficiencies of the representative Brayton cycle and GTCC increase as the turbine inlet temperature increases. However, the net cycle efficiency of the Rankine cycle decreases with an increase in temperature above ~900°C. This is since the steam generator outlet temperature remains the same regardless of the primary cycle maximum temperature. However, the size of the blower that circulates the helium through the steam generator increases, since the blower inlet temperature increases as the reactor outlet temperature increases (in order to stay within reactor temperature differential limitations) resulting in a reduced net cycle efficiency for the Rankine cycle configuration.

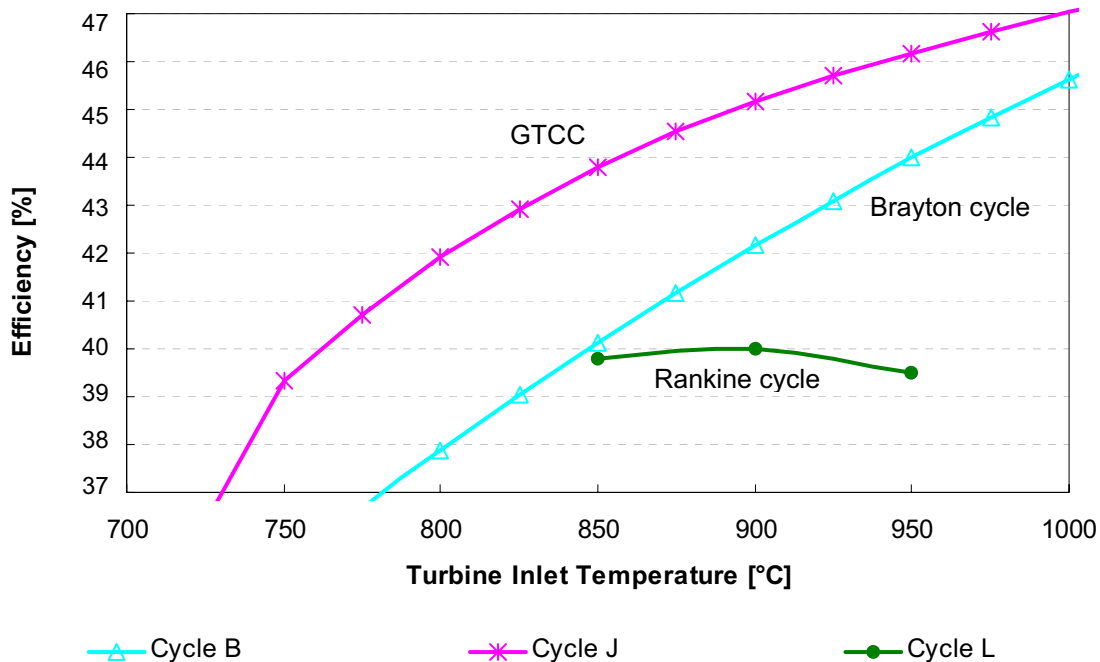


Figure 20.4.31: Net Cycle Efficiency vs. Turbine Inlet Temperature (Brayton Pressure Ratio Fixed at 3.1)

20.4.2.4 Design Point Parameters

This section presents the thermodynamic operating conditions of the reference Brayton cycle (Cycle B), GTCCs (Cycle J and Cycle H) and Rankine cycle (Cycle L). In the iterative process between this special study and the special study for the High Temperature Process Heat, Transfer and Transport, it was found that an indirect Rankine cycle (Cycle L) will be the best suited option for the NNGP. Therefore, Cycle L is evaluated in this section instead of Cycle K. The operating conditions include a T-s diagram of each cycle accompanied by the pressure at each component’s inlet and outlet. The different mass flows, heat exchanger duty and turbo machine power are also presented.

20.4.2.4.1 Brayton Cycle (Cycle B)

The optimum cycle efficiency of Cycle B, 42.3%, is achieved at an overall pressure ratio of approximately 3.2, as shown by Figure 20.4.12. The operating conditions shown below are, therefore, calculated for an overall pressure ratio of 3.2 (identified design point). Figure 20.4.32 shows the numbering structure used for Cycle B on which the presented temperatures and pressures are based.

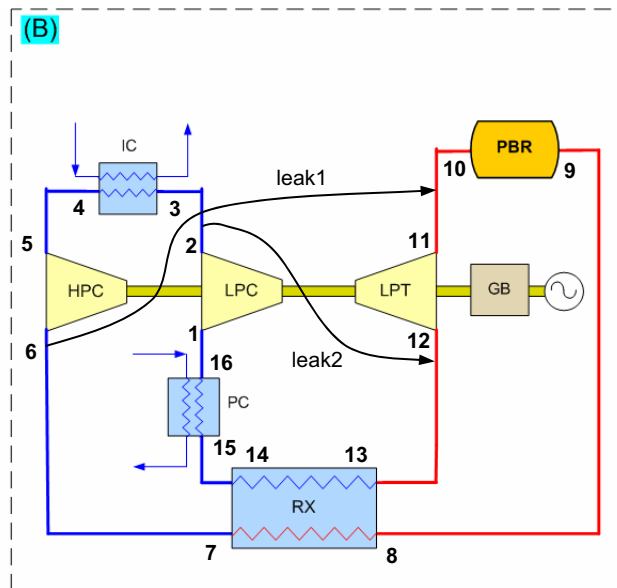


Figure 20.4.32: Numbering for Cycle B

Table 20.4.2 shows the operating pressures at the inlet and outlet of the different components.

Table 20.4.2: Operating Pressure for Cycle B at the Design Point

Position	Pressure [kPa]	Position	Pressure [kPa]
1	2813	9	8713
2	5031	10	8179
3	4985	11	8162
4	4960	12	2917
5	4950	13	2852
6	8855	14	2838
7	8774	15	2832
8	8730	16	2818

Figure 20.4.33 presents a T-s diagram for the design point operating conditions of Cycle B.

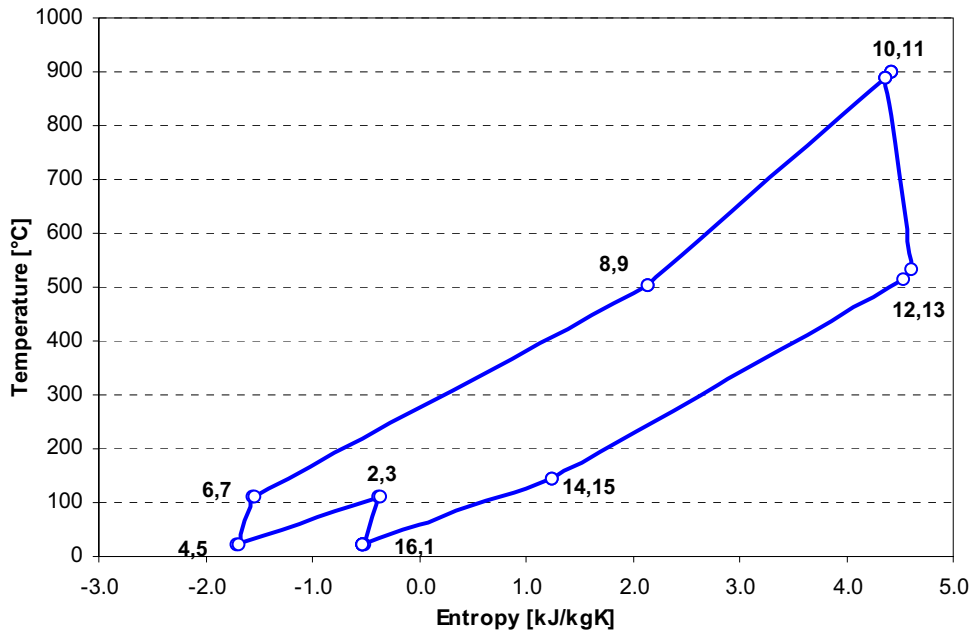


Figure 20.4.33: T-S Diagram for the Design Point Operating Conditions of Cycle B

The total mass flow through the system is 256 kg/s with a leak flow draw-off of 10.8 kg/s after the LPC and a further draw-off of 3.6 kg/s after the HPC. Since the leak flows enter the cycle before and after the LPT, a mass flow of 242 kg/s is achieved through the reactor. The heat exchanger duties and turbo machine loads at the design point of Cycle B are shown in Table 20.4.3.

Table 20.4.3: Cycle B Heat Exchanger Duty and Turbo Machine Load for Cycle B

Component	Duty/Load [MW]
Pre-cooler	161
Inter-cooler	111
Recuperator	494
LPC	116
HPC	111
LPT	455
Net power output	212 MW_e

The net power output (grid power) as presented in Table 20.4.3 is calculated by considering the respective house loads and generator efficiencies. The following equations are used to calculate net grid power output for the Brayton cycles:

$$T_{Excess\ Power} = (T_{Fluidic\ Power} \times \eta_{mec}) - (HPC_{Fluidic\ Power} + LPC_{Fluidic\ Power}) \quad (1)$$

$$Grid\ Power = [(T_{Excess\ Power} \times \eta_{Gen}) - H_L] \times \eta_{TXGen} \quad (2)$$

With:	$T_{Excess\ Power}$	Turbine shaft excess power [MW]
	$T_{Fluidic\ Power}$	Turbine fluidic power [MW]
	η_{mec}	Mechanical efficiency (Assumed to be 0.991)
	$HPC_{Fluidic\ Power}$	High-pressure compressor fluidic power [MW]
	$LPC_{Fluidic\ Power}$	Low-pressure compressor fluidic power [MW]
	η_{Gen}	Generator efficiency (Assumed to be 0.985)
	H_L	House Load (Assumed to be 6.5 MWe)
	η_{TXGen}	Generator transformer efficiency (Assumed to be 0.99)
	$Grid\ Power$	The electrical power exported to the grid [MW]

20.4.2.4.2 Gas Turbine Combined Cycles (Cycle H, J)

This section presents the operating conditions of the reference GTCC cycle (Cycle J), as well as the operating conditions of Cycle H. It was decided to include Cycle H since it has the highest net cycle efficiency of the GTCC configurations under investigation.

Cycle H:

From Figure 20.4.19 it can be seen that Cycle H achieves its maximum cycle efficiency of 45.8% at an overall Brayton pressure ratio of approximately 1.9. The operating conditions of Cycle H (shown below) are, therefore, based on an overall Brayton pressure ratio of 1.9 (design point). Figure 20.4.34 shows the numbering structure used for the Brayton section, as well as the Rankine section of Cycle H.

Figure 20.4.35 presents a T-s diagram of Cycle H at the design point. The diagram presents the operating temperatures for the Brayton section as well as the Rankine section according to the above-mentioned numbering structure.

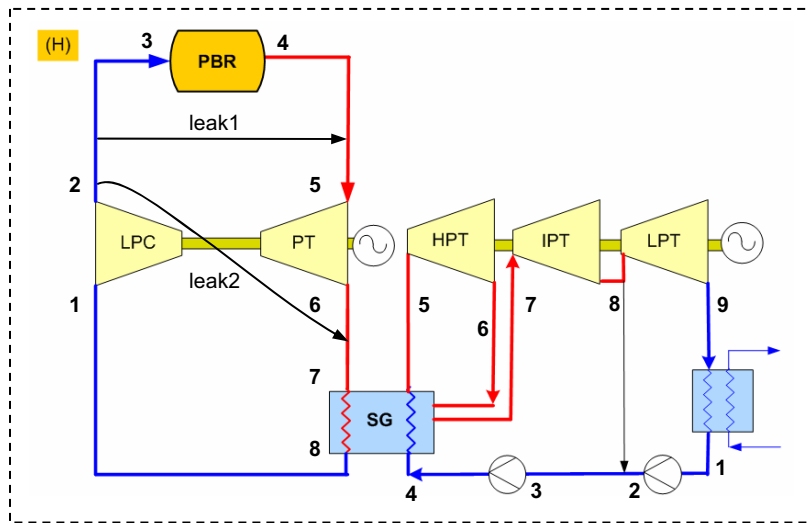


Figure 20.4.34: Numbering for Cycle H

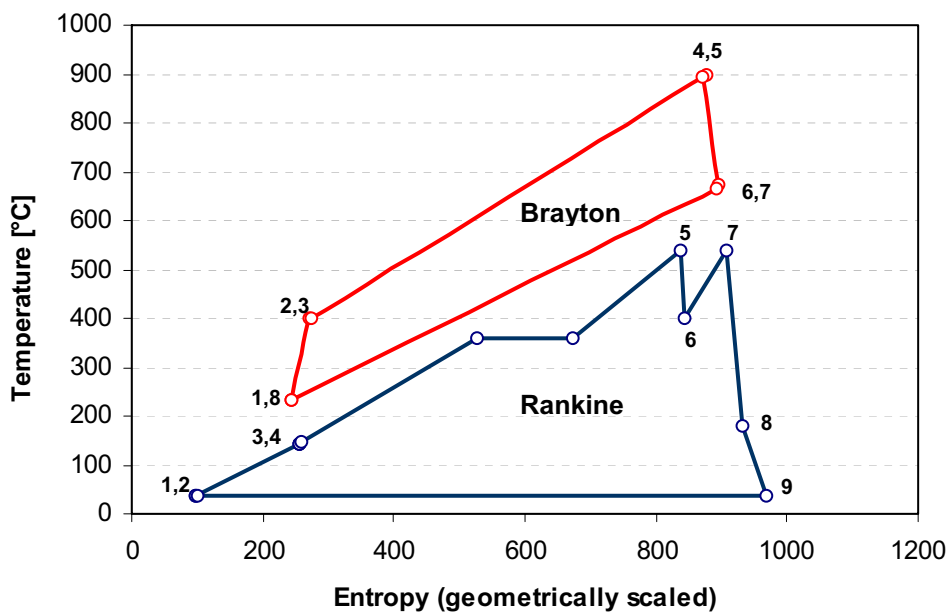


Figure 20.4.35: T-S Diagram for the Design Point Operating Conditions of Cycle H

Figure 20.4.36 presents the temperature in the steam generator as a function of heat transfer. The two lines on the graph represent the steam generator where the top line represents the Brayton side and the bottom line the Rankine side. This graph indicates how the Rankine cycle is custom-designed to exactly fit with the Brayton cycle, with the minimum allowable pinch temperature of 30°C achieved.

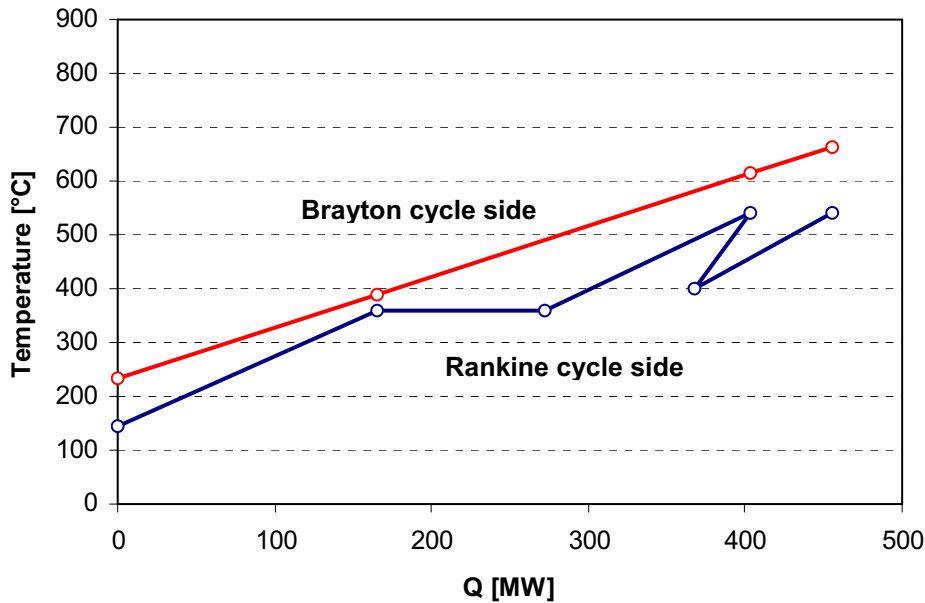


Figure 20.4.36: Heat Transfer vs. Temperature in Steam Generator

Table 20.4.4 shows the operating pressures at the inlet and outlet of the different components for the Brayton section and Rankine section of Cycle H, respectively.

Table 20.4.4: Operating Pressure for Cycle H at the Design Point

Position (Brayton)	Pressure [kPa]	Position (Rankine)	Pressure [kPa]
1	4739	1	6
2	9000	2	376
3	8953	3	376
4	8649	4	18557
5	8632	5	18000
6	4862	6	7292
7	4770	7	7073
8	4746	8	376
		9	6

The total mass flow through the Brayton section is 204 kg/s with a leak flow draw-off of 2.9 kg/s (leak1) after the LPC to cool the turbine inlet and a further draw-off of 8.6 kg/s also after the LPC (leak2) to cool the turbine outlet. A mass flow of 193 kg/s is achieved through the reactor. The total mass flow through the Rankine section is 146 kg/s with a bleed flow (between

point 8 and point 2) of 25 kg/s. The heat exchanger duties and turbo machine loads of the Brayton and Rankine sections of Cycle H are shown in Table 20.4.5.

Table 20.4.5: Cycle H Heat Exchanger Duty and Turbo Machine Load

Component (Brayton)	Duty/Load [MW]	Component (Rankine)	Duty/Load [MW]
LPC	176	SG	455
PT	221	Condenser	258
Net power	38	HPT	35
		IPT	100
		LPT	66
		Net power	191
		Pump 1	4
		Pump 2	0.06
Total net power output		229 MW_e	

The net power output for the Brayton cycle section of the GTCCs is calculated using Equation (1) and (2). The net power output for the Rankine cycle section is calculated by considering the Rankine house loads, pump loads and generator efficiencies. The following equations are used to calculate the net grid power output for the Rankine cycle sections of Cycles H and J:

$$T_{Excess\ Power} = (HPT_{Fluidic\ Power} + IPT_{Fluidic\ Power} + LPT_{Fluidic\ Power}) \tag{3}$$

$$Grid\ Power = (T_{Excess\ Power} - P_{pump1} - P_{pump2}) \times f_{HL} \times \eta_{Gen} \times \eta_{TXGen} \tag{4}$$

- With:
- f_{HL} House Load fraction (0.9915)
 - P_{pump1} Power required by Pump 1 [MW]
 - P_{pump2} Power required by Pump 2 [MW]
 - $HPT_{Fluidic\ Power}$ High-pressure steam turbine fluidic power [MW]
 - $IPT_{Fluidic\ Power}$ Intermediate-pressure steam turbine fluidic power [MW]
 - $LPT_{Fluidic\ Power}$ Low-pressure steam turbine fluidic power [MW]

Cycle J:

Cycle J has a maximum net cycle efficiency of 45.1% at an overall Brayton pressure ratio of 2.2 and the design point operating conditions of Cycle J (shown below) are based on this pressure ratio. Figure 20.4.37 shows the numbering structure used for the Brayton section as well as the Rankine section of Cycle J. The T-s diagram for Cycle J at the design point is shown in Figure 20.4.38. It can be seen from Figure 20.4.38 that the waste heat available before the LPC is utilized to pre-heat the Rankine cycle feed water resulting in increased net cycle efficiency.

The temperatures shown by the diagram correspond to the above-mentioned numbering structure.

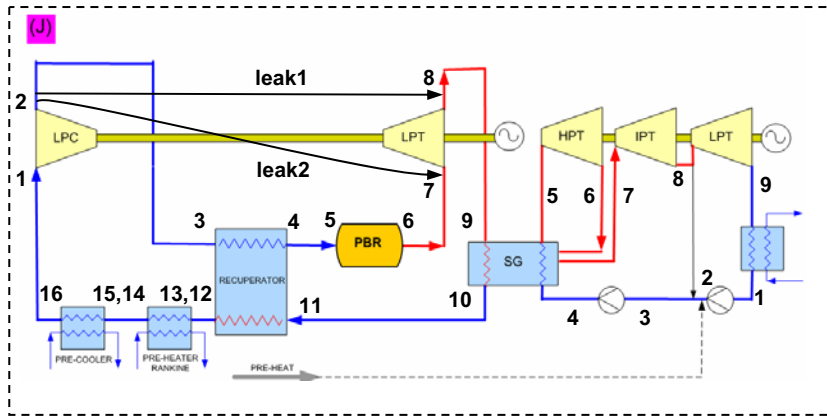


Figure 20.4.37: Numbering for Cycle J

Figure 20.4.39 presents the temperature in the steam generator as a function of heat transfer. The two lines on the graph represent the steam generator where the top line represents the Brayton side and the bottom line the Rankine side. The Rankine cycle is custom-designed to exactly fit the Brayton cycle, with the minimum allowable pinch temperature of 30°C not exceeded.

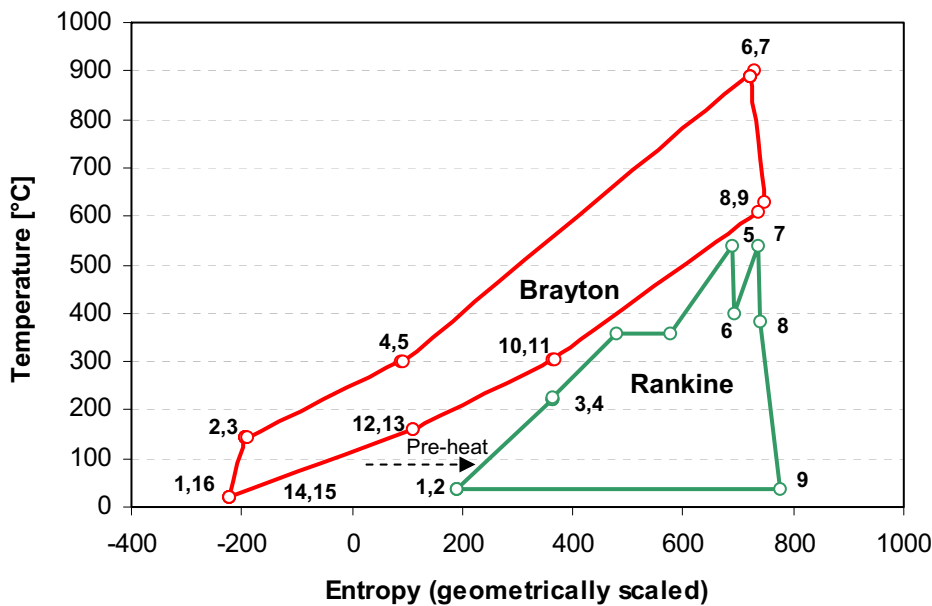


Figure 20.4.38: T-S Diagram for the Design Point Operating Conditions of Cycle J

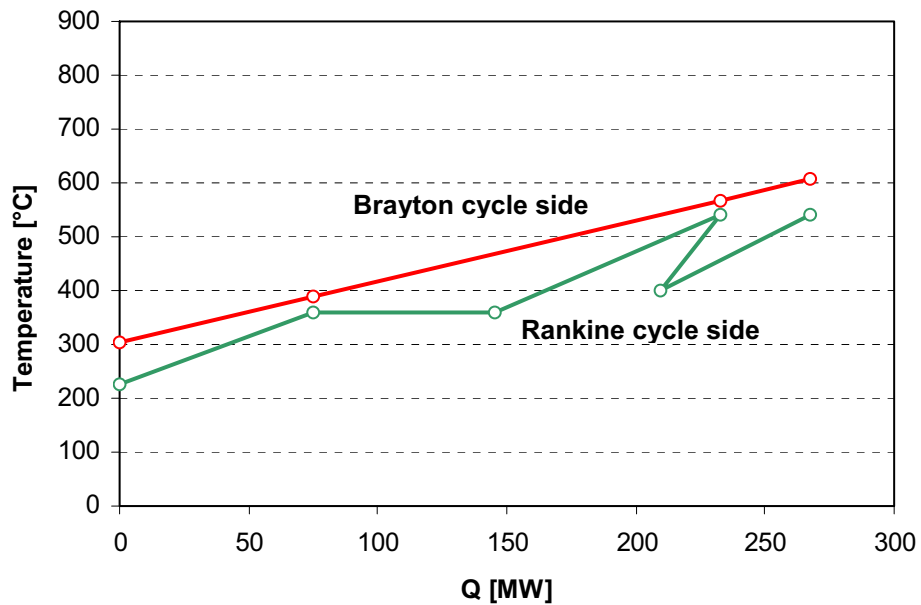


Figure 20.4.39: Heat Transfer vs. Temperature in Steam Generator

Table 20.4.6 shows the operating pressures at the inlet and outlet of the different components for the Brayton section and Rankine section of Cycle J, respectively.

Table 20.4.6: Operating Pressures for Cycle J at the Design Point

Position (Brayton)	Pressure [kPa]	Position (Rankine)	Pressure [kPa]
1	4091	1	6
2	9000	2	2450
3	8925	3	2450
4	8880	4	18557
5	8862	5	18000
6	8675	6	7292
7	8658	7	7100
8	8658	8	2500
9	8658	9	6
10	4263		
11	4178		
12	4157		
13	4149		
14	4128		
15	4120		
16	4099		

The total mass flow through the Brayton section of Cycle J is 170 kg/s with a leak flow draw-off of 7.1 kg/s (leak1) after the LPC and a further draw-off of 2.4 kg/s also after the LPC (leak2). A mass flow of 160 kg/s is therefore achieved through the reactor. The total mass flow through the Rankine section is 97 kg/s with a bleed flow (between point 8 and point 2) of 12 kg/s. The heat exchanger duties and turbo machine loads of the Brayton and Rankine sections of Cycle J are presented by Table 20.4.7.

Table 20.4.7: Cycle J Heat Exchanger Duty and Turbo Machine Load

Component (Brayton)	Duty/Load [MW]	Component (Rankine)	Duty/Load [MW]
LPC	109	SG	267
LPT	221	Condenser	179
Net power	102	HPT	23
		IPT	29
		LPT	78
		Pump 1	0.2
		Pump 2	2
		Net power	124
Total net power output		226 MW_e	

20.4.2.4.3 Rankine Cycles (Cycle L)

Figure 20.4.40 shows the numbering structure used for the cycle analysis of Cycle L. Figure 20.4.41 shows the T-s diagram for the Rankine section of Cycle L. The temperatures and pressures in the primary heat transport system are shown in Table 20.4.8.

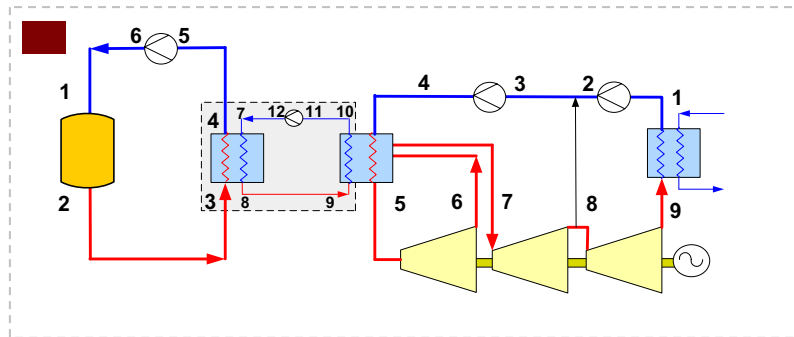


Figure 20.4.40: Numbering for Cycle L

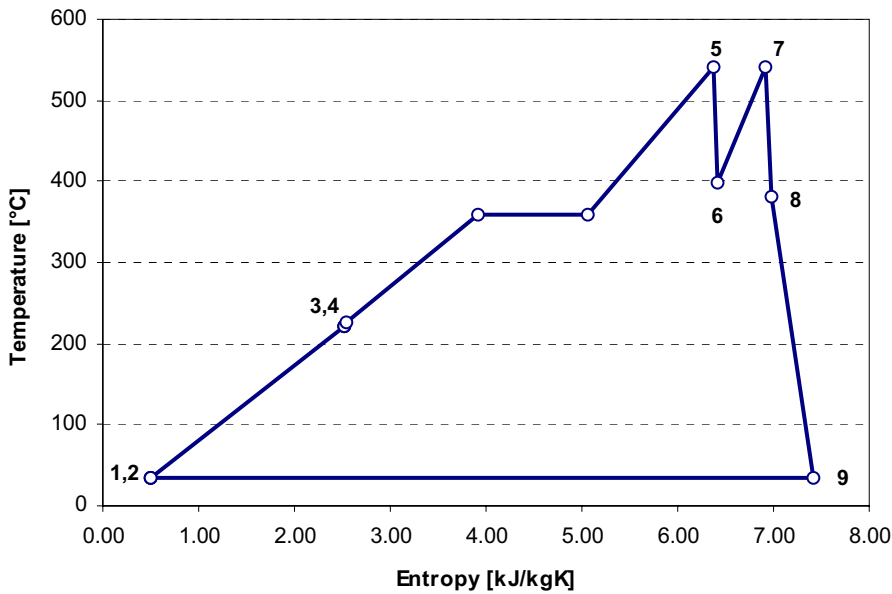


Figure 20.4.41: T-S Diagram for the Rankine Section of Cycle L

Table 20.4.8: Operating Pressures and Primary/Secondary Circuit Temperatures for Cycle L

Position (Primary/Secondary circuit)	Pressure [kPa]	Temperature [°C]	Position (Rankine)	Pressure [kPa]
1	8982	350	1	6
2	8766	950	2	2378
3	8749	950	3	2378
4	8697	339	4	18557
5	8679	339	5	18000
6	9000	350	6	7292
7	8782	289	7	7073
8	8730	900	8	2378
9	8712	900	9	6
10	8412	276		
11	8395	276		
12	8800	289		

The total mass flow through the primary heat transport circuit of Cycle L is 160 kg/s. The total mass flow through the Rankine section is 188 kg/s with a bleed flow (between point 8 and point 2) of 50 kg/s. The heat exchanger duties and blower loads of the primary and secondary circuits as well as the Rankine section of Cycle L are presented in Table 20.4.9.

Table 20.4.9: Cycle L Heat Exchanger Duties and Turbo Machine Loads

Component	Duty/Load [MW]
Primary blower	9
Secondary blower	11
SG	520
Condenser	294
HPT	45
IPT	57
LPT	128
Pump 1	0.47
Pump 2	5
Rankine power	217
Net power	197
Net efficiency	39.4%

The net power output for Cycle L is calculated by considering the Rankine house loads, the respective pump loads, generator efficiencies and the required blower power. The following equations are used to calculate the net grid power output for Cycle L:

$$T_{Excess\ Power} = (HPT_{Fluidic\ Power} + IPT_{Fluidic\ Power} + LPT_{Fluidic\ Power}) \tag{5}$$

$$Grid\ Power = [(T_{Excess\ Power} - P_{pump1} - P_{pump2}) \times f_{HL} \times \eta_{Gen} - P_{Blower1} - P_{Blower2}] \times \eta_{TXGen} \tag{6}$$

- With:
- $P_{Blower1}$ Power required by primary circuit blower [MW]
 - $P_{Blower2}$ Power required by secondary circuit blower [MW]
 - $HPT_{Fluidic\ Power}$ High-pressure steam turbine fluidic power [MW]
 - $IPT_{Fluidic\ Power}$ Intermediate-pressure steam turbine fluidic power [MW]
 - $LPT_{Fluidic\ Power}$ Low-pressure steam turbine fluidic power [MW]

20.4.3 SUMMARY AND RECOMMENDATIONS

In this study various cycle configurations were compared in order to identify representative Brayton, Combined and Rankine cycles for the NGNP. The most promising Brayton cycles, GTCCs and Rankine cycles were analyzed and compared with regard to thermodynamic performance and practical considerations when employed in conjunction with a given PBMR. A representative cycle was chosen for each group of cycle configurations.

For the Brayton cycle configurations, it was found that a single-shaft cycle with inter-cooling would be the best option in terms of net cycle efficiency and turbo-unit size. The representative Brayton cycle (Cycle B - Figure 20.4.6) has a net cycle efficiency of 42.3%. For the GTCCs, a single-shaft recuperative Brayton cycle without inter-cooling was found to be the most suitable cycle configuration. Although the cycle (Cycle J - Figure 20.4.9) does not have the highest net cycle efficiency (45.1%) of the GTCCs under investigation, the turbo-machines employed by the cycle builds on the PBMR DPP design. Cycle J was therefore chosen as the representative GTCC on the basis of readiness of technology. A single conventional Rankine cycle coupled to a PBMR through a steam generator was chosen as the representative Rankine cycle (Cycle K - Figure 20.4.11). The representative Rankine configuration uses proven Rankine cycle technology and has a net cycle efficiency of 41.2%.

The influence of a direct versus indirect PCS was also investigated for each group of cycle configurations. As expected, it was indicated that the net cycle efficiency of the cycles in each group decreases for an indirect configuration.

The influence of the coupling configuration of the hydrogen plant with the PCS, as well as the size of the hydrogen production plant, was also considered. The sensitivity of cycle efficiency to the hydrogen plant size was compared for Brayton and Rankine cycles. It was found that the net cycle efficiency of the representative Rankine cycle is not as sensitive to the coupling configuration and hydrogen production plant size as the representative Brayton cycle.

Considering the results presented in the study and the above mentioned conclusions it is recommended that the feasibility of the three representative cycle configurations identified by this study be further evaluated by NGNP Special Study 20.3 [2] in order to identify the optimum cycle configuration for the NGNP application.

REFERENCES

1. Greyvenstein, R., Rousseau, P.G., Greyvenstein, G.P. and Van Ravenswaay, J.P. 2005. “The CYCLE-C Computer Tool: Techno-Economic Comparison of Power Conversion Configurations for HTGR Application”. Paper 5701. Proceedings of ICAPP '05, Seoul Korea.
2. NNGP Preconceptual Design Report: “Special Study 20.3: High Temperature Process Heat, Transfer and Transport Study,” NNGP-20-RPT-003, January 2007.
3. Matzner, D. 2004. “PBMR Project Status and the way Forward”. 2nd International Topical Meeting on High Temperature Reactor Technology. Beijing, China. September 2004.
4. IST Presentation, “DEVELOPMENT OF BLOWERS FOR THE PBMR ENVIRONMENT – Reliable, Versatile and Maintenance-free,” Proceedings HTR2006: 3rd International Topical Meeting on High Temperature Reactor Technology, October 1-4, 2006, Johannesburg, South Africa
5. M-Tech Quality Manual, MTQS-4.2.2, Revision 4.
6. ANSI/ANS 10.4: 1987, “Guidelines for the Verification and Validation of Scientific and Engineering Computer Programs for the Nuclear Industry”.

BIBLIOGRAPHY

None

DEFINITIONS

A	-	heat transfer area
C_a	-	axial velocity
dT	-	temperature difference
htr	-	hub-tip-ratio
k	-	constant
m	-	mass flow
N	-	rotational speed
rpm	-	revolutions per minute
r_t	-	tip radius
SF	-	blade safety factor
U	-	heat transfer coefficient
z	-	number of stages
ρ_{blade}	-	turbo machine blade material density
ρ_{inlet}	-	inlet density
σ_{max}	-	maximum allowable blade stress
Ψ	-	work coefficient
Φ	-	flow coefficient

REQUIREMENTS

NONE

LIST OF ASSUMPTIONS

1. Pebble Bed Reactor based on PBMR DPP reactor design uprated to 500 MW_{th}.
2. Helium used for primary and secondary heat transport fluids.
3. Appendix A and Appendix B provide the input parameters used in the cycle analysis.

TECHNOLOGY DEVELOPMENT

Since the selected representative Brayton cycle and the representative GTCC build on the current PBMR DPP design very little technology development will be required. Furthermore, considering that the steam generator of the selected representative Rankine cycle has an inlet temperature of approximately 900°C, the Rankine steam generator will have to be custom designed. However, very little additional technology development for the representative Rankine cycle will be required, since it relies on proven technology.

The following components present in the selected representative cycles will require some technology development:

1. Helium blower for primary and secondary loop circulation. The proposed Helium blower will be based upon the Howden blower design that is used for the DPP. Currently such a circulator is in operation in the PBMR Helium Test Facility [4].
2. Reactor core outlet pipe material qualification at ROT > 900°C.
3. High temperature steam generator with inlet temperatures of larger than 900°C.

APPENDICES

APPENDIX A: COMPONENT MODELS

This section provides a discussion of the various component models used to indicate the size of the turbo machines, heat exchangers and blowers.

Turbo Unit Models

The compressor and turbine models determine the relative size of the compressors and turbines, respectively. The component models for the compressors and turbines are very similar. The size of the turbo unit was defined as the sum of the compressor size and turbine size. Table 20.4.10 summarizes the required input and output for the compressor and turbine models.

Table 20.4.10: Summary of Turbo Unit Model Inputs and Outputs

Fixed input values	Sizing Model	To be solved	Output
$k_{1,2,3,4,5}$ η_s Φ Ψ Blade material η_c $C_{a,c}$	$C_{Comp/Turb} = k_1[k_2r_t^2(k_3z + k_4) + k_5]$	r_t z	$C_{Comp/Turb}$

The following variables are fixed input to the compressor and turbine models:

- Φ - flow coefficient
- Ψ - work coefficient
- $C_{a,c} = 135$ m/s - axial velocity

Compressor specific inputs

- k_1, k_2, k_3 - proportionality constants for compressor

- k_4, k_5 - fixed constants for compressor
- Blade material properties
- $\eta_c = 0.89$ - isentropic efficiency

Turbine Model specific inputs

- k_1, k_2, k_3 - proportionality constants for turbine
- k_4, k_5 - fixed constants for turbine
- Blade material properties
- $\eta_c = 0.91$ - isentropic efficiency

The following variables are obtained from the cycle analysis for both the compressors and turbines:

- C_p - specific heat at constant pressure
- dT - temperature rise (drop) over compressor (turbine)
- m - mass flow [kg/s]
- ρ - fluid density [kg/m³]

The size model is used to find the optimum speed and safety factor for the compressor and turbine, respectively.

- **N** - rotational speed [rev/s]
- **SF** - safety factor [-]

The input values above are used together with the following equations to solve the number of stages, tip radius and hub-tip-ratio.

The *work coefficient* is defined as:
$$\psi = \frac{C_p (dT / z)}{U_m^2}$$

The *flow coefficient* is defined as:
$$\phi = \frac{C_a}{U_m}$$

The *centrifugal tensile stress* is defined by:
$$\sigma_{real} = \frac{\sigma_{max}}{SF} = \frac{2}{3} \left[\frac{\rho_b}{2} U_t^2 \left(1 - \left(\frac{r_r}{r_t} \right)^2 \right) \right]$$

The *continuity equation* states that:

$$m = \rho C_a \pi r_t^2 \left(1 - \left(\frac{r_r}{r_t} \right)^2 \right)$$

- **z:** **number of stages** [-]
- **r_t:** **tip radius** [m]
- $\frac{r_r}{r_t}$: **hub-tip-ratio** [-]

At this stage the compressor and turbine sizes (r_t and stages) have been solved. The turbo unit size can therefore be determined.

Choice of Φ and ψ

The choice of Φ and ψ is significant since these two parameters basically define the geometry of the machine, its performance and also its off-design behavior.

Compressor:

One would like to have Φ as small as possible to minimize the frontal area and ψ as large as possible to minimize the number of stages. The choice of reaction, Φ and ψ are also influenced by the permissible amount of diffusion in the blades. The de Haller criterion sets the upper limit on the fluid deflection, stating that $\frac{V_2}{V_1} \leq 0.72$. Usually, the goal is to use the maximum deflection in order to minimize the number of stages and therefore the size. Typical values for reaction, Φ and ψ were chosen based on a combination of (i) information contained in literature on the subject, (ii) experience gained in the development of the PBMR cycle and (iii) discussions with experts in the field.

Turbine:

Typical values for reaction, Φ and ψ were also chosen for the turbine model.

Recuperator Model

The recuperator component model solves only for the heat transfer area; this gives an indication of the size of the heat exchanger. The heat transfer area is calculated with the NTU-method. The NTU value for a concentric tube, counter flow heat exchanger is given by:

$$NTU = \frac{\eta_{\text{Recuperator}}}{1 - \eta_{\text{Recuperator}}}$$

$$NTU = \frac{UA}{C_{\min}} = \frac{UA}{(\dot{m}C_p)_{\min}}$$

From the above-mentioned equations it can be shown that:

$$UA = \left(\frac{\eta_{\text{Recuperator}}}{1 - \eta_{\text{Recuperator}}} \right) \dot{m}C_p$$

For un-finned, tubular heat exchangers, the AU value is also defined as:

$$\frac{1}{AU} = \frac{1}{A_i U_i} = \frac{1}{A_o U_o} = \frac{1}{h_i A_i} + \dots + \frac{1}{h_o A_o}$$

where

i	=	primary side / low-pressure
o	=	secondary side / high-pressure
h _i	=	primary side heat transfer coefficient
h _o	=	secondary side heat transfer coefficient

U₀ was set at 1094 [W/m².K]. It was decided to use U as a constant value for all the cycles at all the pressure ratios. Thus the heat transfer area used in all the analyses for the recuperator is:

$$A_o = \frac{\left(\frac{\eta_{\text{Recuperator}}}{1 - \eta_{\text{Recuperator}}} \right) \dot{m}C_p}{1094}$$

An efficiency for the recuperator is selected by using the above-mentioned equation to plot the heat transfer area as a function of the recuperator efficiency. The mass flow was taken as 192 kg/s, C_p as 5195 [J/kg.K] and U as 1094 [W/m².K]. It was decided to use a recuperator efficiency of 97% - see Figure 20.4.42.

Concentric tube counter-flow heat exchanger

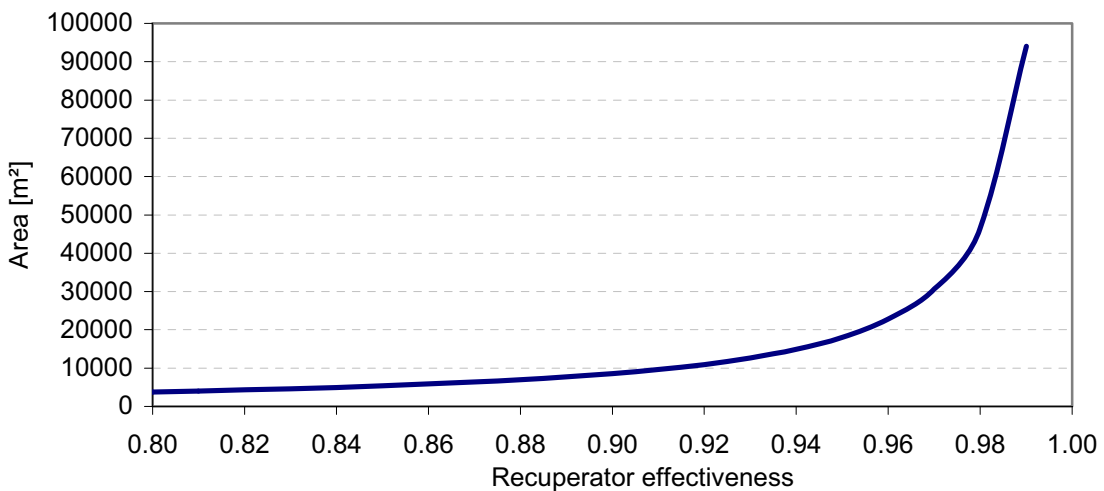


Figure 20.4.42: Recuperator Efficiency vs. Heat Transfer Area for Recuperator

Pre-cooler and inter-cooler

The heat transfer area for the coolers is also calculated with the NTU-method. From the NTU-method the heat transfer areas can be calculated with the following equations:

$$Ai_{pc} = -\left(\frac{1}{C_r}\right)\ln(1 + C_r \ln(1 - \eta_{pc}))\dot{m}C_p / U$$

$$Ai_{ic} = -\left(\frac{1}{C_r}\right)\ln(1 + C_r \ln(1 - \eta_{ic}))\dot{m}C_p / U$$

The heat transfer coefficient U is simply assumed to be 320 [W/m².K], which is a typical value.

An efficiency for the coolers is selected by using the area equation to plot the heat transfer area as a function of the heat exchanger efficiency. The mass flow was taken as 200 kg/s, Cp as 5195 [J/kg.K] and U as 320 [W/m².K]. The values of the mass flow, Cp and U are not as important, since they will only shift the graph up or down. It was decided to use a cooler efficiency of 83% - see Figure 20.4.43.

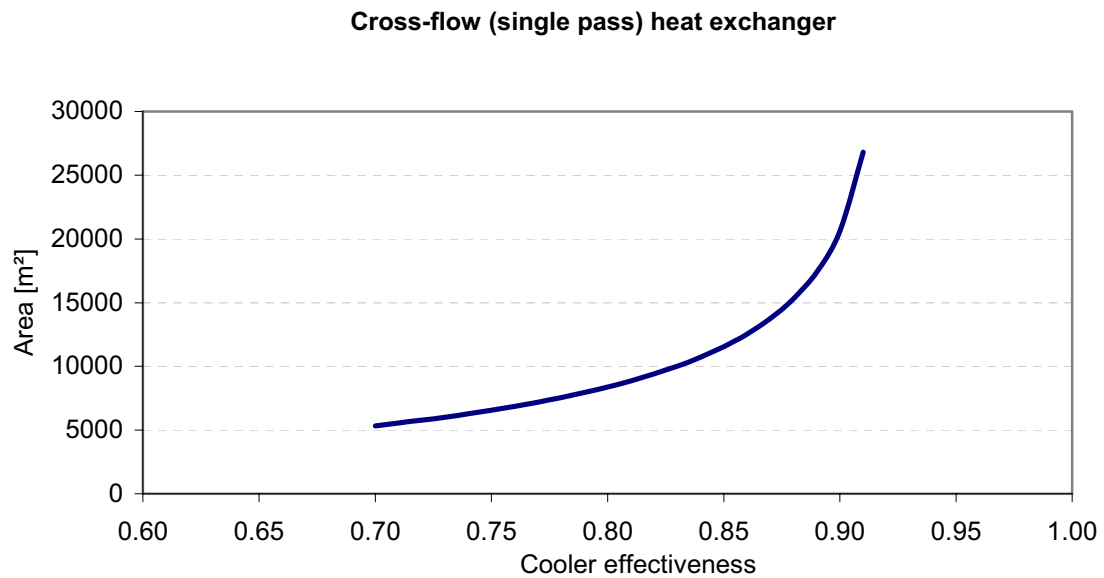


Figure 20.4.43: Heat Exchanger Efficiency vs. Heat Transfer Area for Coolers

Intermediate Heat Exchanger Model

The heat transfer area of the IHX is calculated with the same relationship as explained under the recuperator model section.

$$A_{IHX} = \frac{\left(\frac{\eta_{IHX}}{1 - \eta_{IHX}} \right) \dot{m} C_p}{U_{IHX}}$$

For the IHX, both the effectiveness (η_{IHX}) and heat transfer coefficient (U_{IHX}) are calculated. The effectiveness is calculated from the specified IHX temperature difference (dT_{IHX}),

$$\eta_{IHX} = \frac{(T_{h,i} - T_{h,o})}{(T_{h,i} - T_{c,i})} \quad \text{where } h = \text{hot}, \quad c = \text{cold}$$

The heat transfer coefficient will be different for various working fluids and is calculated as a function of the conductivity (k), which is a function of temperature.

$$k_1 = \text{function}(t)$$

$$k_2 = \text{function}(t)$$

$$h_1 = \frac{Nu \, k_1}{d_{IHX}}, \quad \text{where } Nu = 3.66 \text{ (assuming laminar flow)}$$

$$h_2 = \frac{Nu \, k_2}{d_{IHX}}, \quad \text{where } Nu = 3.66$$

$$U_{IHX} = \left(\frac{1}{h_1} + \frac{1}{h_2} \right)^{-1}$$

Blower model

The blower size is calculated simply to be proportional to the blower power output.

$$t_{outlet} = t_{inlet} + \frac{t_{inlet}}{\eta_{blower}} \left[\left(\frac{p_{inlet}}{p_{outlet}} \right)^{(\gamma-1)/\gamma} - 1 \right]$$

$$Q_{Blower} = \dot{m} C_p (t_{outlet} - t_{inlet}) \cdot$$

APPENDIX B: INPUT PARAMETERS

This section provides a detailed list of all the relevant inputs to the cycle analysis tool. Table 20.4.11 shows the relevant input values together with a description of each parameter.

Table 20.4.11: Input Parameters to Cycle Analysis Tool

Variables	Value	Units	Description
Brayton cycle inputs			
η_c	89	[%]	compressor isentropic efficiency
η_t	91	[%]	turbine isentropic efficiency
$C_{a,c}, C_{a,t}$	135	[m/s]	diffuser outlet velocity (compressor/turbine)
t_{min}	22.5	[°C]	minimum cycle coolant (helium) temperature
t_{max}	900	[°C]	maximum cycle coolant temperature
p_{max}	90	[bar]	maximum cycle pressure
pressure ratio	vary	[-]	total pressure ratio over all compressors
PBR	500	[MWth]	Pebble Bed Reactor thermal power
k_{PBMR}	40	[-]	loss coefficient for PBR - fixed $k_{PBMR} = \frac{1}{2} \frac{1}{A^2} K = \frac{\rho_{avg} \Delta P}{\dot{m}^2}$
%dP _{HXs}	0.995	[-]	0.5% pressure loss on each side for each heat exchanger in cycle
%dP _{PIPING}	0.998	[-]	0.2% pressure loss assumed for each pipe in the cycle
Brayton House load	6.5	[MW]	Brayton section house load
House load	0.8 of Brayton	[MW]	Combined Cycles G, J
House load	0.6 of Brayton	[MW]	Combined Cycles H, I
η_{Gen}	98.5	[%]	generator efficiency
η_{TXGen}	99.0	[%]	generator transformer efficiency
η_{blower}	80	[%]	blower isentropic efficiency
Rankine cycle inputs			
t_{min}	35	[°C]	condenser temperature
t_{max}	≤ 540	[°C]	maximum allowable outlet temperature for steam generator
p_{max}	180	[bar]	pressure in steam generator
%dP _{RH}	3	[%]	losses in reheater

Variables	Value	Units	Description
Brayton cycle inputs			
%dP _{SG}	3	[%]	losses in steam generator
t _{PINCH}	30	[°C]	pinch temperature for steam generator
CD _x	> 0.88	[-]	minimum allowable condenser two-phase fraction
η _{turbine}	89	[%]	turbine efficiency
η _{pump}	72	[%]	pump efficiency
%dP SG helium side	0.966	[-]	pressure drop through steam generator on helium side
Rankine House load	0.00850	[-]	Rankine house load as percentage of Rankine grid output 0.85%
Fluid properties			
γ _{He}	1.667	[-]	helium: ratio of specific heats
R _{He}	2078.0	J/kg.K	helium: gas constant
C _{pHe}	5195.0	J/kg.K	helium: specific heat at constant pressure
Turbo unit inputs			
η _{mech}	99	[%]	mechanical shaft efficiency
η _s	89	[%]	stage efficiency - internal stage - compressor
η _s	91	[%]	stage efficiency - internal stage - turbine
N _{PT}	100	[rev/s]	the power turbine speed was fixed at 6000 rpm
Heat exchanger inputs			
U _{Recuperator}	1094	[-]	heat transfer coefficient for the recuperator
η _{Recuperator}	97	[%]	recuperator effectiveness
dT _{IHX}	50	[°C]	temperature difference over the IHX for indirect cycles
Leak flows			
Single Shaft	5.6	[%]	percentage of total mass flow
leak 1	25	[%]	percentage of total leak flow before turbine
leak 2	75	[%]	percentage of total leak flow after turbine
Single Shaft: No IC	5.2	[%]	percentage of total mass flow
leak 1	100	[%]	percentage of leak
Two Shaft	6.1	[%]	percentage of total mass flow
leak 1	50	[%]	percentage of leak
leak 2	50	[%]	percentage of leak
3-shaft designs	7.3	[%]	percentage of total mass flow
leak 1	30	[%]	percentage of leak
leak 2	30	[%]	percentage of leak

Variables	Value	Units	Description
Brayton cycle inputs			
leak 3	40	[%]	percentage of leak

APPENDIX C: SPECIAL STUDY 20.4 SLIDES

Appendix C provides the slides presented on this special study at the December 2006 monthly meeting at the Shaw Group offices in Stoughton, MA.

APPENDIX C: SPECIAL STUDY 20.4 SLIDES



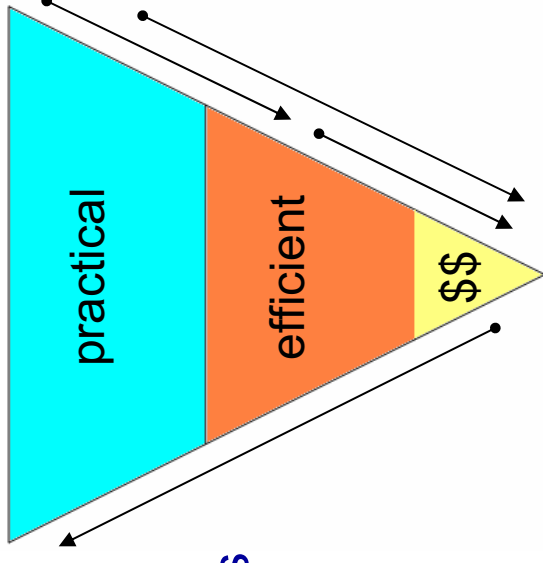
SPECIAL STUDIES:
20.3 - HEAT TRANSPORT SYSTEM
20.4 - POWER CONVERSION SYSTEM

Part 2 – Power Conversion System Options

December 6, 2006

Background

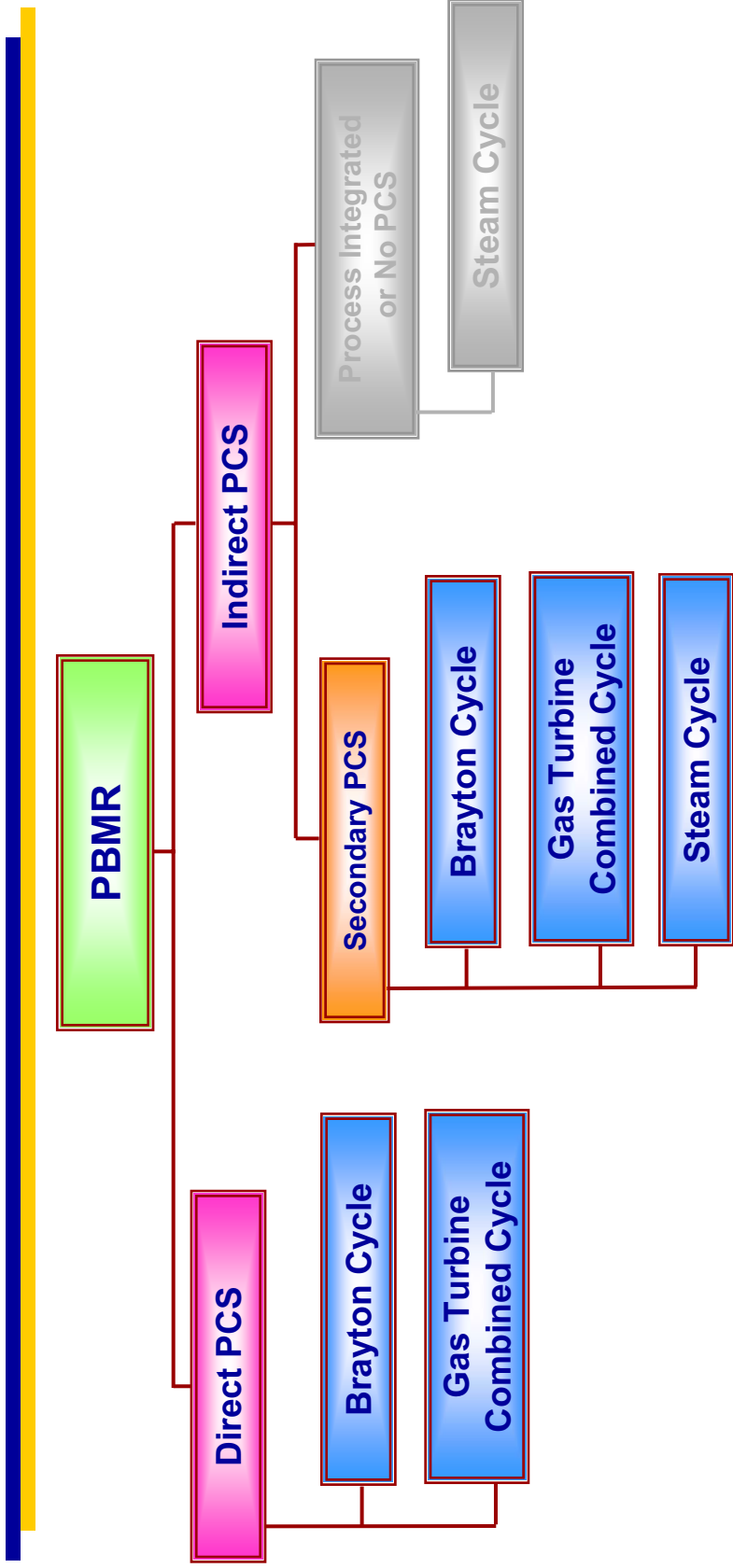
- The choice of Power Conversion System (PCS) is a vital step in the Preconceptual Design of the NGNP
- The PCS directly influences
 - Plant net efficiency
 - Practicality of the component designs
 - Plant flexibility
 - Plant cost
 - Potential technology growth
- Identifying the optimum PCS is a complex problem which is influenced by a large number of interdependent variables



Objective

- **Analyze and compare the performance of three PCS families being considered in conjunction with Heat Transport System (HTS) options**
 - **Gas Turbine (Brayton) Cycles**
 - **Gas Turbine Combined Cycles (CCGT)**
 - **Rankine Cycles**

PCS Options Investigated

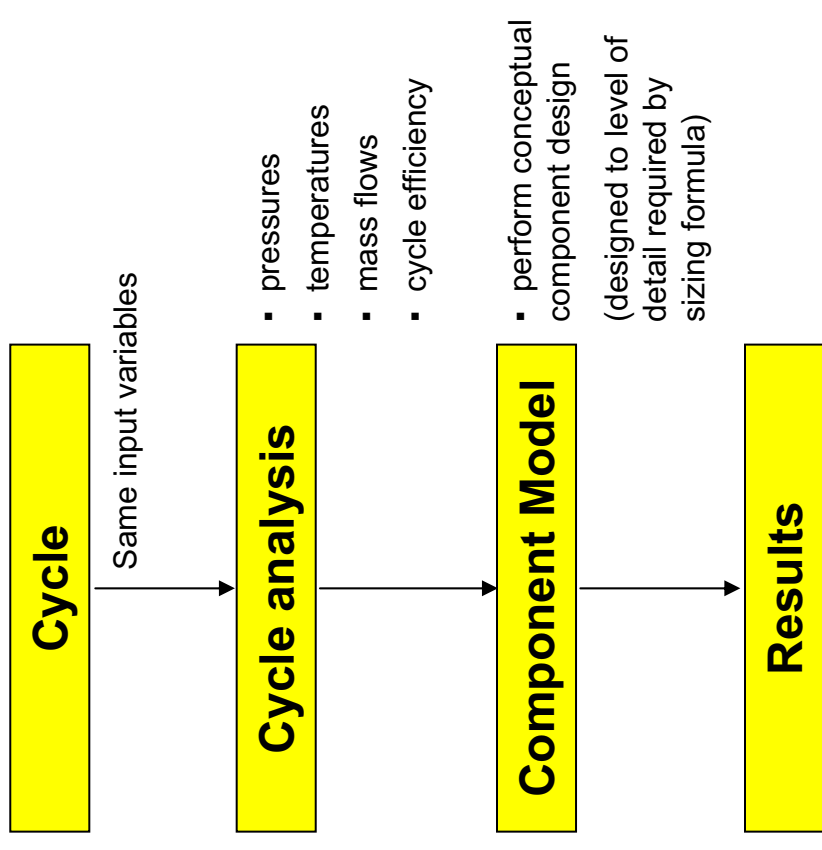


Part 2 Outline

- Introduction
- ➔ Analysis Methodology
- Evaluation
 - Brayton Cycles
 - GTCC
 - Rankine Cycles
- Cycle Trade-offs
- Summary

Analysis Methodology

- **Integrated analysis approach**
- **Systematically compares various cycle configurations based on the same input parameters**
- **Evaluate the efficiency as a function of various design parameters**



Influence of H₂ Production Unit

- **The size of the H₂ Production Unit (HPU) will be relatively small**
 - ~5 - 50MWt per 20.7
- **It is, therefore, assumed that the size of the HPU will not significantly influence the choice of the best cycle configuration within a given family (Brayton, GTCC, Rankine)**
 - Therefore, when comparing cycle variations within these three individual groups, the HPU size is not directly considered
- **For the optimum cycle within each family, the influence of HPU size is subsequently evaluated**

Cycle Analysis

- Input variables together with basic thermodynamic relations, are used to calculate the temperatures and pressures at each component's inlet and outlet
- **Brayton cycle**
 - Fixed heat exchanger efficiencies
 - Fixed pressure drop percentages for piping and heat exchangers
 - Fixed reactor design
 - Fixed compressor and turbine efficiencies
- **Rankine cycle**
 - Maximum steam pressure is fixed
 - Upper limit is set for maximum steam temperature
 - Turbine and pump efficiencies are fixed
 - Fixed pressure drop percentages through SG and re-heater
 - Optimize RIT for maximum GTCC efficiency
 - Limit low pressure turbine outlet quality to more than 88%

Cycle Optimization

- **Gas Turbo Units**
 - Combination of speed, blade safety factor, etc. was optimized to ensure the minimum capital cost (smallest machine) at every operating point
- **GTCC**
 - Rankine Cycle was custom-designed to exactly fit the Brayton cycle at every considered operating point
 - Brayton cycle and Rankine cycle were optimized to ensure the maximum combined efficiency at every operating point

Input Parameters

- **Generic inputs**
 - PBR power = 500 MW_{th}
 - DPP Reactor design
 - Primary and secondary fluid = Helium
- **Brayton Cycle inputs**
 - Turbine inlet temperature = 900°C (assumed for 20.4)
 - Min helium coolant temp = 22.5°C (assumed for 20.4)
 - $\eta_{\text{compressor}} = 89\%$; $\eta_{\text{turbine}} = 91\%$; $\eta_{\text{blower}} = 80\%$
 - Compressor outlet axial velocity = 135 m/s
 - $\eta_{\text{recuperator}} = 97\%$
 - IHX pressure drop = 0.5% of inlet pressure
 - Piping pressure drop = 0.2% of inlet pressure
 - Brayton house load (HL) = 6.5 MW_e
 - Primary circuit maximum pressure = 9 MPa
 - IHX approach temperature = 50°C (indirect cycles)
 - Secondary circuit pressure = 8.8 MPa
- **Reactor and Brayton Cycle constraints**
 - Maximum RIT = 500°C (Core Barrel < 427°C)
 - Maximum mass flow = 200 kg/s (V < 100m/s)
 - Maximum Turbo Unit pressure ratio = 3.5
- **Rankine Cycle inputs**
 - Maximum steam pressure = 180 bar
 - Condenser temperature = 35°C
 - Turbine exhaust quality = ~0.88
 - $\eta_{\text{turbine}} = 89\%$; $\eta_{\text{pumps}} = 72\%$
 - SG and re-heater pressure drop = 3% of inlet pressure
 - Piping pressure drop ignored
 - $HL_{\text{Rankine}} = 0.9915 * \text{Power}_{\text{Rankine}}$
 - Pinch Temperature = 30°C
- **Rankine Cycle constraints**
 - Max steam temperature ≤ 540°C
- **GTCC inputs**
 - (G)(J) $HL_{\text{CC}} = 0.8 * HL_{\text{Brayton}} + 0.9915 * \text{Power}_{\text{Rankine}}$
 - (H)(I) $HL_{\text{CC}} = 0.6 * HL_{\text{Brayton}} + 0.9915 * \text{Power}_{\text{Rankine}}$

Part 2 Outline

- **Introduction**
- **Analysis Methodology**
- ➔ **Evaluation**
 - **Brayton Cycles**
 - **GTCC**
 - **Rankine Cycles**
- **Cycle Trade-offs**
- **Summary**

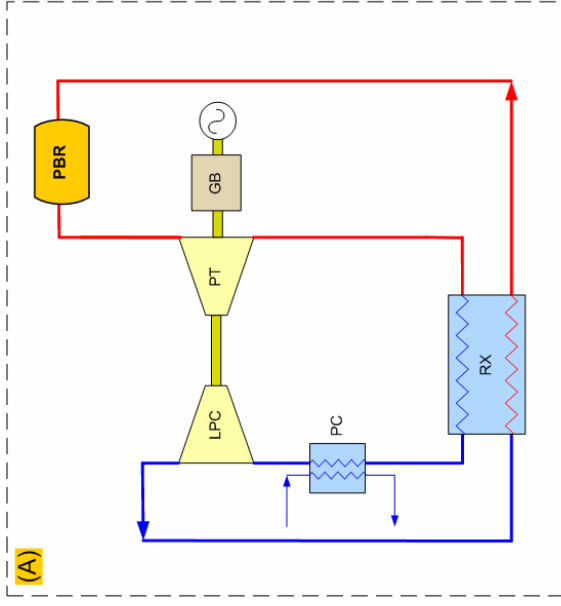
Brayton Cycle Configurations

- **(A) Single-shaft**
- **(B) Single-shaft with inter-cooling**
- **(C) Two-shaft with inter-cooling**
- **(D) Three-shaft with inter-cooling**
- **(E)* Three-shaft with two-step inter-cooling**

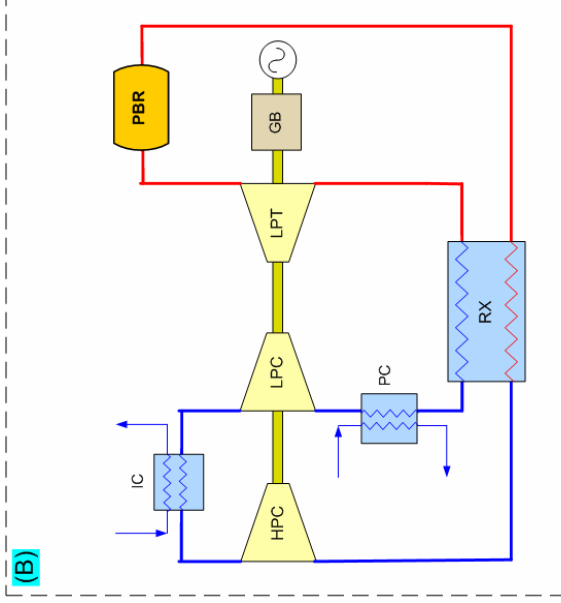
*Indirect Cycle F to follow later

Brayton Cycle Options A, B, C

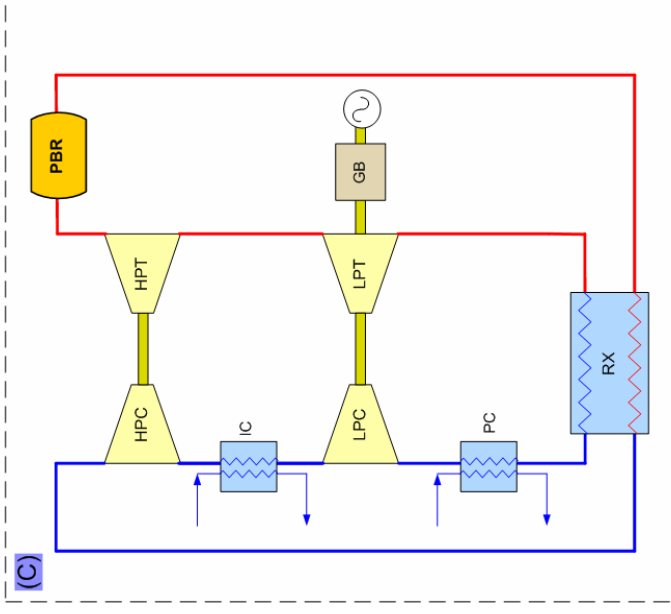
(A) Single-shaft



(B) Single-shaft with inter-cooling



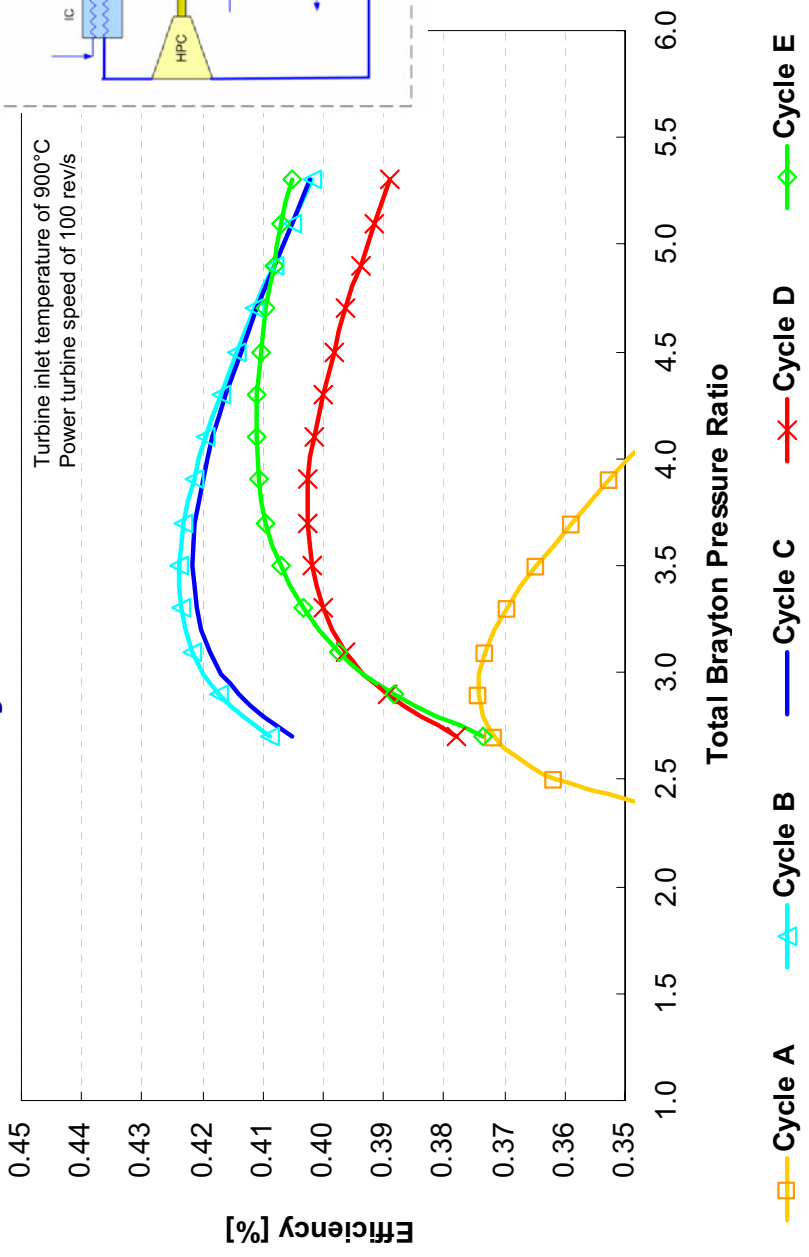
(C) Two-shaft with inter-cooling



Brayton Cycles

Net Cycle Efficiency

Net efficiency vs. Pressure ratio



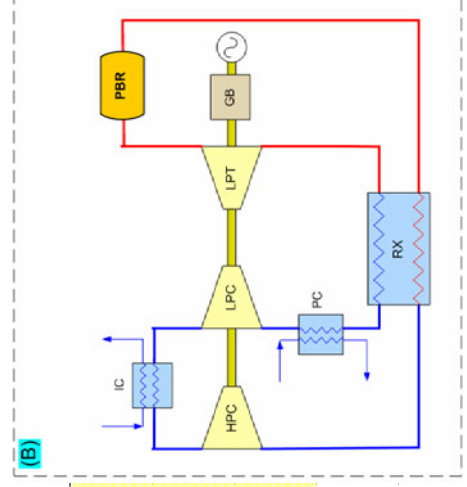
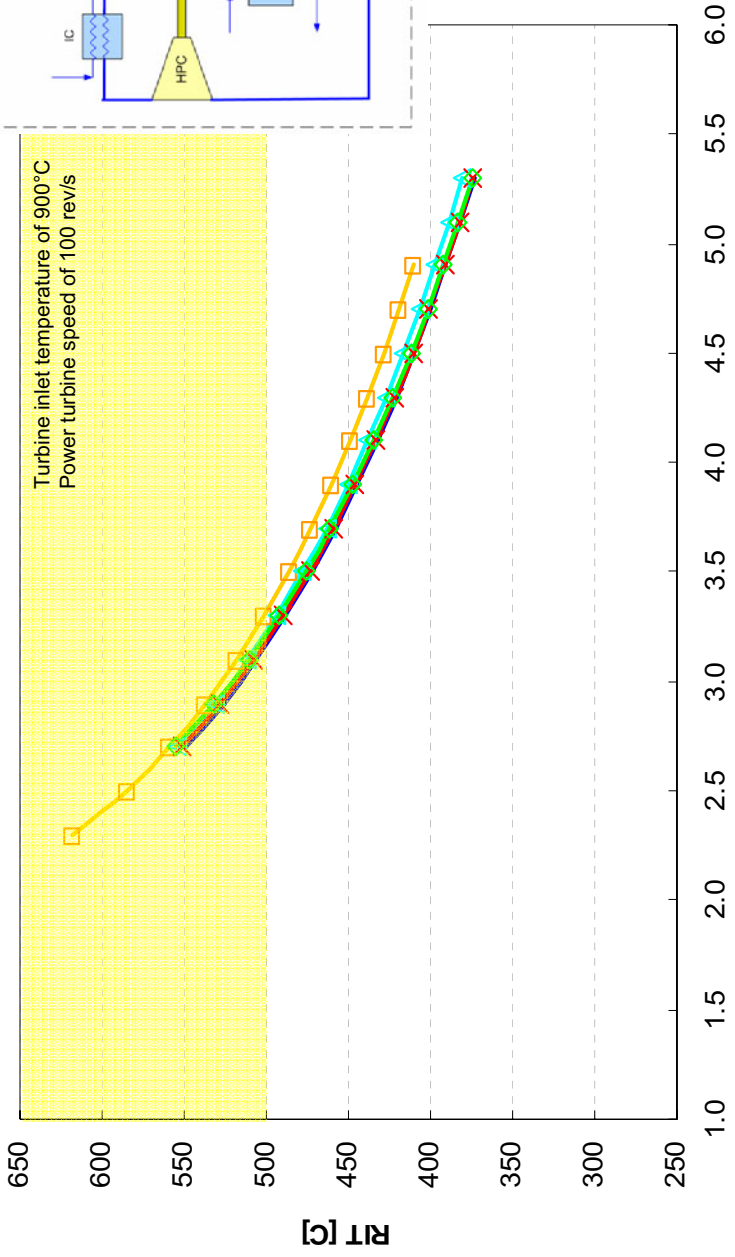
- (A) 1-Shaft
- (B) 1-Shaft IC
- (C) 2-Shaft IC
- (D) 3-Shaft IC
- (E) 3-Shaft ICx2

• Best efficiency – Cycle B: Single shaft Brayton cycle with intercooler

Brayton Cycles

RIT

RIT vs. Pressure ratio



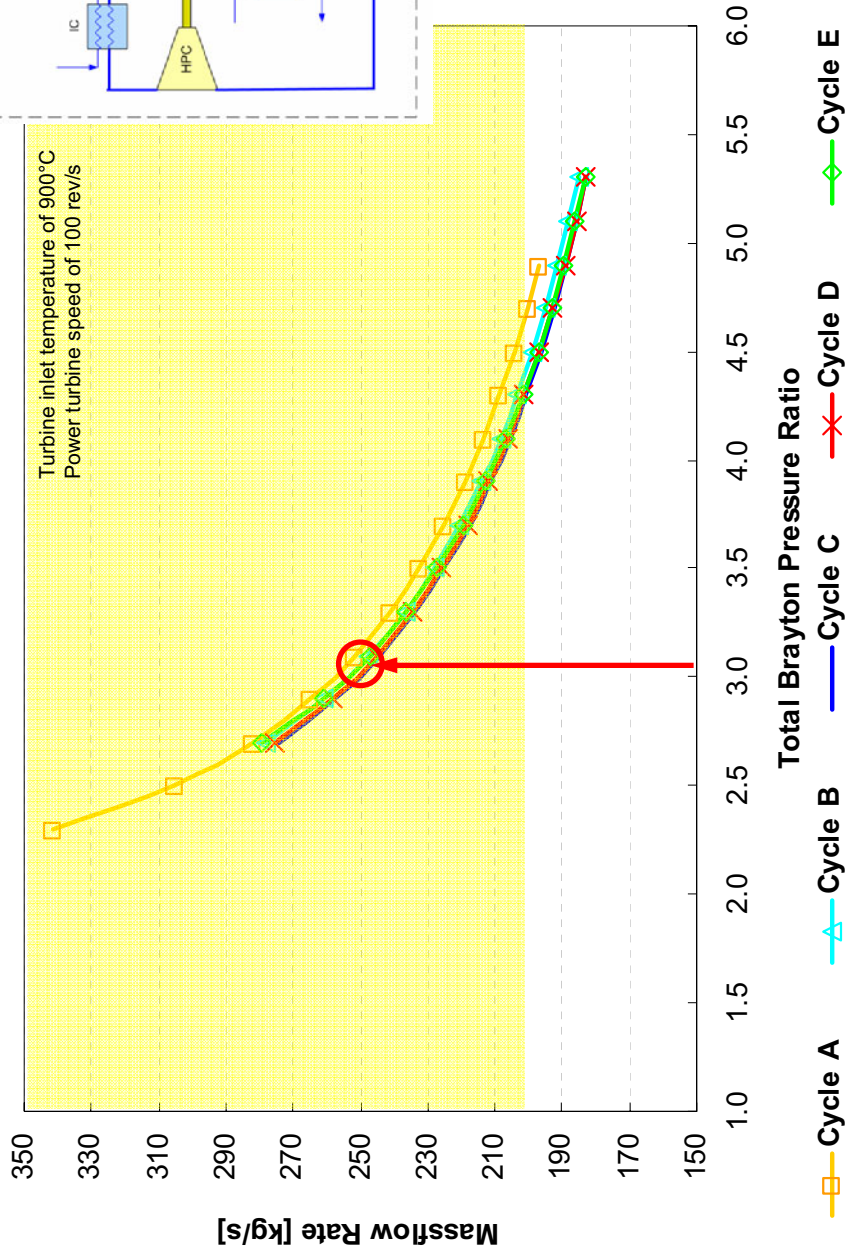
- (A) 1-Shaft IC
- (B) 1-Shaft IC
- (C) 2-Shaft IC
- (D) 3-Shaft IC
- (E) 3-Shaft ICx2

- **Maximum RIT of 500°C; to enable Core Barrel to operate below 427°C**
- **All cycles to operate above 3.1 pressure ratio to enable RIT < 500°C**

Brayton Cycles

Mass Flow Rate

Mass flow rate vs. Pressure ratio



- (A) 1-Shaft
- (B) 1-Shaft IC
- (C) 2-Shaft IC
- (D) 3-Shaft IC
- (E) 3-Shaft ICx2

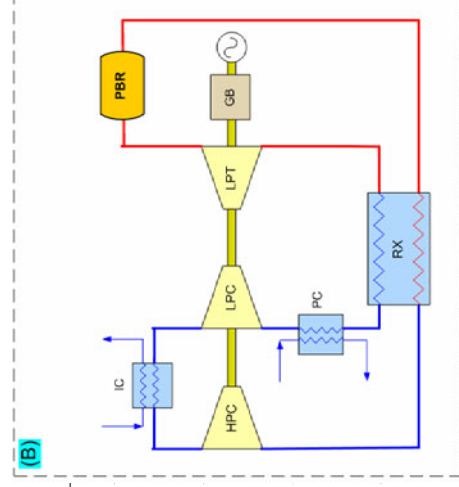
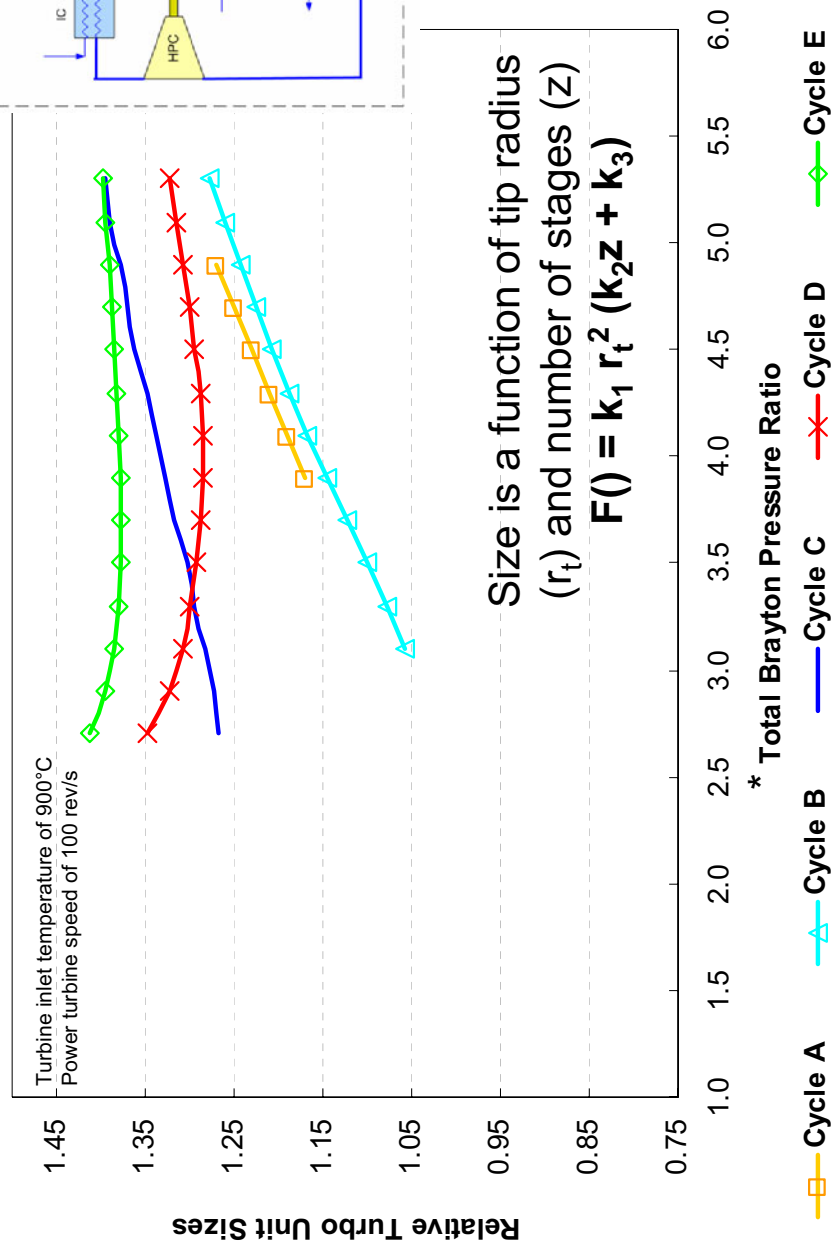
• **Maximum mass flow of ~200 kg/s; to limit reactor core velocity**

➤ Brayton cycles unable to operate at their maximum cycle efficiency within reactor design envelope at 500 MW

Brayton Cycles

Relative Turbo Unit Size

Relative turbo unit size vs. Pressure ratio



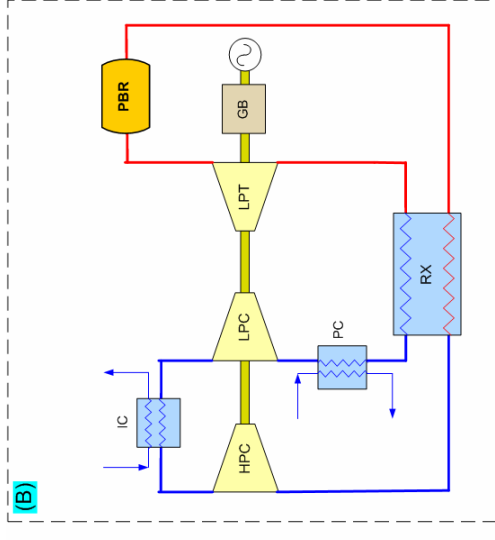
- (A) 1-Shaft
- (B) 1-Shaft IC
- (C) 2-Shaft IC
- (D) 3-Shaft IC
- (E) 3-Shaft ICx2

- Single-shaft designs have highest gradients (fixed rotational speed)
- Three-shaft designs have lowest gradient (only third shaft has a fixed rotational speed) – free shafts rotational speed optimized

(*See appendix for effect of rotational speed and ROT)
 20.3/20.4: Part 2 - 12/6/2006

Choice of Brayton Cycle

- **Criteria**
 - Performance
 - Efficiency (MEDIUM)
 - Cycle B highest
 - Component Size (LOW)
 - Turbo Units Cycle B lowest
 - Design Envelope (HIGH)
 - mass flow rate < 200 kg/s; $280 < RIT < 500$; pressure ratio < 3.5
 - All Brayton cycles exceed the mass flow rate limitation at 500 MWt



- **Conclusion**
 - **Cycle B preferred Brayton Cycle**
 - However, Cycle B exceeds the mass flow rate limitation (at 500MW)

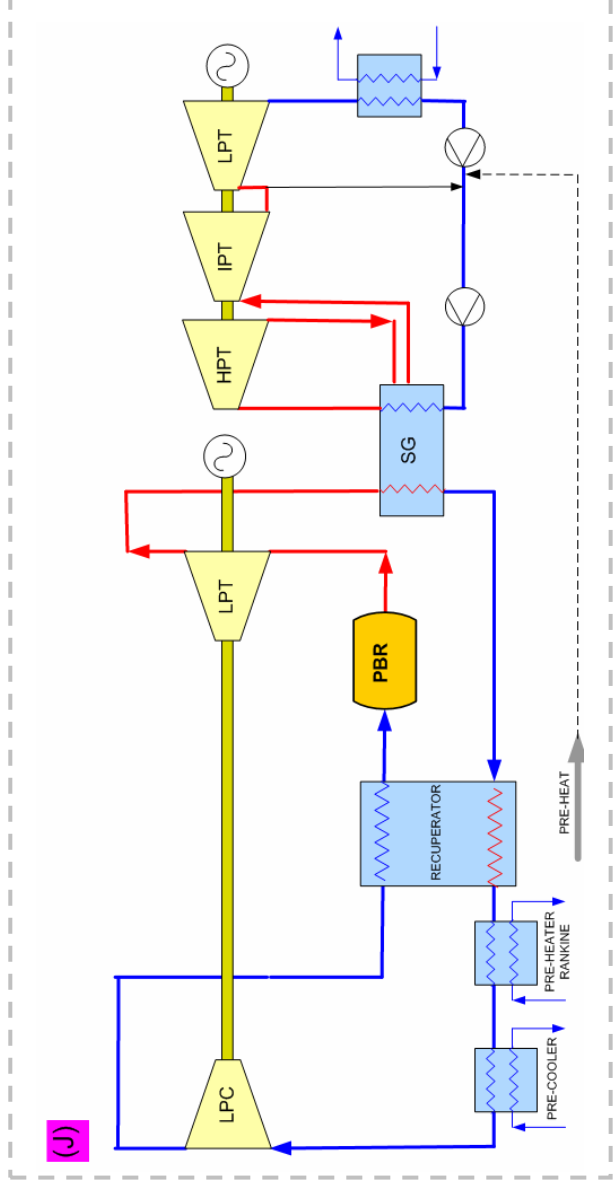
GTCC Configurations

- **(G) Single-shaft recuperative Brayton with inter-cooling**
- **(H)* Single-shaft Brayton without inter-cooling**
- **(J) Single-shaft recuperative Brayton without inter-cooling**

*Indirect Cycle I to follow later

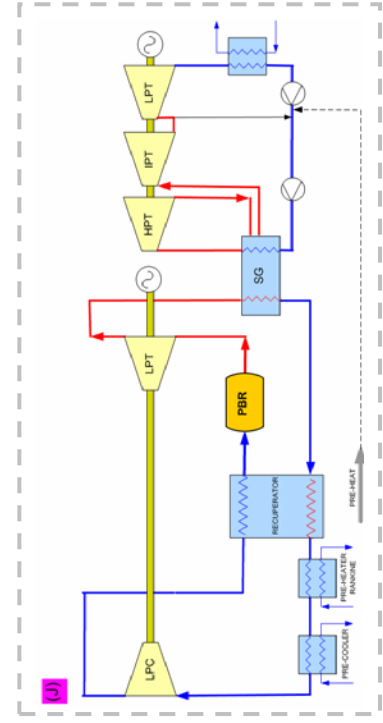
GTCC Configurations

J

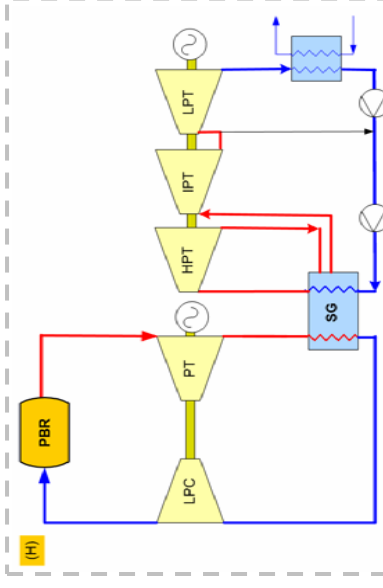
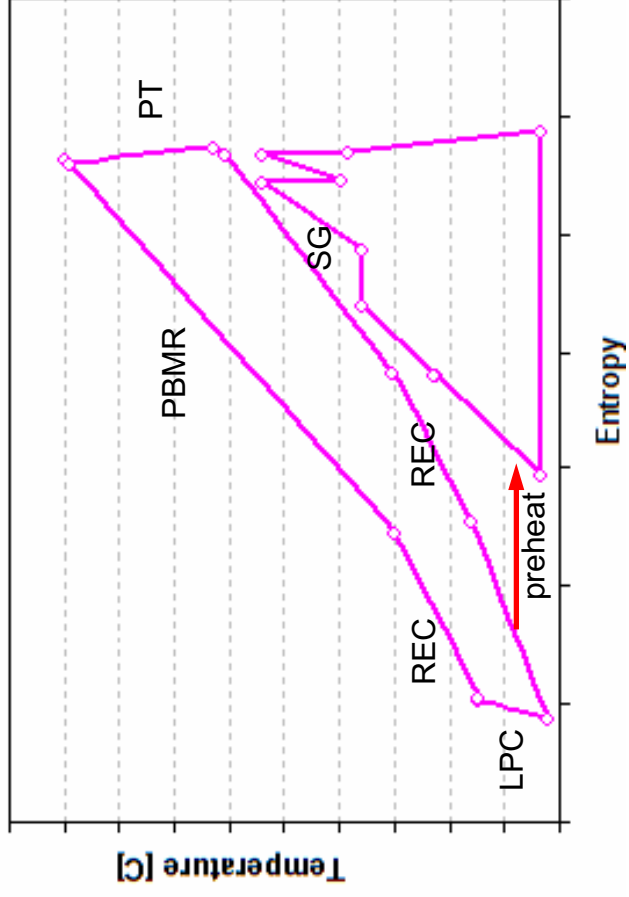


J: Single-shaft recuperative Brayton without inter-cooling

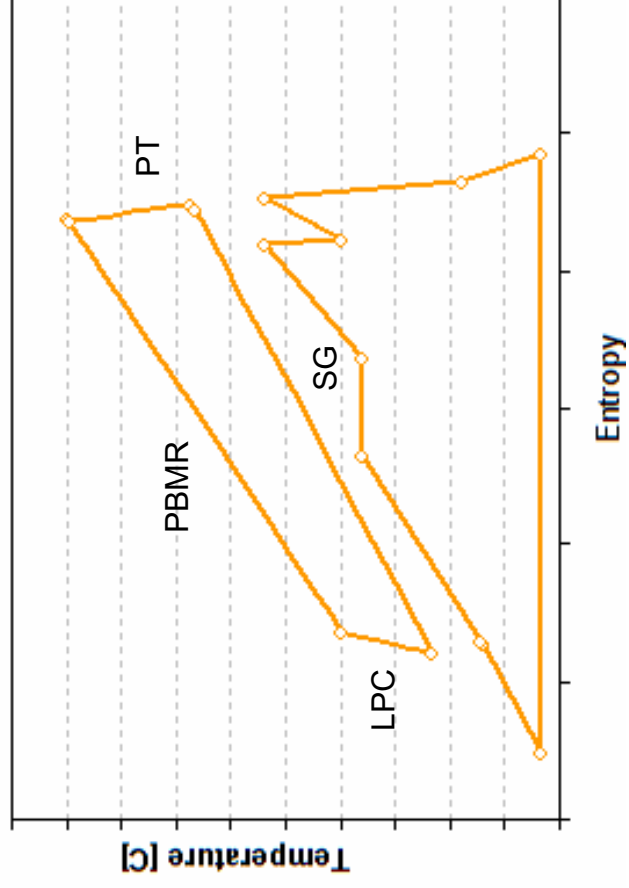
Brayton/Rankine Cycle Power Tradeoff



Cycle (J)

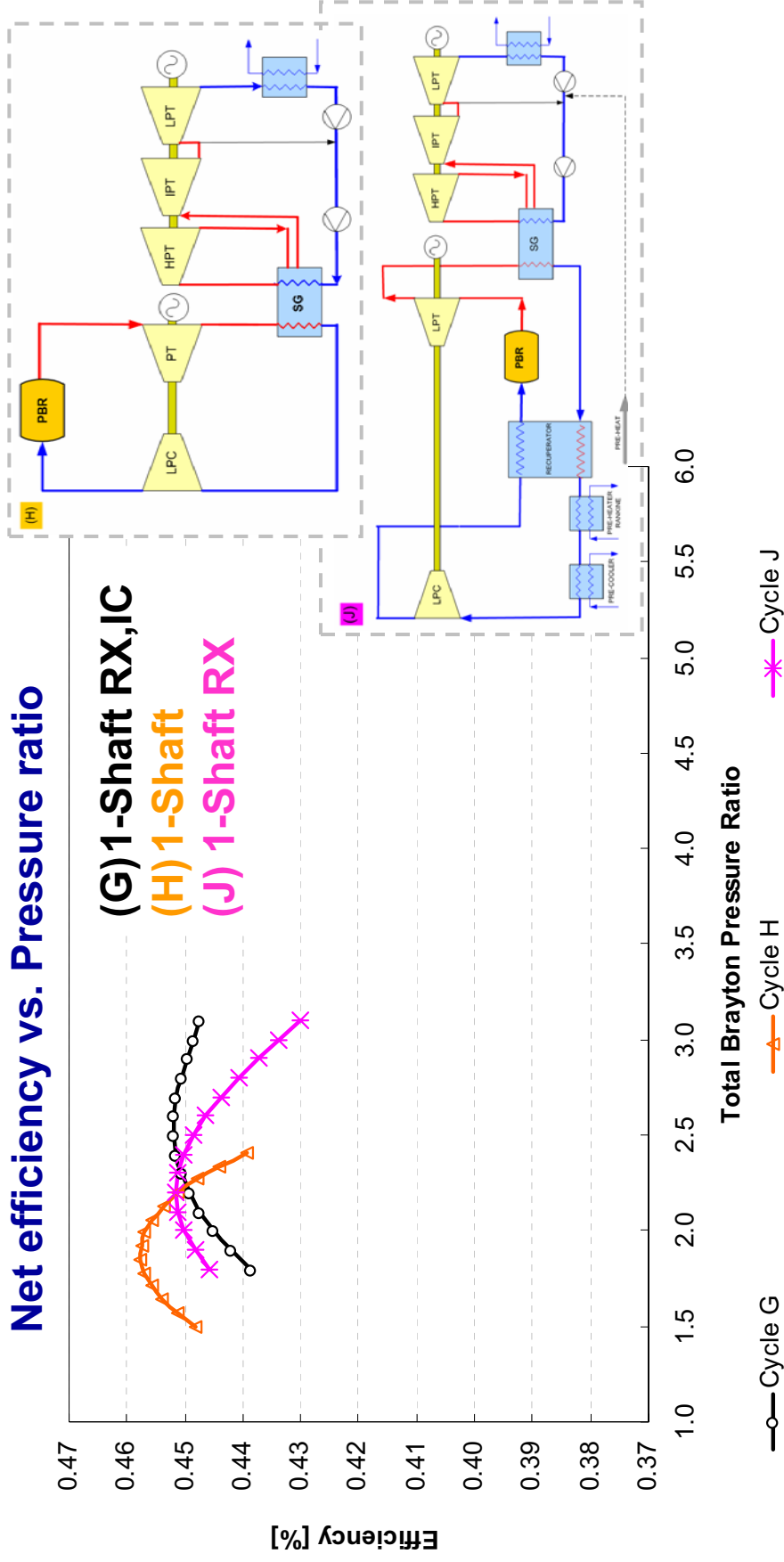


Cycle (H)



GTCC

Net Cycle Efficiency

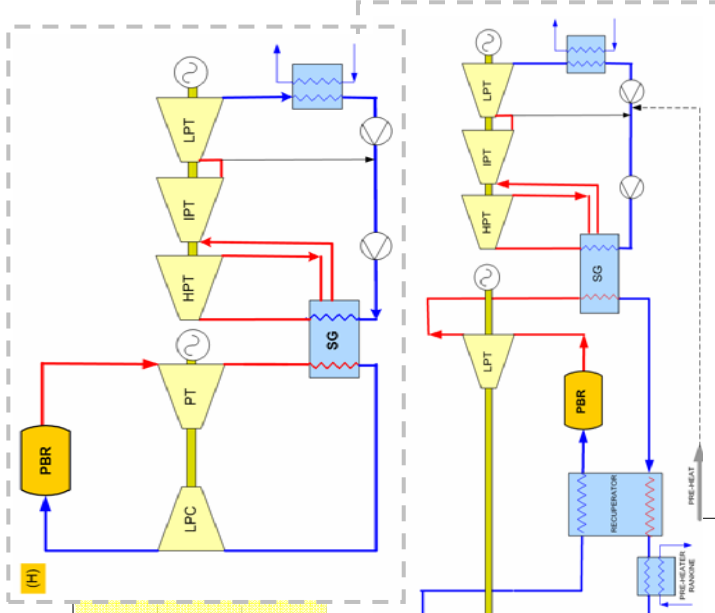
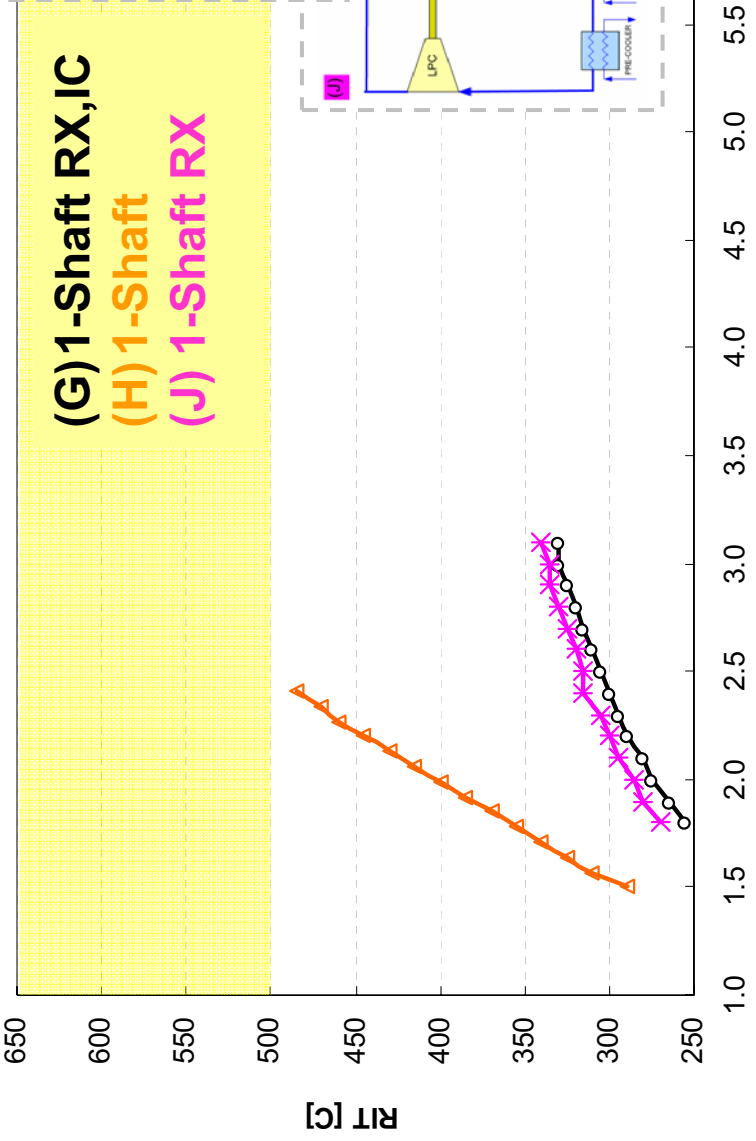


- Cycle H has highest net cycle efficiency, however only a small difference exists between GTCC efficiencies

➤ Resulting from optimization and preheat at (G) and (J)

GTCC RIT

Reactor inlet temperature vs. Pressure ratio



Total Brayton Pressure Ratio

- Cycle G
- △— Cycle H
- *— Cycle J

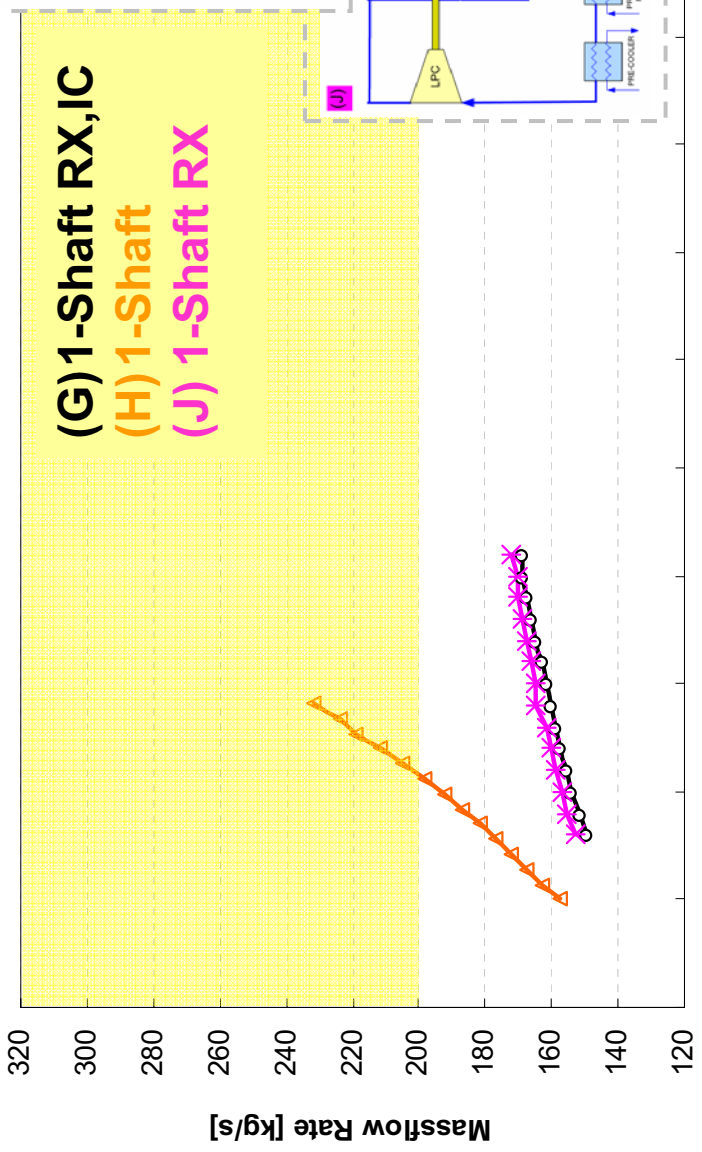
● **Maximum RIT of 500°C; to enable Core Barrel to operate below 427°C**

➤ All GTCCs are able to operate at its maximum efficiencies within the envelope

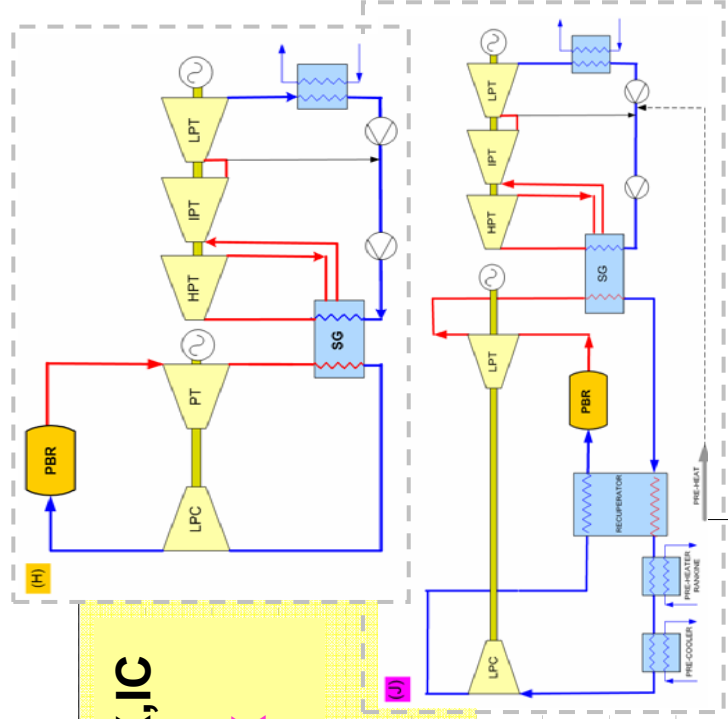
GTCC

Mass Flow Rate

Mass flow rate vs. Pressure ratio



(G) 1-Shaft RX,IC
 (H) 1-Shaft
 (J) 1-Shaft RX



Total Brayton Pressure Ratio

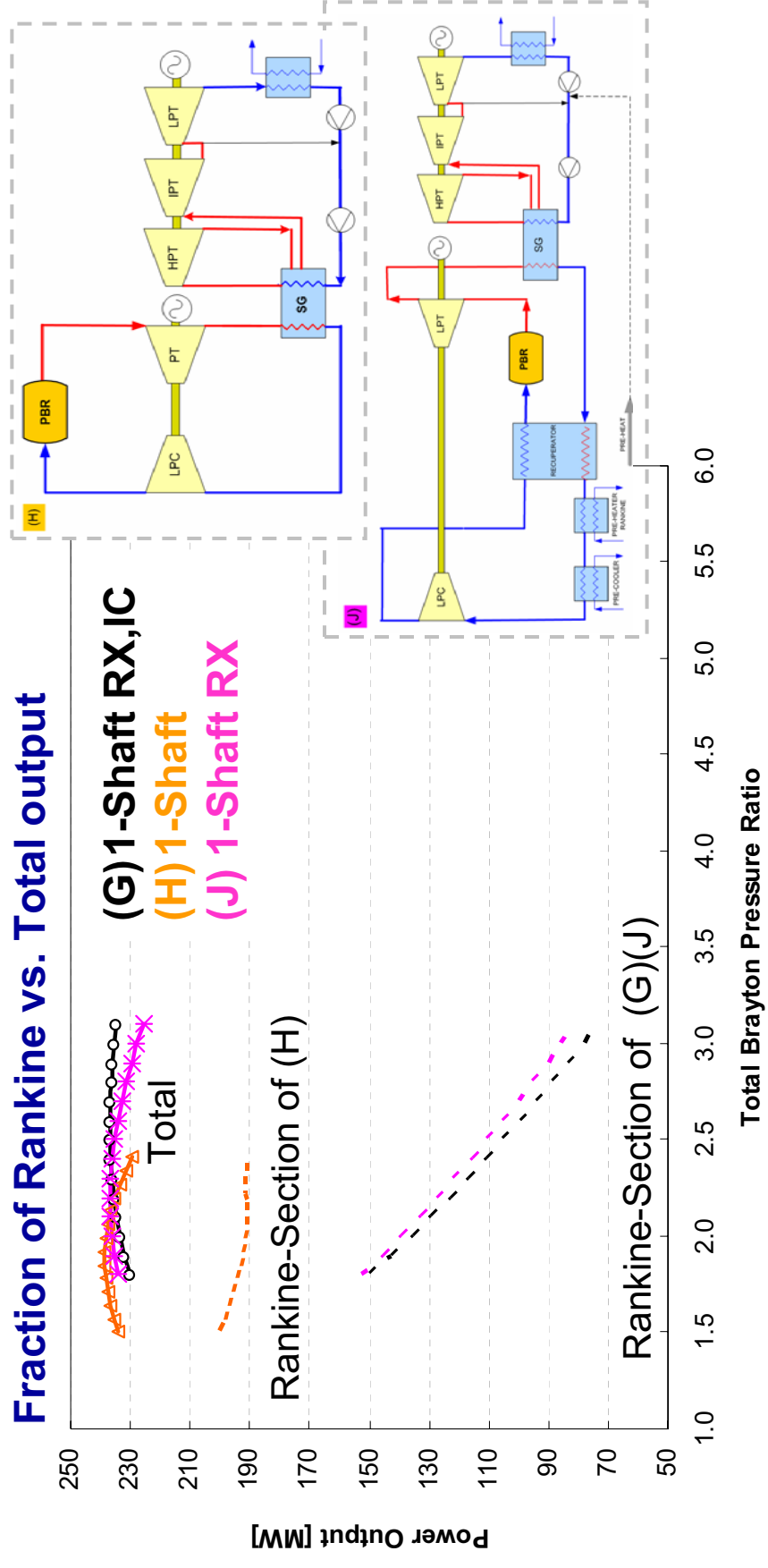
—○— Cycle G —△— Cycle H —*— Cycle J

• **Maximum mass flow of ~200 kg/s; to limit reactor core velocity**

➤ All the GTCCs are able to operate at its maximum efficiencies within the envelope

GTCC

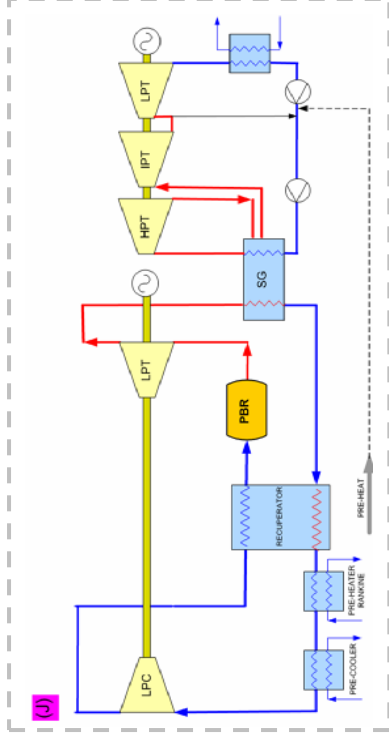
Work Split



- Cycle H: ~80% Rankine and 20% Brayton (large Rankine)
- Cycle J: ~50% Rankine and 50% Brayton (equal split)

Choice of GTCC

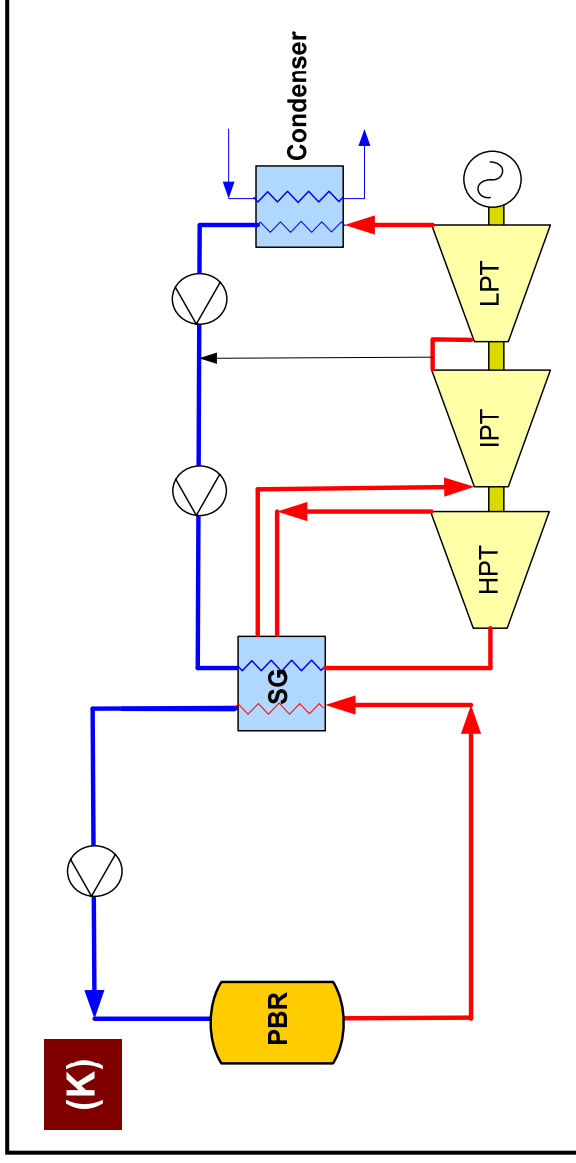
- **Criteria**
 - **Performance (MEDIUM)**
 - *Net Cycle Efficiency* –
 - Cycle H – 45.8%,
 - Cycle J – 45.1%
 - **Design Envelope (HIGH)**
 - *All GTCCs within envelope*
 - **Readiness (HIGH)**
 - *Cycle H -*
 - Compressor inlet temperature $\sim 200^{\circ}\text{C}$ – new turbo machine design (PBMR DPP 23°C)
 - Cooling flow required
 - *Cycle J:*
 - Builds on current PBMR DPP Brayton design (layout)
 - Utilizes PBMR DPP helium turbo machinery (operating conditions similar to DPP)



- **Conclusion**
 - Cycle J and H both good choices, however, Cycle J is perceived as lowest risk due to known Brayton turbo machinery
 - Cycle J selected as reference GTCC

Choice of Rankine

- Evaluated a single “representative” Rankine cycle and hence Cycle K chosen by default
 - Efficiency = 42%
 - Primary side mass flow = 160 kg/s (within reactor design envelope)
 - RIT = 300°C (within reactor design envelope)

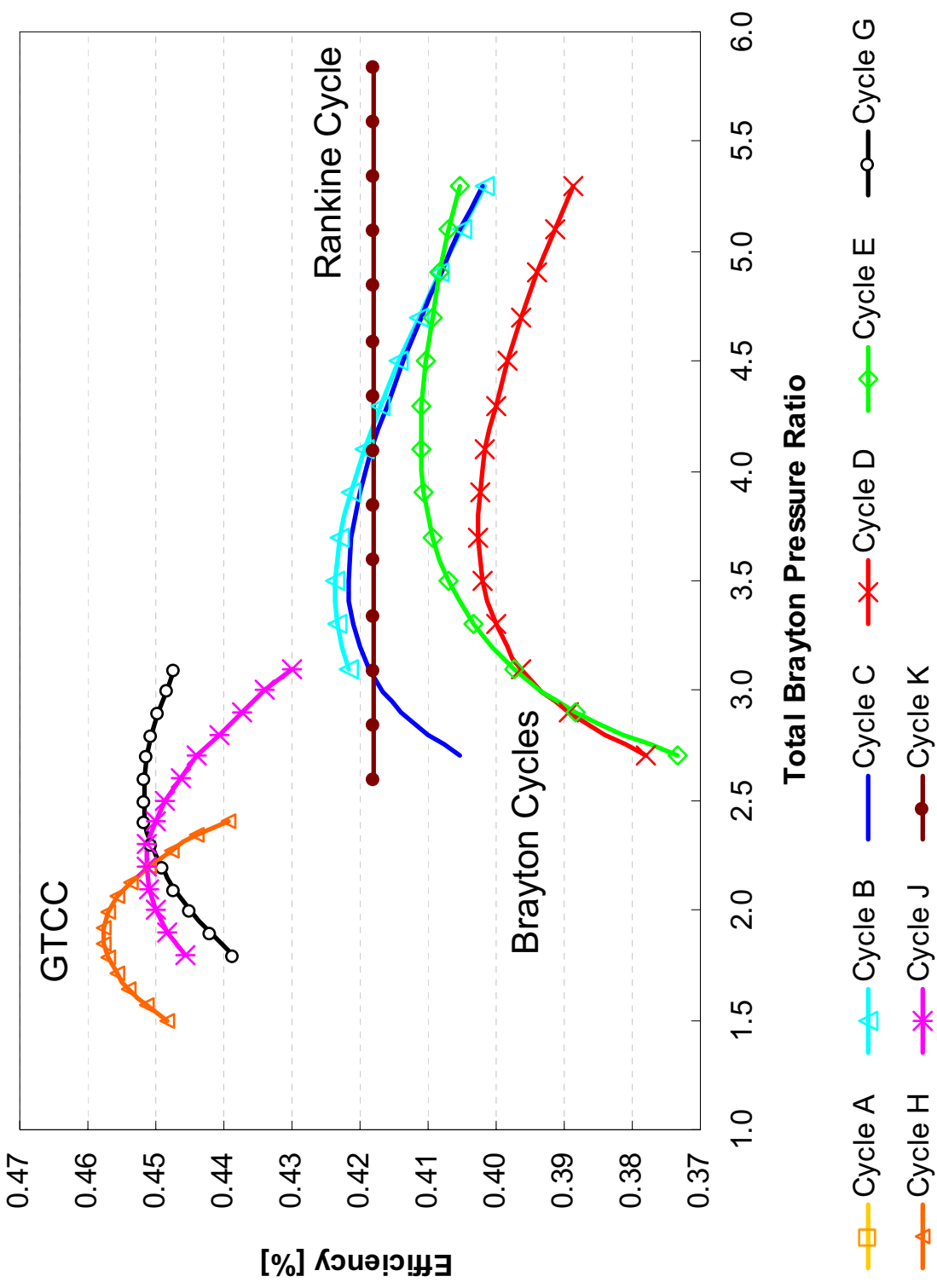


Part 2 Outline

- **Introduction**
- **Analysis Methodology**
- **Evaluation**
 - Brayton Cycles
 - GTCC
 - Rankine Cycles
- ➡ **Cycle Trade-offs**
- **Summary**

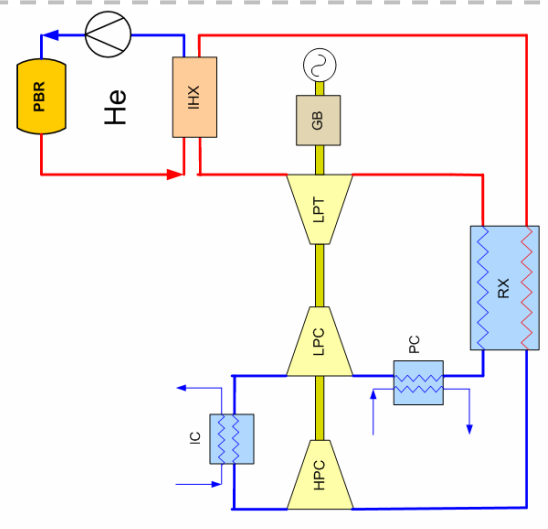
Net Cycle Efficiencies

Direct Cycles A, B, C, D, E, G, H, J, K



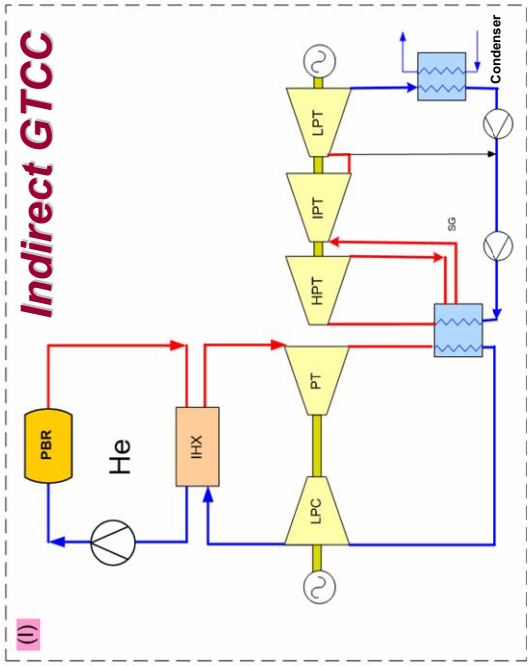
Direct- vs. Indirect Cycles

(F) **Indirect Brayton**



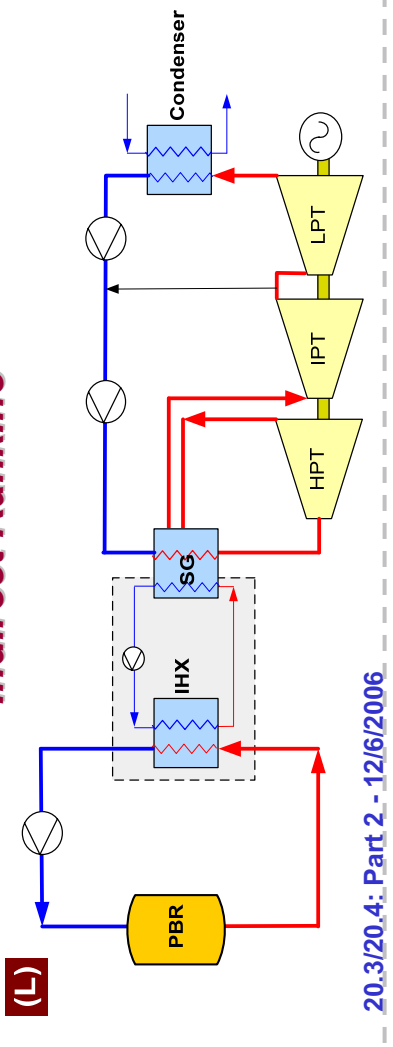
(F) **Indirect single-shaft with inter-cooling**
(Indirect version of Cycle B)

(I) **Indirect single-shaft Brayton**
(Indirect version of Cycle H)



(L) **Indirect secondary steam cycle**
(Indirect version of Cycle K)

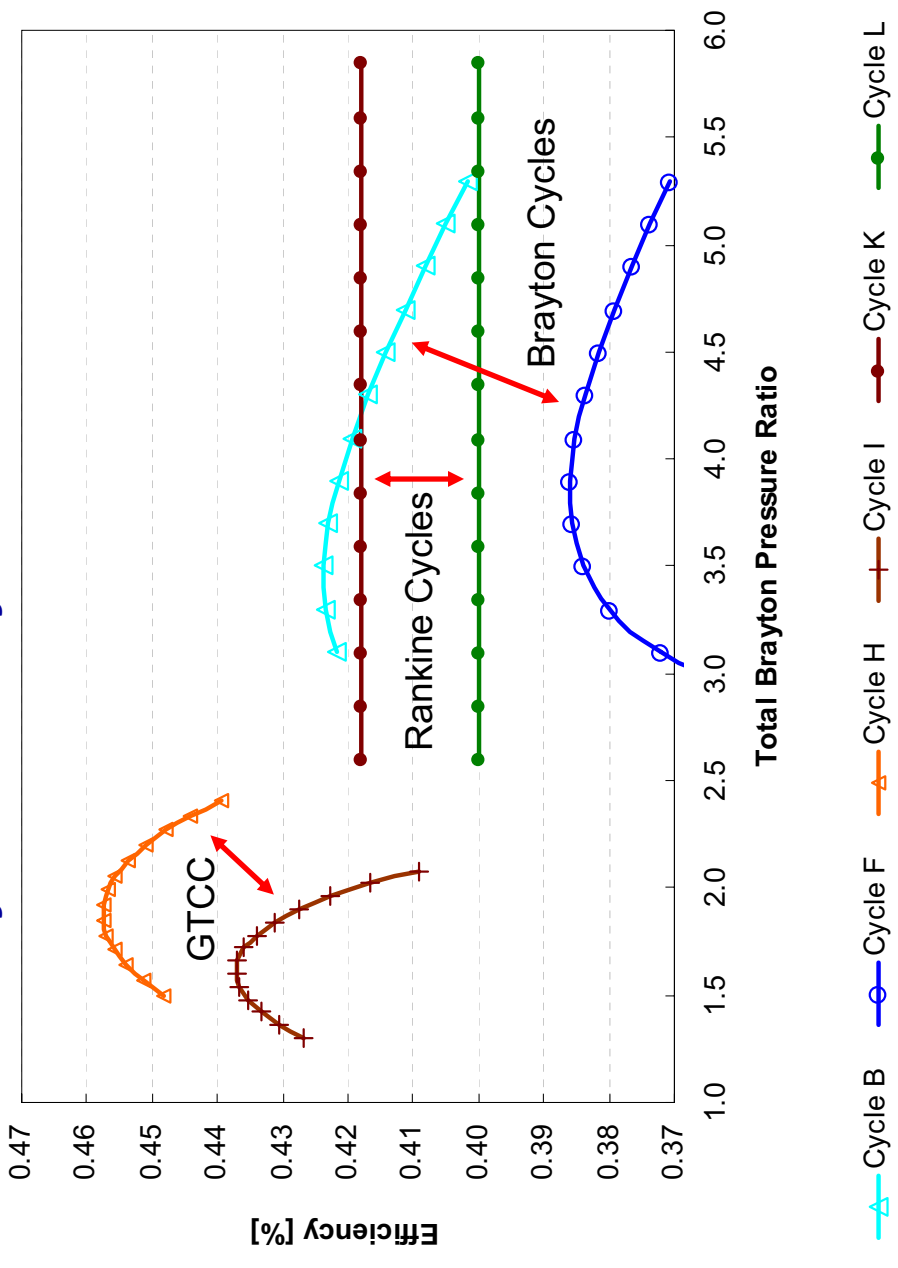
Indirect Rankine



Indirect Cycles

Net Cycle Efficiency

Net cycle efficiency vs. Pressure ratio



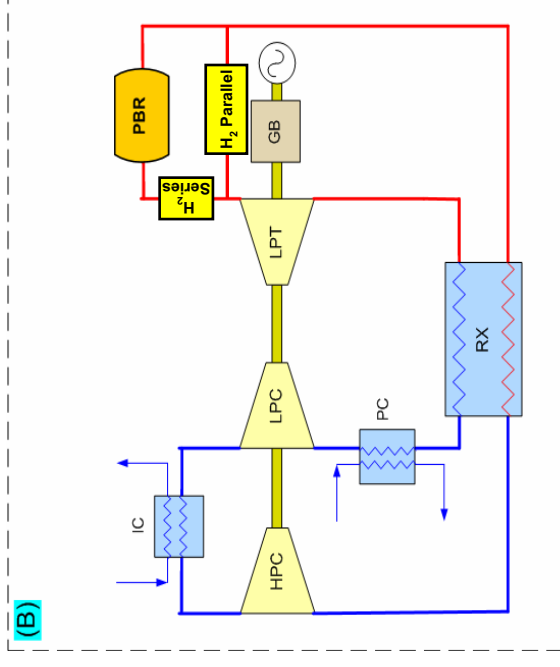
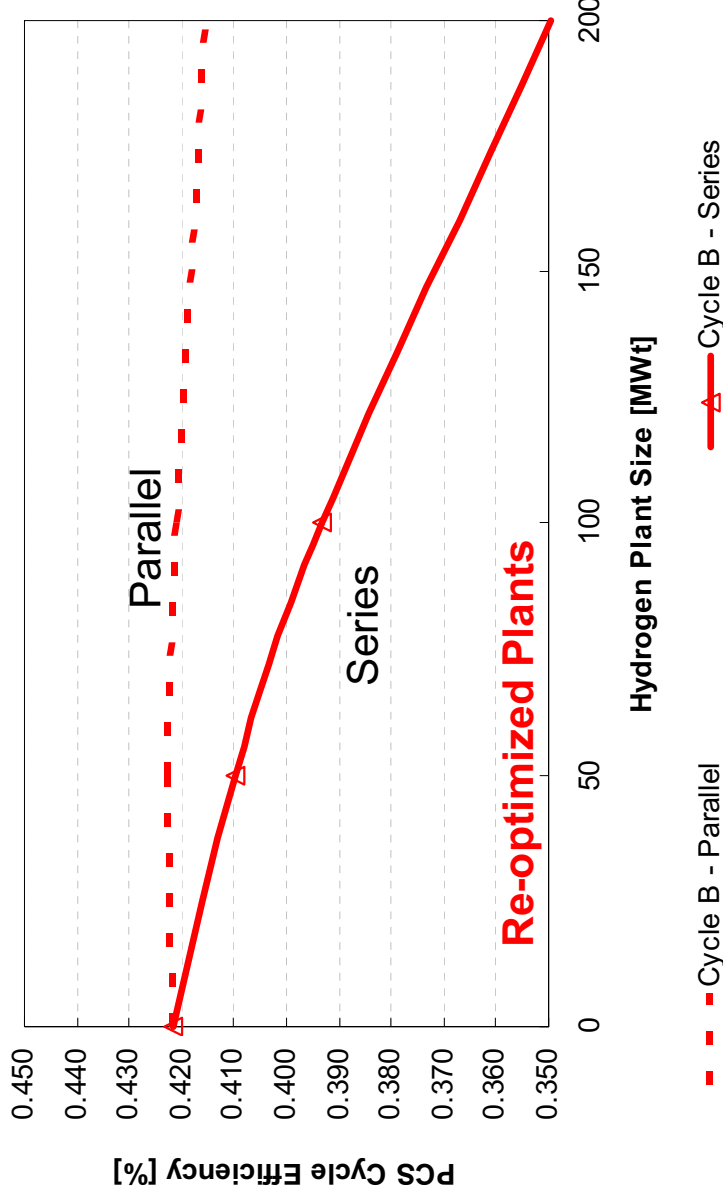
- Indirect Cycles reduces the net cycle efficiency by:
 - Brayton Cycle ~4%, GTCC ~2%, Rankine Cycle ~2%

Configuration Trade-offs

Brayton Series vs. Parallel

- Effect of H₂ plant size and configuration on Direct Brayton Cycle (B) thermal efficiency

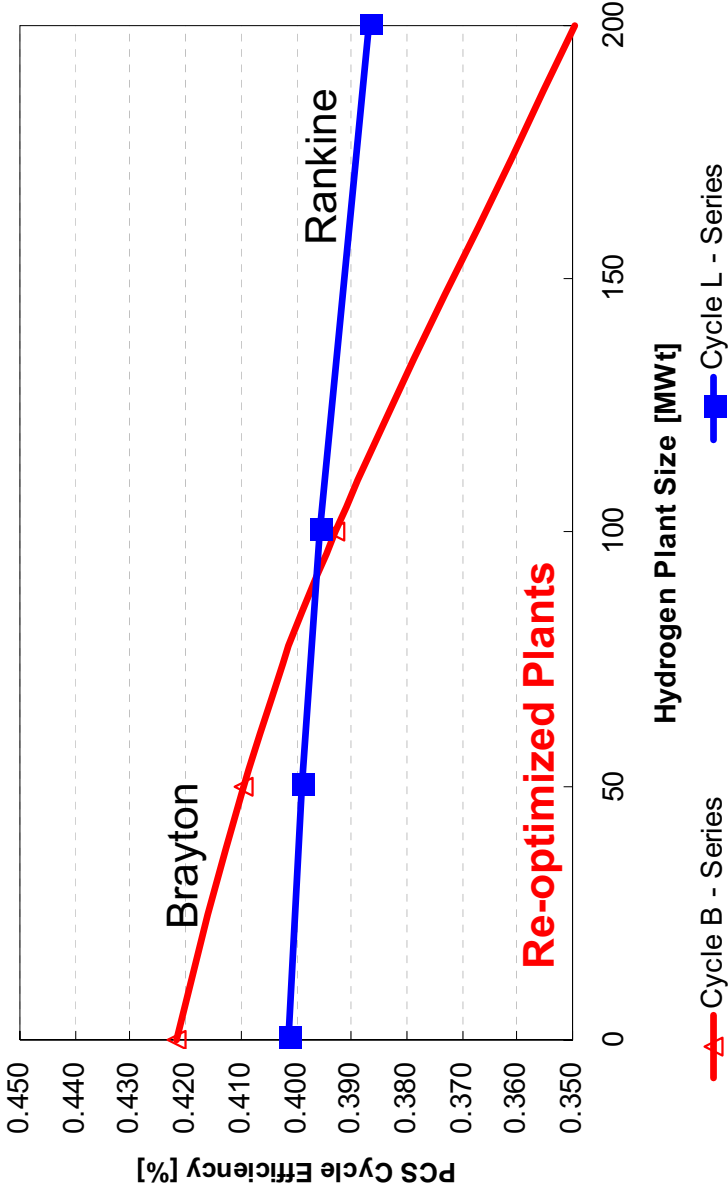
➤ Please note: parallel blower house load not included; parallel mixing not included



Configuration Trade-offs

Influence of Hydrogen plant size

- Effect of H₂ plant size coupled in series on the thermal efficiency of a Direct Brayton Cycle (B) vs. Rankine Cycle (L)
 - Rankine cycle efficiency > Brayton cycle efficiency above 100 MW hydrogen plant



Part 2 Outline

- **Introduction**
 - **Analysis Methodology**
 - **Evaluation**
 - Brayton Cycles
 - GTCC
 - Rankine Cycles
 - **Cycle Trade-offs**
-  **Summary**

Summary

- Cycle B chosen as reference Brayton Cycle PCS
 - Best efficiency
 - Turbo machine growth path
- Cycle J chosen as reference GTCC PCS
 - Builds on current PBMR DPP Brayton design
- Conventional Rankine Cycle chosen for reference Rankine Cycle PCS

